4. SITE 323

The Shipboard Scientific Party[1]

SITE DATA

Position: 63°40.84'S, 97°59.69'W (Bellingshausen Abyssal Plain)

Water Depth:
5004 corrected meters, echo sounding
4993 meters, drill pipe measurement

Number of Holes: 1

Number of Cores: 21

Penetration: 731 meters

Total Length of Cored Section: 199.5 meters

Total Core Recovered: 76.73 meters

Percentage Core Recovered: 38%

Oldest Sediment Cored:
Depth Subbottom: 701.0 meters
Nature: Brown clay
Age: Late Cretaceous
Velocity: 1.85 ±0.04 km/sec

Basement:
Depth Subbottom: 701.0 meters
Penetration: 30.0 meters
Nature: Basalt
Velocity: 3.65-4.80 km/sec

Principal Results: A single hole was drilled into the Bellingshausen Abyssal Plain south of the Eltanin Fracture Zone, and 66.5 meters of claystone and 10.2 meters of basalt were recovered from 731 meters of penetration. The upper 500 meters (Miocene and Pliocene) is diatomaceous clay and claystone; a single ice-rafted granite cobble was found at about 360 meters in Miocene claystone. Between about 500 and 640 meters (?Oligocene to early Miocene) the claystone lacks biogenic silica. Below this (640-670 meters) lies iron-rich and nannofossil-rich brown claystone of Danian age, and Maestrichtian brown zeolitic claystone (670-700 m). This overlies aphanitic aphyric basalt rich in iron and titanium, and low in magnesium oxide. The (1) evidence of fractionation, (2) the absence of glass, palagonite, or hyaloclastite, and (3) the low hummocky relief of acoustic basement suggest that the basalt may represent one or more sills. However, the Maestrichtian age (70 m.y.) determined from fossils in the sediments overlying the basalt is close to the 76 m.y. age suggested by the nearest magnetic anomaly (?32).

Background and Objectives

Site 323 lies southwest of the Eltanin Fracture Zone on the Bellingshausen Abyssal Plain about 150 miles north of the base of the Antarctic continental rise (Figures 1, 2). Water depths exceed 4000 meters throughout the region, and in the vicinity of Site 323 they exceed 5000 meters. Water depths less than 4000 meters occur to the south along the Antarctic coast, to the northwest near the East Pacific Ridge, and over a few seamounts more than 150 miles away (Heezen and Tharp, 1972). Tectonically, the site lies in the deep oceanic part of the Antarctic plate. A seismic profile through the site (*Eltanin*-42, 1700 hr, 20 March 1970) (Figure 3) shows a smooth abyssal plain underlain by less than a kilometer of sediment resting upon a moderately smooth basement.

The regional geology of the Southeast Pacific Basin and the adjacent land masses is poorly known. The closest land areas lie about 350 miles southward at Peter I Island and along the coast of West Antarctica at Thurston Island (about 480 miles south). The rocks of coastal West Antarctica record a complex history of Phanerozoic sedimentation, volcanism, plutonism, regional metamorphism, and orogenic deformation; no rocks of definitely Precambrian age are known at the present (Craddock, 1970, 1972). Several orogenic cycles have been identified, and the youngest is the Andean of Cretaceous to early Tertiary age. Cenozoic volcanic rocks crop out extensively in coastal West Antarctica. Thurston Island consists of Paleozoic and Mesozoic igneous and metamorphic rocks. Peter I Island is a basaltic volcano, probably Miocene in age, and other seamounts lie nearby in the Southeast Pacific Basin (Heezen and Tharp, 1972).

Only a few magnetic profiles have been run near Site 323, and the pattern of magnetic anomalies has not yet been firmly established. Pitman et al. (1968) postulate the existence of anomalies 32 and 29 to the west, and to the north in another crustal block. If the crust at Site 323 originated at the Pacific-Antarctic Ridge, then their map shows a predicted age substantially older than anomaly 32, which formed about 76 m.y.B.P.

Little is known of the sediments beneath the Southeast Pacific Basin and the history of physical and biological events which they may record; present knowledge is summarized by Goodell et al. (1973). Piston cores taken here suggest that the abyssal plain is

---

[1] Charles D. Hollister, Woods Hole Oceanographic Institution, Woods Hole, Massachusetts (Co-chief scientist); Campbell Craddock, University of Wisconsin, Madison, Wisconsin (Co-chief scientist); Yury A. Bogdanov, P.P. Shirshov Institute of Oceanology, U.S.S.R. Academy of Sciences, Moscow, U.S.S.R.; N. Terence Edgar, Scripps Institution of Oceanography, La Jolla, California (Present address: U.S. Geological Survey, Reston, Virginia); Joris M. Gieskes, Scripps Institution of Oceanography, La Jolla, California; Bilal U. Haq, Woods Hole Oceanographic Institution, Woods Hole, Massachusetts; James R. Lawrence, Lamont-Doherty Geological Observatory, Columbia University, Palisades, New York; Fred Rögl, Eidg. Technische Hochschule, Zurich, Switzerland (Present address: Naturhistorisches Museum, Vienna, Austria); Hans-Joachim Schrader, Institut und Museum der Universität Kiel, Kiel, Germany; Brian E. Tucholke, Lamont-Doherty Geological Observatory, Columbia University, Palisades, New York; Walter R. Vennum, Sonoma State College, Rohnert Park, California; Fred M. Weaver, Florida State University, Tallahassee, Florida; Vasily N. Zhivago, P.P. Shirshov Institute of Oceanology, U.S.S.R. Academy of Sciences, Moscow, U.S.S.R.

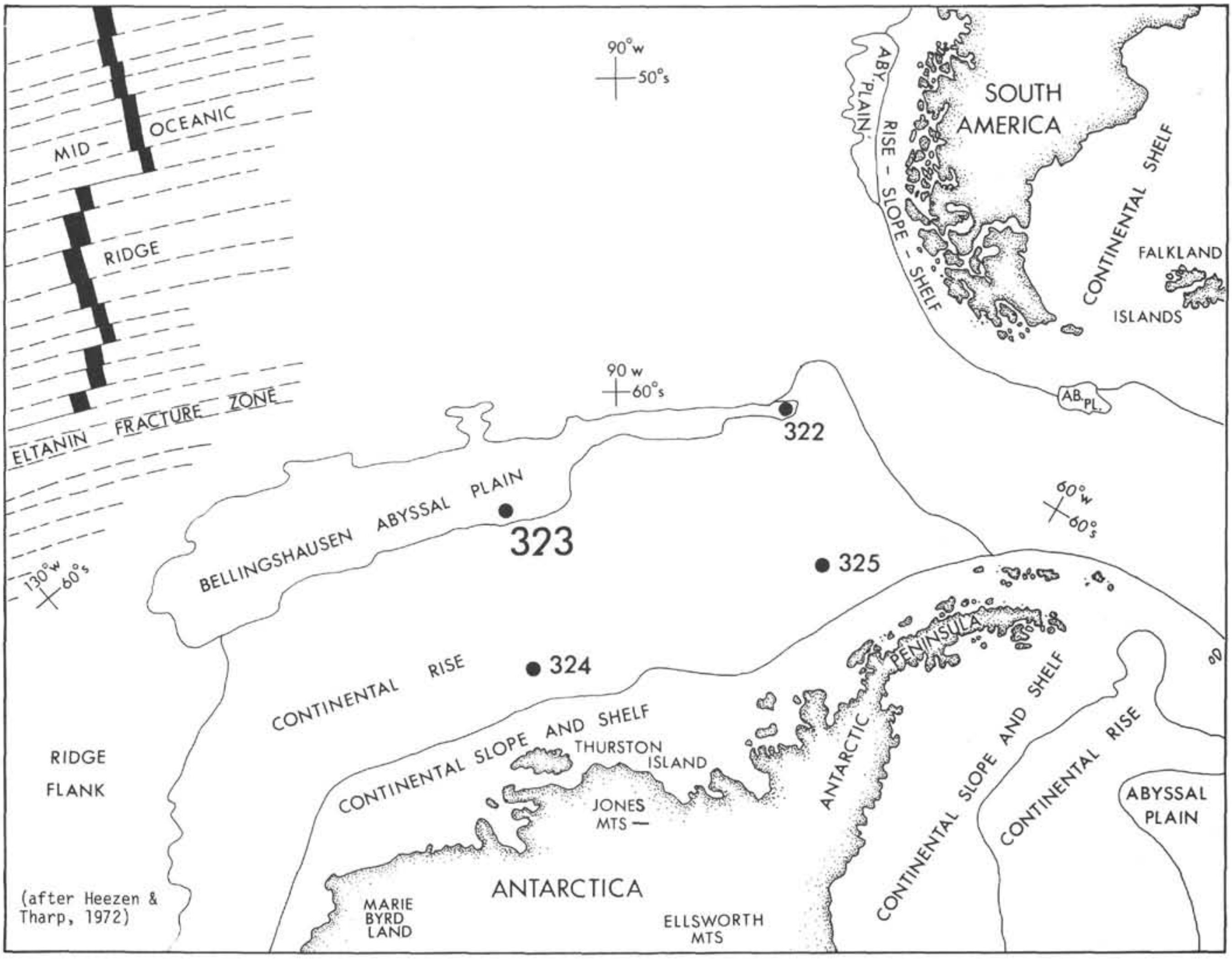

Figure 1. *Location of Site 323.*

underlain by fine-grained distal turbidite sediments. Site 323 lies about 250 miles south of the axis of the Antarctic Circumpolar Current which flows eastward through the Scotia Sea at a rate of more than 200 million m^3/sec (Gordon, 1967, 1972; Reid and Nowlin, 1971). Weissel and Hayes (1972) infer from magnetic anomalies that oceanic crust began to form between East Antarctica and Australia about 55 m.y.B.P.; this may define the earliest date at which the present circumpolar circulation pattern could have formed. Kennett et al. (1972) report a regional unconformity of Oligocene age in the southwestern Pacific Ocean Basin, and they attribute it to paleocirculation changes related to the separation of Australia from East Antarctica and to glacial episodes in Antarctica. If the crust at Site 323 is Mesozoic in age the sedimentary layer is rather thin and the section may contain one or more unconformities.

The history of continental glaciation in Antarctica should be recorded by the sediments in the adjacent ocean; one of our prime objectives was to recover that record. On the continent evidence for Tertiary glaciation in the Jones Mountains (74°S, 94°W) was first reported by Craddock et al. (1964) and later summarized by Rutford et al. (1972). LeMasurier (1972) in describing the volcanic history of Marie Byrd Land suggested the existence of a West Antarctic ice sheet since the Eocene. Margolis and Kennett (1970) studied the quartz grains and foraminifers in 18 piston cores from the South Pacific and inferred that Antarctic glaciation occurred during much of the time since the Eocene, but with a warm episode in the Miocene. During DSDP Leg 28 glaciomarine sediments, including beds as old as Oligocene, were found in holes in the Ross Sea at Site 270. We attempted to resolve this apparent discrepancy in the history of Antarctic glaciation by obtaining a record of ice-rafting processes at our drilling sites.

Objectives

The principal objective at Site 323 was to establish the age of the oceanic crust by drilling into basement. Other objectives were: to determine lithology, provenance, and processes of sedimentation; to determine the history of Antarctic glaciation; to determine the biostratigraphic sequence and paleobiogeographic

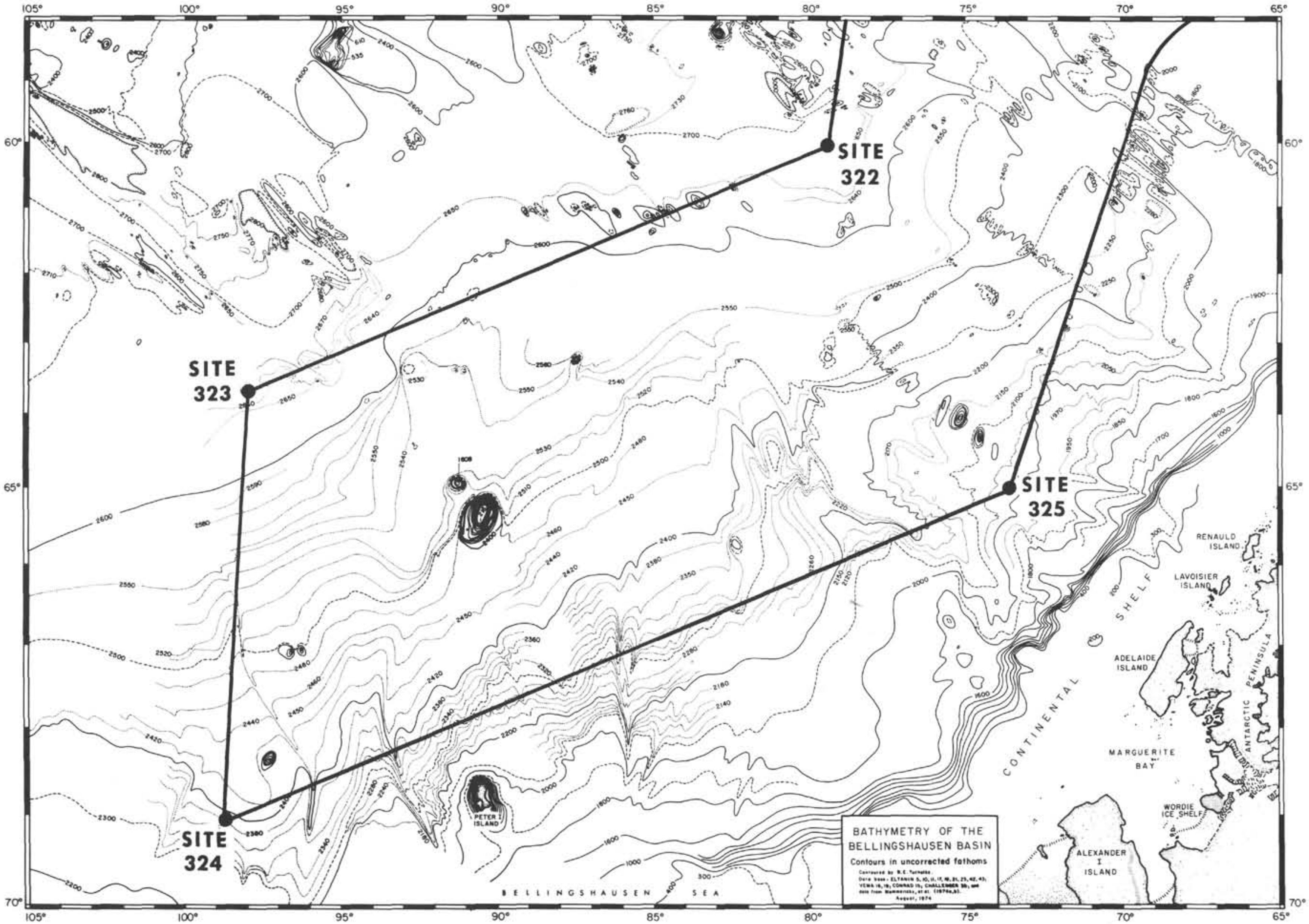

Figure 2. *Bathymetric map of the Bellingshausen region (see also foldout in back cover).*

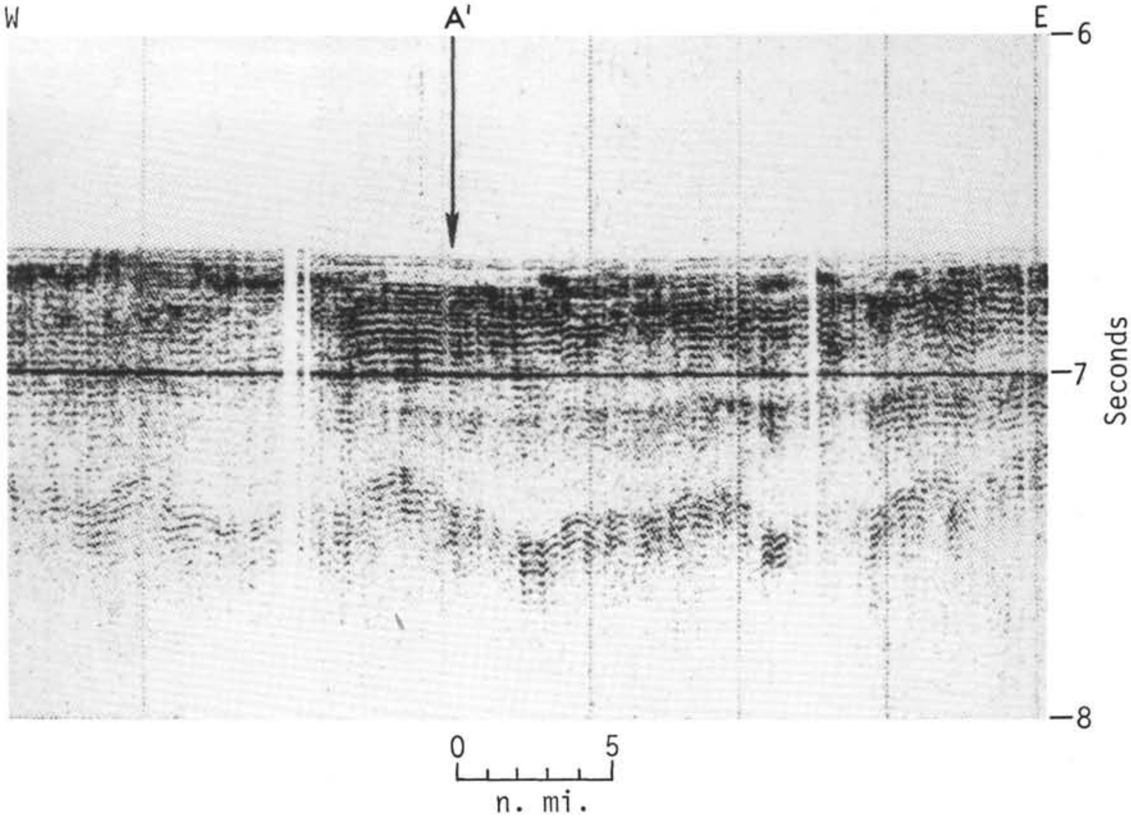

Figure 3. *A west-east* Eltanin 42 *seismic profile near Site 323. See track chart (Figure 4) for location. (A' is 0000 hr, 23 March 1970.)*

environment; to obtain specimens of basement rock for studies of composition, alteration, age, and paleomagnetism; to obtain samples of pore waters and solid phases for studies of geochemical gradients and halmyrolysis.

OPERATIONS

The ship arrived in the vicinity of Site 323 at approximately 1130 hr on 6 March 1974. At 1202 hr speed was reduced to about 7 knots and a brief seismic reflection survey was run (Figures 4 and 5). The beacon (16kHz O.R.E.) was dropped at 1345 hr, reaching the sea floor (4993 m drill pipe measurement from sea surface) at about 1425 hr. The vessel was stabilized over the beacon at 1425 hr and the drill string lowered, making bottom contact at 5003 meters below the rig floor at 0750 hr, 7 March.

A total of 21 cores was attempted in the hole. Recovery averaged 38% for the entire hole, and ranged from 7% to 99% in the sedimentary sequence and from 1% to 55% in the basalt. A summary of coring is given in Table 1.

Approximately 10 meters of basalt were recovered from a total penetration of 30 meters at an average coring rate of 0.11 meters per minute. At least once during cutting the last two cores (20 and 21), an abrupt increase in coring rate occurred leading to speculation that the basalt is a sill between thin sediment layers. No sediment however was recovered in either Cores 20 or 21.

Upon departure from the site, a short loop to the northwest was made to begin seismic profiling before we passed over the beacon (at 0653 hr, 11 March) enroute southward to Site 324.

LITHOLOGY

Sediments and igneous rocks were penetrated to a depth of 731 meters at Site 323, and 66.5 meters of sediment and 10.2 meters of basalt were recovered. Sediments at this site are dominated by clays and claystones, but biogenic components are more common than at Site 322. Diatom clays and diatom oozes predominate in the upper 465 meters of the section; radiolarians are also restricted to this interval. The base of the siliceous sediments is marked by the occurrence of silicified claystones (cherts) in Cores 8, 9, and 10 (408-512 m). Calcareous foraminifers and nannoplankton occur only near the bottom of the hole at 655 to 674 meters in Cores 15 and 16. The only megascopic evidence of ice rafting encountered in Miocene sediments is in Core 7, Section 2 (granite cobble) and 7, CC (ice-rafted gravel in clay). Estimates of principal components from smear slides are given in Figure 6.

The lithologic sequence is divided into six primary units based on sediment color, relative induration, and composition (Table 2). Contacts between the units are preserved in three places. (1) The contact between the siliceous and nonsiliceous claystones of Units 2 and 3 occurs in Core 10; it appears to be a gradational contact

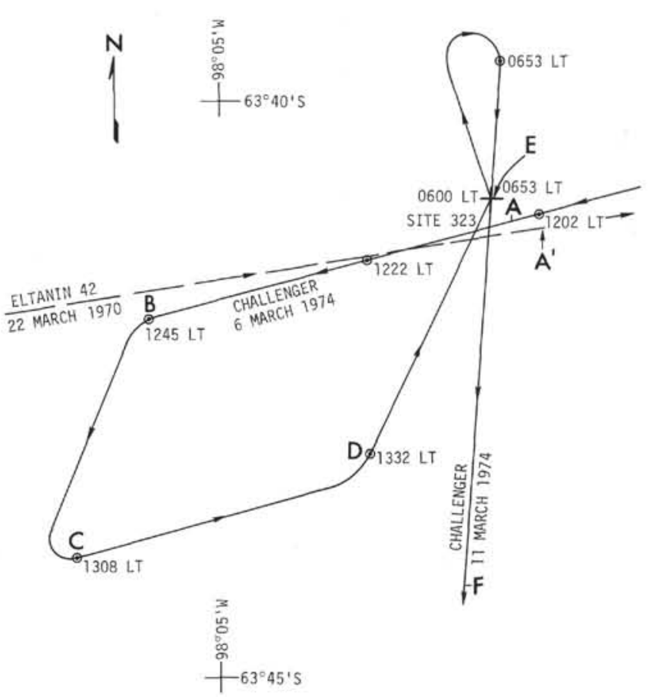

Figure 4. Glomar Challenger *1974 track approaching and departing Site 323, and* Eltanin *1970 track. Letters indicate positions shown on seismic profiles, Figures 3 and 5.*

because discrete chert cobbles are present between nonsiliceous claystones down through Core 10, Section 3. Although it is possible that the cherts in Core 10 were displaced from higher in the hole, this is unlikely inasmuch as the cobbles are not excessively abraded as would be expected if they had been worked downhole by the bit. Furthermore, sonic velocities determined on cherts in Cores 8 through 10 consistently decrease downhole (see Tucholke, Edgar, and Boyce, this volume) in a manner compatible with a gradient of downward decreasing silicification. (2) The contact between Units 3 and 4 is a sharp mineralogical and color change from gray claystones to underlying, iron-bearing, brown claystones in Core 14. (3) The contact between Units 4 and 5 occurs at 666.5 meters in Core 16, Section 2 and marks a sharp change from claystone rich in nannofossils and amorphous iron oxides to claystone devoid of these components but bearing zeolites.

Units 1 and 2 are differentiated on the basis of induration, and the contact is assumed to occur at 266 meters just below Core 3. The sparse sampling and poor core recovery in the upper part of the hole make exact determination of the contact difficult. Core 3 contains soft claystone, but the coring rate decreased sharply below this core, and this criterion is used to establish the contact.

The contact between Unit 5 and basalt occurs in Core 18, Section 6. The continuity of the core, however, is broken here, and sediment from the actual contact is probably missing.

Unit 1 (0-266 m) consists largely of unconsolidated gray diatom clays and diatom oozes of late middle Miocene to Holocene age, and it correlates with relatively rapid drilling and coring rates. Contacts between subtle color changes in the clays are often sharp. Semi-indurated clays near the base of the unit are still pliable and appear to be transitional to the claystones of Unit 2. Silts and sands usually occur as distinct intervals 7-15 cm thick interbedded with clays. Sand stringers and pods 1-2 cm thick are common and appear to be beds disturbed by coring; their upper and lower contacts are normally sharp. No size grading was observed in any of these beds. Primary structures within the sand, silt, and clay units are virtually nonexistent; the few that may have been present have been destroyed by coring.

The sediments of Unit 1 are primarily composed of detrital quartz and clay minerals. Feldspar and heavy minerals comprise up to 10% of the silts and sands. One exceptional sample (3-3, 121 cm) is a quartz silty sand containing about 35% heavy minerals, which may indicate mechanical concentration. Rock fragments appear sporadically in quantities usually less than 10%, as do opaque minerals, pyrite, and glauconite which are present in trace quantities.

The biogenic fraction is dominated by fragmentary diatoms comprising up to 60% of the sediment, but the average is about 10%. Radiolarians and sponge spicules are much less common (3%-5%) but in some samples exceed 10%.

Unit 2 spans 241.5 meters of lower through middle Miocene sediment from just below Core 3 to Core 10, Section 2. It is characterized by grayish claystones with abundant diatoms, radiolarians, and sponge spicules, and is distinguished from Unit 1 by the dominance of indurated claystones and by the sharply reduced drilling and coring rates.

Sediment recovery was generally poor throughout Units 1 and 2, and it appears likely that thick sequences of unconsolidated or poorly consolidated silt and sand were penetrated, but not trapped by the dog-type core catchers used at this site. (A similar situation was experienced at Site 322.)

Core 4 (75-85 m) taken at the top of Unit 2 is atypical, consisting of: (1) a drilling slurry of claystone fragments and (2) a well-sorted, very coarse sand. The sand contains angular to subangular rock fragments with traces of abraded pelecypod fragments. Although the sand is totally disturbed by drilling, its size sorting is unlike that of drill cuttings, and it is probably representative of an unconsolidated sand layer.

The claystones down to Core 7 (370 m) have little internal structure or color variation. Yellowish-brown claystone galls were occasionally observed in drill slurry but never in distinct beds. Smear-slide mineralogy of these galls is similar to that of the gray claystones. Some faint bedding, trace fossils (burrowing), and silty-sand pods were observed in Cores 7-10.

The claystones of this interval are mineralogically similar to the clays of Unit 1 except for occurrences of authigenic calcite (5-1, 135 cm and 7-1, 95 cm) which represent the only carbonate detected in either Unit 1 or 2, and the presence of cherts in the lower part (Cores 8-10) of Unit 2.

The cherts are lithified claystones developed by precipitation of cryptocrystalline silica. They are generally dark gray (N3) in color and can be scratched

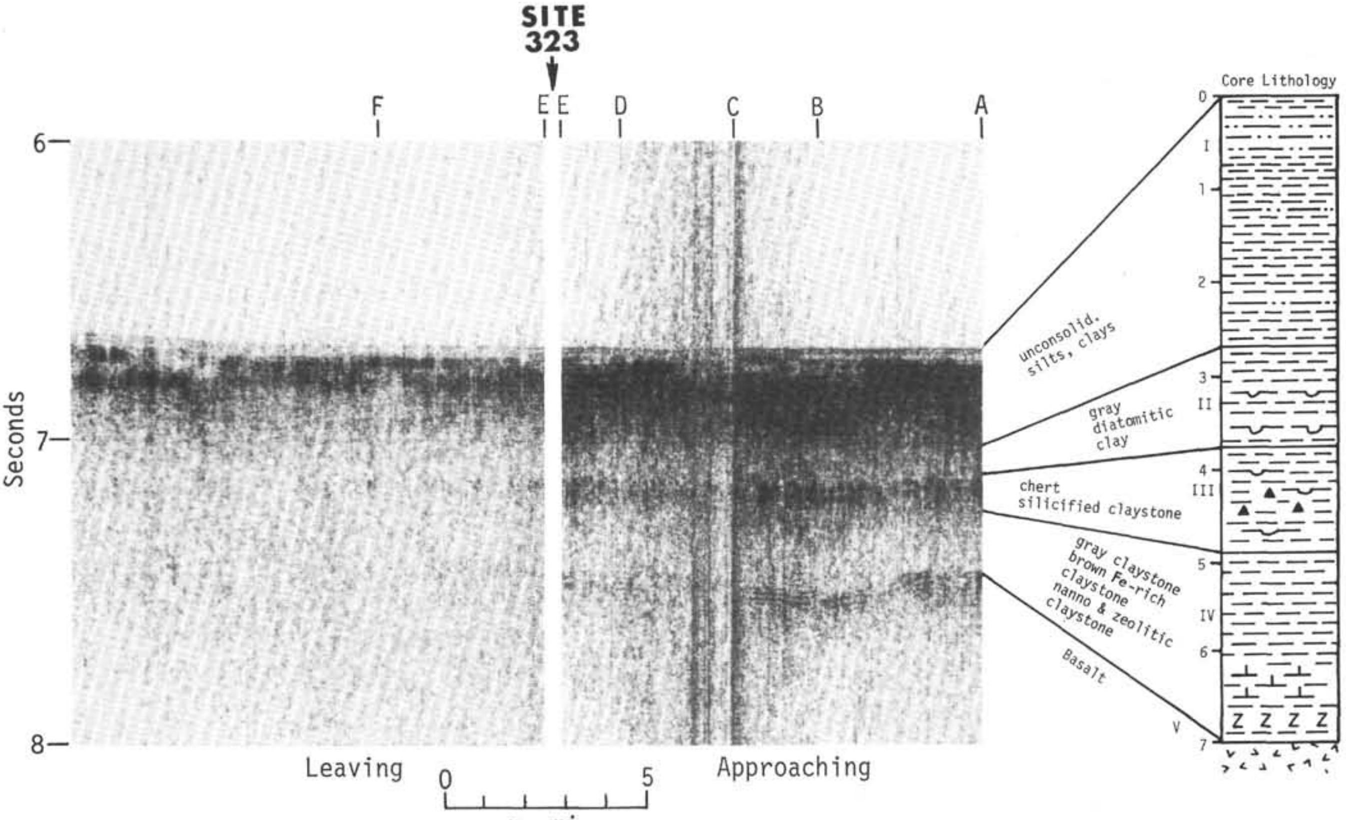

Figure 5. Glomar Challenger *seismic profile approaching and leaving Site 323. See Figure 4 for location. Acoustic units are discussed in the text.*

easily or with difficulty with a knife, depending on the degree of lithification; the most strongly lithified samples have a subconchoidal fracture, but most are less well lithified and can be described as porcelanitic cherts (Lancelot, 1973). The siliceous cement is predominantly cristobalite, with lesser amounts of tridymite (Zemmels and Cook, this volume). Such cherts were encountered in the following locations: 8-1, 110-120 cm; 8, CC; 9-2, 117-140 cm; 10-1, 92-96 cm; 10-2, 4-6, 12-14, and 135-138 cm; 10-3, 62-63 cm, 124-125 cm. The lithification of these claystones has not disturbed the fine faint bedding and trace fossils. Silicification is strongly localized; the transition from unlithified claystone to chert usually occurs over a few centimeters and in some cases within a centimeter (notably at 9-2, 117 cm and 10-1, 95 cm). Faint corroded relics of diatoms and radiolarians are observed in the aggregate of cryptocrystalline silica and clay minerals comprising the cherts. The cherts mark the deepest occurrence of biogenic or reprecipitated silica in more than trace quantities.

The 130.5 meters of sediment composing Unit 3 (lower Miocene) have the same megascopic lithology as the grayish claystones of Unit 2, although Unit 3 claystones are, on the whole, slightly more silty. The single most important distinction between the units is lack of biogenic silica in Unit 3, whereas recrystallized calcite and pyrite are commonly observed. Clay minerals dominate in the sediment. Quartz varies from less than 5% to more than 75%, and feldspars occur sporadically in quantities less than 5%. Heavy minerals average less than 5% but are consistently observed throughout the unit, whereas only scattered occurrences were observed in the two overlying sedimentary units.

Calcite occurs most commonly in Core 13 (617-626.5 m), and two thin (3 mm) quartz-silt layers are enriched (50%) in authigenic calcite. No other calcite was noted in the smear slides, although severely corroded foraminifers were observed in megascopic descriptions of Cores 11 through 13 (550-626 m). Cores 11 and 12 contain traces to more than 5% pyrite and pyritized diatoms occur in Core 11, Section 1.

The claystones of this unit also exhibit distinct internal structures including very fine laminae (bedding planes) which are often associated with sharp color changes between shades of gray and gray-brown. Bioturbation is uncommon but is distinct in Sections 12-2, 13-5, 13-6, 14-1, and 14-2. No sedimentary structures diagnostic of current reworking of the sediments were noted.

Units 4 and 5, in contrast to the overlying gray claystones, are composed almost entirely of brownish pelagic claystones. Clay minerals, amorphous iron and manganese oxides, nannofossils and zeolites are the primary constituents of the sediments; traces of opaque

TABLE 1
Coring Summary, Site 323

	Cored Interval			Recovered			
Core	Total Depth (m)	Subbottom Depth (m)	Cored (m)	(m)	(%)	Lithology	Age
1	5078.5-5088.0	75.5-85.0	9.5	7.35	77	Diatom clay and ooze with silt and sand stringers	Pliocene
2	5164.0-5173.5	161.0-170.5	9.5	1.6	17	Diatom clay and ooze	Pliocene
3	5259.0-5268.5	256.0-265.5	9.5	2.8	29	Sandy and silty claystone	Late Miocene
4	5316.0-5325.5	313.0-322.5	9.5	3.35	35	Sand	Middle to early Miocene
5	5335.0-5344.5	332.0-341.5	9.5	0.7	7	Claystone	Middle to early Miocene
6	5344.5-5354.0	341.5-351.0	9.5	1.1	12	Diatom claystone and clayey diatomite	Middle to early Miocene
7	5363.5-5373.0	360.5-370.0	9.5	3.5	37	Clay and diatom claystone	Middle to early Miocene
8	5411.0-5420.5	408.0-417.5	9.5	1.6	17	Diatom clay, clayey silt and claystone	Middle to early Miocene
9	5458.5-5468.0	455.5-465.0	9.5	2.5	26	Diatom claystone, silicified clay	Miocene
10	5506.0-5515.5	503.0-512.5	9.5	3.0	32	Clayey silt and silty claystone	Early Miocene-? Oligocene
11	5553.5-5563.0	550.5-560.0	9.5	3.1	33	Quartz-silty claystone	Early Miocene-? Oligocene
12	5601.0-5610.5	598.0-607.5	9.5	2.2	23	Claystone and siltstone	Early Miocene-? Oligocene
13	5620.0-5629.5	617.0-626.5	9.5	7.7	97	Claystone and siltstone	Early Miocene-? Oligocene
14	5639.0-5648.5	636.0-645.5	9.5	2.7	27	Quartz-silty claystone	(Barren)
15	5658.0-5667.5	655.0-664.5	9.5	9.4	99	Fe-claystone and nannofossil claystone	Late Danian
16	5667.5-5677.0	664.5-674.0	9.5	6.2	63	Fe-claystone and nannofossil claystone	Late-Middle Danian
17	5677.0-5686.5	674.0-683.5	9.5	1.5	16	Claystone	Maestrichtian
18	5696.0-5705.5	693.0-702.5	9.5	7.7	81	Claystone, zeolitic claystone, and basalt	Maestrichtian
19	5705.5-5715.0	702.5-712.0	9.5	5.2	55	Basalt	(Barren)
20	5715.0-5724.5	712.0-721.5	9.5	3.4	36	Basalt	(Barren)
21	5724.5-5734.0	721.5-731.0	9.5	0.13	1	Basalt	(Barren)
Total	5734.0	731.0	199.5	76.73	38		

Recovery of total sequence penetrated = 10.5%.

minerals and manganese micronodules are found, but detrital quartz, feldspar, heavy minerals, and recrystallized calcite are conspicuously absent.

The 28.5-meter-thick Unit 4 consists of iron-rich dusky yellow-brown claystone of Danian age. Bedding is very poorly defined and the sediment is extensively mottled by burrowing. From Core 15, Section 6 to Sample 16-2, 55 cm the sediment is a yellow-brown nanno-claystone.

Below Sample 16-2, 55 cm, Unit 5 (Maestrichtian to Danian) is brownish zeolitic claystone. Zeolites are very common (10%-50%) immediately above the contact with basalt. Amorphous iron oxide is rare in this unit and nannoplankton are rare. The claystones are structureless and devoid of trace fossils except for a *Zoophycos* burrow at 110 cm in Core 18, Section 4 and minor mottling in Core 18, Section 5. Sharp color contrasts are developed around the *Zoophycos* burrow (yellow-gray, green-gray, brown) but no mineral differences were detected in these varicolored sediments. The lower half of Unit 5 also has numerous corroded foraminifers (*Cyclammina*) detected as tiny white specks in the brown claystone (see Rögl, this volume). Montmorillonite is the dominant mineral component in both Units 4 and 5 (Zemmels and Cook; Gorbunova, both this volume).

The base of Unit 5, immediately overlying basalt at 701 meters, shows no effects of contact metamorphism. However, the continuity of the core is broken at the sediment-basalt contact, and metamorphosed sediments may have been lost.

Interpretation of the Sedimentary Record

The brown claystones, iron-rich claystones, and nannofossil claystones comprising Units 4 and 5 appear to be Danian to Maestrichtian or older. They bear a striking resemblance to the Line Islands Oceanic Formation described by Cook (1972) in the equatorial Pacific Ocean. Both Units 4 and 5 and the Line Islands Formation lie directly above basalt and are characterized by dusky yellow-brown and brown claystones containing amorphous iron and manganese oxides with lesser amounts of volcanogenic minerals. The enrichment of metallic oxides in this time-transgressive unit may be caused by precipitation from bottom waters enriched in metals by submarine volcanic hydrothermal exhalations near spreading centers. Sediments of this type have also been found on the East Pacific Rise in regions

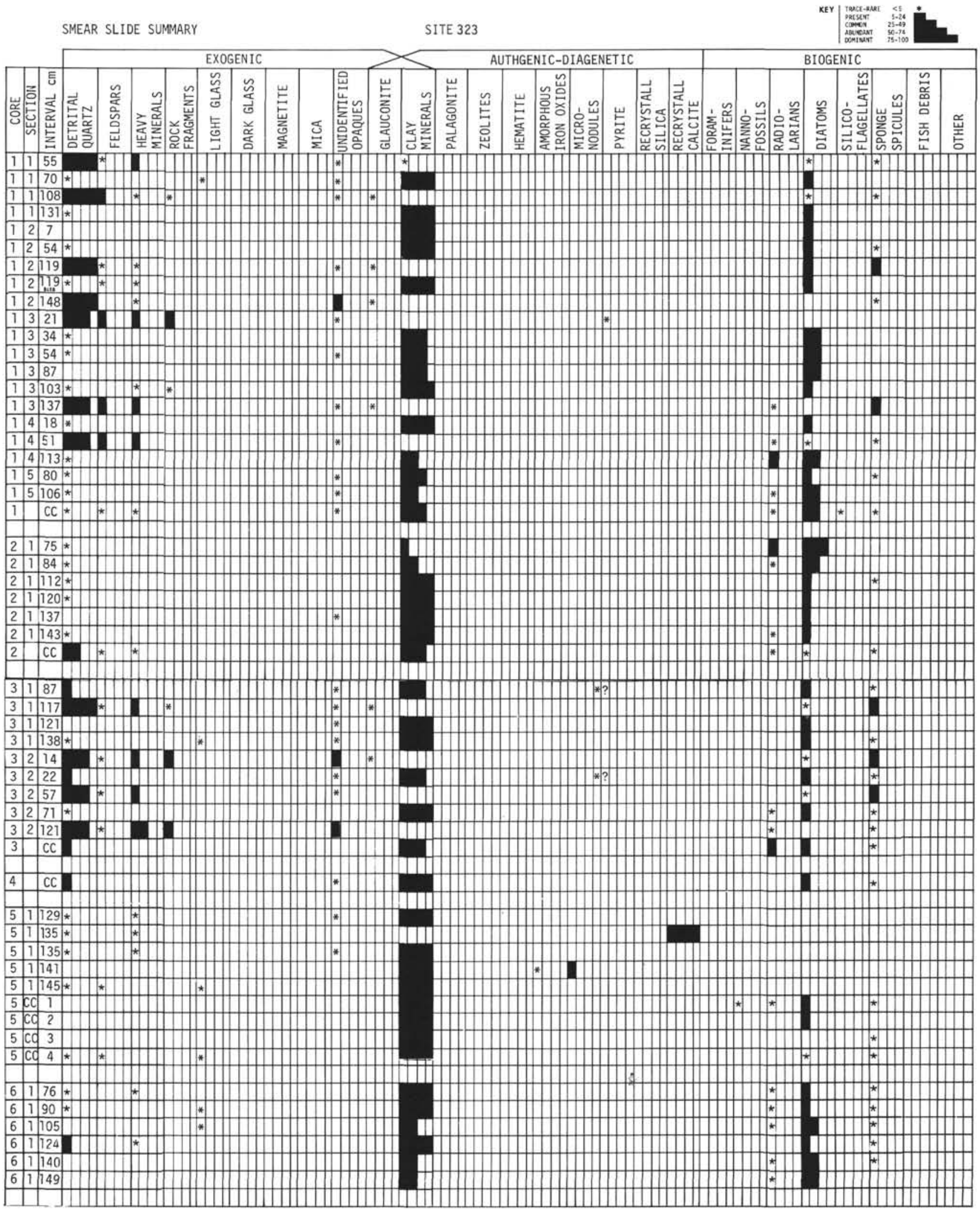

Figure 6. *Estimate of principal components from smear slides, Site 323.*

of high heat flow (Böstrom and Peterson, 1966). The absence of terrigenous detritus and the fine laminations and extensive burrow mottling in Units 4 and 5 indicate pelagic sedimentation in an isolated quiescent environment.

In the bottom of Core 15 and the top of Core 16 both the diverse Danian benthonic foraminiferal assemblage and the good preservation and abundance of Danian nannoplankton indicate a shallow depositional environment (middle to upper bathyal, <2000 m). It is

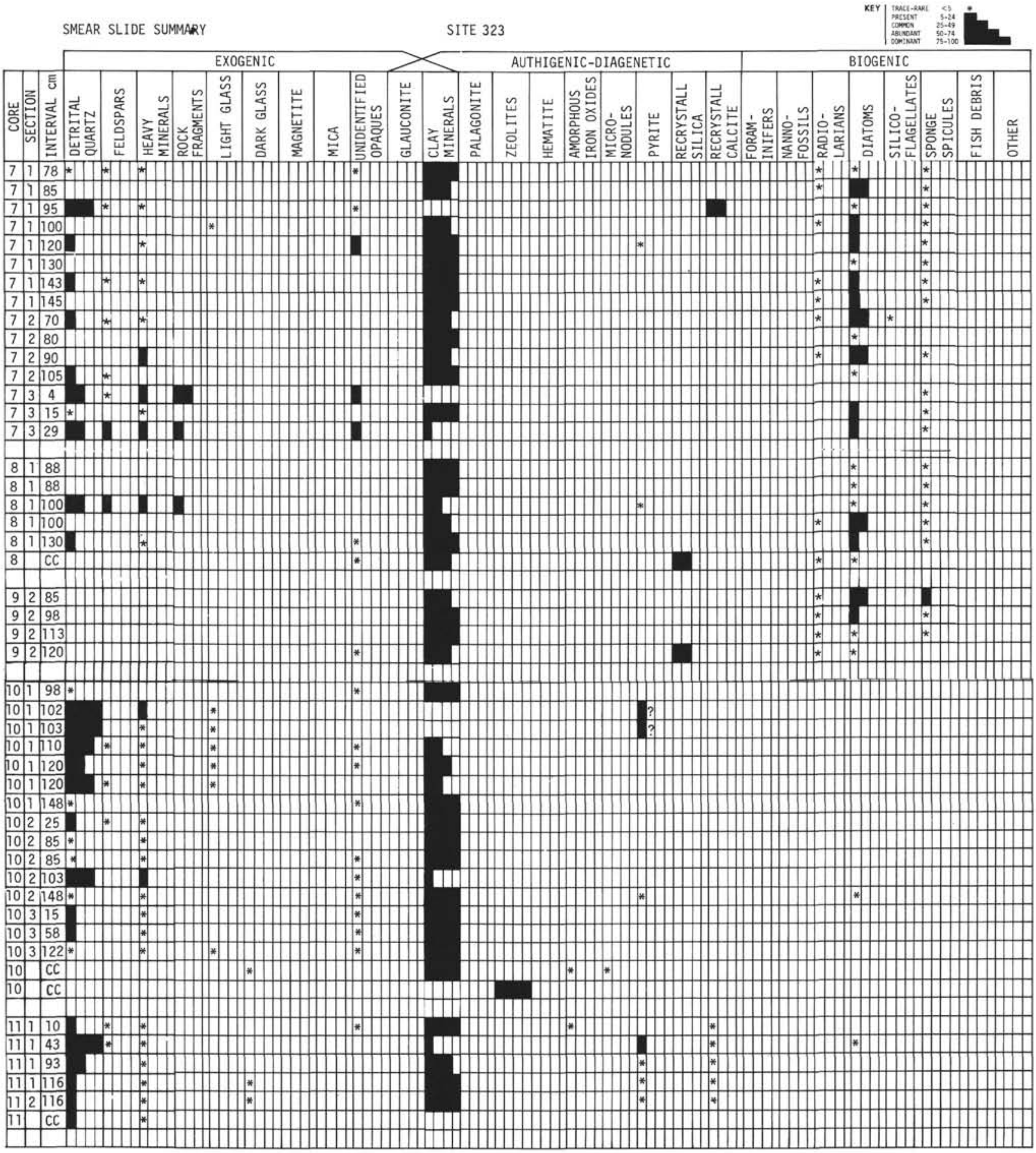

Figure 6. *(Continued).*

likely that the basaltic sill beneath Unit 5 was intruded near the spreading center that formed the underlying crust. If this was a normal, shallow, spreading ridge crest, then the sea floor could have been relatively shallow (1000-2000 m) in Danian time, and Units 4 and 5 were deposited in the middle to upper bathyal range of 200-2000 meters.

Unfortunately, we have little knowledge at present of the variation in level of the carbonate compensation depth in these high latitudes during late Cretaceous and early Tertiary. However, if the above interpretation of depth of deposition is correct, the carbonate distribution in Unit 5 suggests a shallow CCD during the Maestrichtian, CCD depression in the Danian, and a shoaling CCD (supplementing the effect a subsiding sea floor) after the early Paleocene. This temporal variation of the CCD is nearly the reverse of fluctuations deduced in the equatorial Pacific.

Significant changes occur in the sedimentary environment at the base of the lower Miocene Unit 3. Accumulation rates increase to roughly 1.5 cm/1000 yr, and an influx of terrigenous detritus (quartz, feldspar,

Figure 6. *(Continued)*.

TABLE 2
Summary of Lithologic Units, Site 323

Unit	Lithology	Subbottom Depth (m)	Unit Thickness (m)	Age
1	Gray unconsolidated sandy silt, diatom clay, diatom ooze	0-266	266	Holocene to Miocene
2	Gray diatom claystone and chert	266-507.5	241.5	Middle to early Miocene
3	Gray claystone devoid of biogenic silica	507.5-638	130.5	Early Miocene
4	Fe-claystone, nanno-claystone	638-666.5	28.5	Danian
5	Brown zeolitic claystone	666.5-701	34.5	Maestrichtian
6	Basalt	701-731	>30	–

heavy minerals, and probably clays) is apparent. The paucity of feldspars and absence of rock fragments in this unit indicate that the sediment is compositionally mature. Furthermore, there is little variation in the relative abundance of the various mineral components (notably heavy minerals) throughout the entire section, suggesting a constant sediment supply from a single source. The mechanism of sediment emplacement/transport is uncertain. No textural peculiarities or primary sedimentary structures were observed which would distinguish turbidites from bottom-current-deposited material (contourites). The reducing conditions suggested by the presence of pyrite argue against significant bottom-water circulation, although the pyrite could be formed in microreducing conditions below the sediment surface. Deposition of clay and fine silt from a nepheloid layer associated with a newly developed flow of bottom water appears to offer the most reasonable mechanism for the deposition of Unit 3.

Biogenic calcite and silica are also largely absent in this unit. Whether this is indicative of a shallow carbonate compensation level and/or reduced surface productivity is unknown at present. Recrystallized calcite is scattered throughout the unit in amounts from 5% to 25%. This calcite may have been derived from solution of calcareous tests, suggesting at least some surface productivity.

The mineralogical changes from Unit 3 to Unit 2 include disappearance of pyrite and the influx of common siliceous organisms. Both of these changes may relate to the intensification of circulation of surface and bottom water, which in turn may correlate with the first effective circulation of the Antarctic Circumpolar Current. The oceanic barrier to circumpolar circulation between New Zealand and Antarctica was apparently first breached in the Oligocene (Houtz et al., 1975); a second major barrier probably also existed between South America and Antarctica, but we are unable to say as yet when this barrier became sufficiently fragmented to allow circumpolar circulation.

The cherts (silicified claystones) at the base of Unit 2 have apparently resulted from the intrastratal remobilization and precipitation of biogenic silica. The degree of lithification and sonic velocities of the cherts are greater in the more abundant, shallow cherts where biogenic silica is most common, and a gradient of decreasing silica appears to exist towards the bottom of Unit 2.

Other than the cherts, Units 2 and 1 are quite similar in mineralogy, and both contain a less mature mineral assemblage than Unit 3. Feldspars and rock fragments are commonly observed. Displaced shallow-water diatoms, shell fragments (Core 4), and the immaturity of the mineral assemblage indicate rapid emplacement of the sediments by turbidity currents. The fine grain size of the Unit 2 claystones and the variable but generally coarser grain size of Unit 1 sediments (sands are also indicated by poor core recovery and hole instability) suggest that Site 323 has received turbidites first by distal deposition and subsequently as more proximal deposits. This effect relates simply to the gradual development of the Antarctic continental rise which later allowed higher energy turbidity currents to reach the area.

Unfortunately, the coring process has obscured primary structures in the unconsolidated Unit 1 sediments, and no structures are observed in either Unit 1 or 2 that are diagnostic of turbidity-current deposition. The silts and fine sands cored in these units are often well sorted and have probably been reworked by bottom currents.

GEOCHEMISTRY

Sediments

The sediments above 638 meters are dominated by terrigenous material. Diatoms disappear below 400 meters, apparently due to recrystallization to porcellanite and siliceous claystones. In addition to the formation of porcellanite around 450 and 500 meters, the alteration of volcanic material is significant (Anderson and Lawrence; Kastner, this volume).

The clay mineral suite below 638 meters is dominated by illite/smectite, with >80% smectite. This material is associated with clinoptilolite and possibly authigenic feldspar (Zemmels and Cooke; Drever, this volume). There is a variance in opinion as to the genesis of this secondary mineral assemblage (see Geochemistry Introduction and Summary, this volume). Of interest is the decrease in the K/Al ratio in the clay fraction and the constancy of this ratio in the bulk sediment. This evidence can again be used with equal strength in the case for or against diagenetic alteration of terrigenous material.

Of considerable interest are the high Fe/Mn-bearing sediments between 638 and 669 meters, which sandwich two or three rather thin layers of nannofossil chalk. These sediments are also enriched in trace metals (Bogdanov et al.; Drever, both this volume) as well as in strontium and phosphorus. Barium increases toward basement, below this metal-enriched zone. Bogdanov et al. suggest a hydrothermal origin of this material, as a result of the upward motion of waters of hydrothermal origin through the basalts and overlying sediments. These fluids would first lose their Ba, due to barite precipitation. Subsequently, oxidation and precipitation of Fe and Mn, as well as the other metals, would occur in the oxidizing upper sediment layers. Although speculative in nature, this interpretation is in agreement with the observation of possible "hydrothermal" alteration in the underlying basalts (Kastner, this volume).

Interstitial Water

Interstitial water concentration gradients of calcium, magnesium, and potassium suggest three main reaction zones: in the upper 100 meters of Pleistocene/Pliocene sediments; in the layers between 450-500 meters; in the basal sediments and/or underlying basalts. Reactions in the upper zone may involve alteration of terrigenous material. In the chert zones between 450-500 meters the recrystallization of biogenous silica to opal-CT is associated with alteration of volcanic debris (source for calcium) to smectite (sink for magnesium) and authigenic K-feldspar (sink for potassium). In the lower

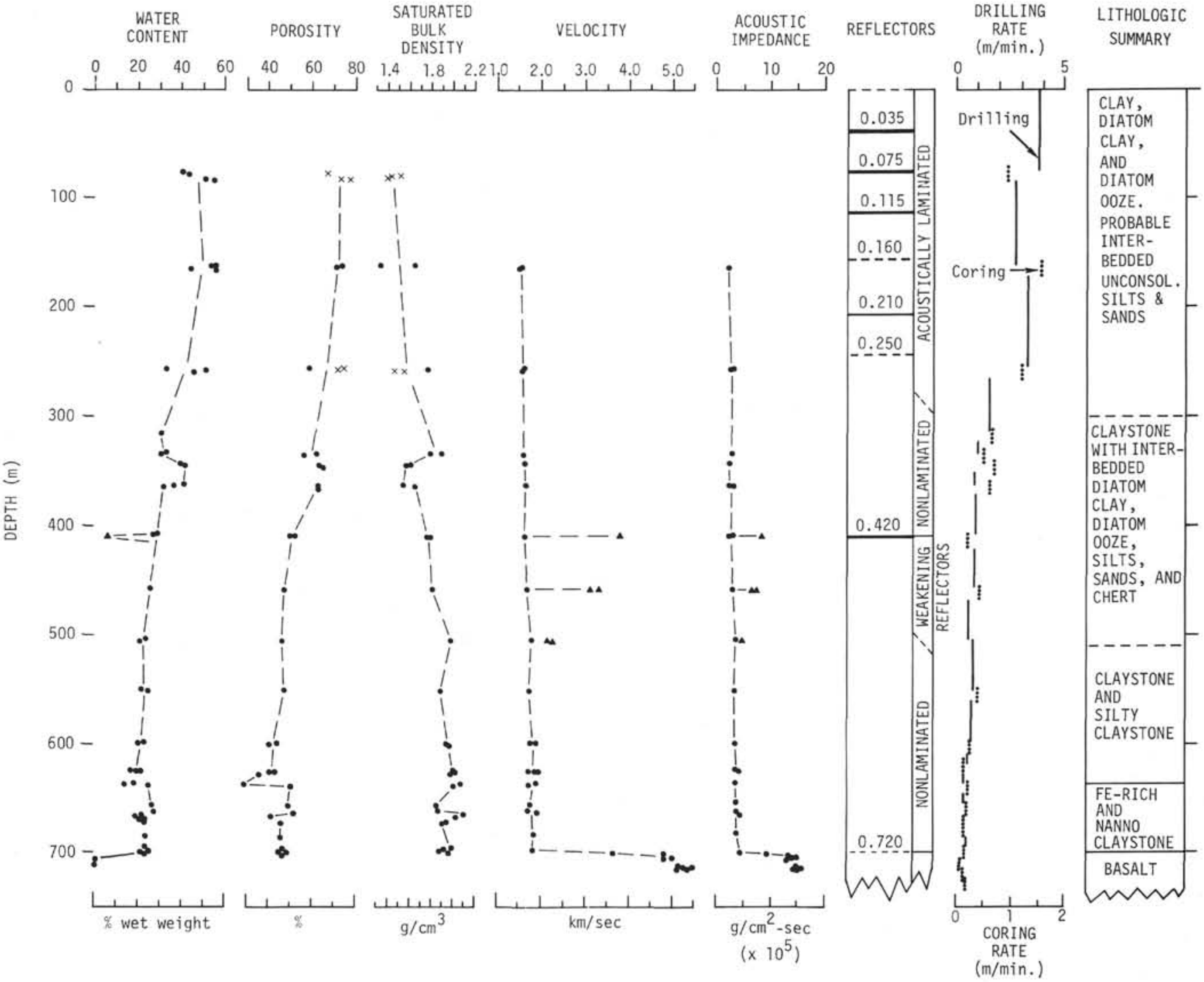

Figure 7. *Summary of physical properties, acoustic character, and lithology of sediments at Site 323. Velocities are those measured perpendicular to bedding or on unoriented samples. Relative strength of reflectors is indicated by heavy solid lines (strongest) to dotted lines (weakest), and the depth of each reflector (in seconds reflection time) is indicated. Values determined by the syringe technique are marked by x; silicified claystones (cherts) are indicated by triangles.*

TABLE 3
Summary of Physical Properties, Site 323

Sample (Interval in cm)	Estimated Depth (m)	Velocity (km/sec)		GRAPE Special 2-Min Count Sat. Bulk Density (g/cc)		Sat. Bulk Density (g/cc)	Wet Water Content (%)	Grain Density (g/cc)	Porosity (%)	Impedance (g/cm² sec) × 10⁵	Lithology Remarks
		∥ Beds	⊥ Beds	∥ Beds	⊥ Beds						
1-1, 125-128	76.75						42				Disturbed diatom clay
1-3, 94	79.44					1.52[a]	44	2.60[a]	68[a]		Detrital diatom clay
1-5, 5	81.55					1.42[a]	52	2.59[a]	74[a]		Disturbed clayey, diatom ooze
1-5, 37	81.87					1.39[a]	56	2.81[a]	78[a]		Disturbed clayey, diatom ooze
2-1, 79-81	161.79						55				Clayey diatom ooze
2-1, 79-81	161.79					1.32	56	2.23	74		Clayey diatom ooze
2-1, 84	161.84	1.58								2.09[b]	Clayey diatom ooze
2-1, 93-98	161.93						56				Clayey diatom ooze
2-1, 106-108	162.06					1.65	43	3.26	71		Diatom-rich clay
2-1, 120	162.20	1.52		1.56						2.42	Diatom-rich clay
3-1, 106-107	257.06					1.77	33	2.88	59		Silty claystone
3-1, 108	257.08	1.69	1.67	1.86						3.16	Silty claystone
3-2, 23	257.73	1.73	1.66	1.87	1.82					3.05	Silty claystone
3-2, 73	258.23					1.45[a]	52	2.79[a]	75[a]		Diatom
3, CC	259.10					1.54[a]	47	2.98[a]	73[a]		Diatom
4, CC	316.10						31				Disturbed clay
5-1, 141	333.41	1.67	1.62	1.82	1.82	1.90	33	3.39	62	3.02	Claystone
5, CC	333.55		1.63		1.81	1.79	31	2.79	66	3.03	Claystone
6-1, 140	342.90					1.61	40	2.68	64		Clayey diatomite
6-1, 144	342.94	1.73	1.69	1.60	1.58					2.70	Clayey diatomite
6, CC	343.05	1.73	1.66	1.62	1.62	1.57	42	2.65	66	2.74	Clayey diatomite
7-1, 140	361.40	1.71	1.65	1.62	1.64	1.53	41	2.46	63	2.67	Diatom-rich claystone
7-2, 113	362.63	1.75	1.66	1.74	1.68	1.66	37	2.46	63	3.16	Claystone gall
7-3, 31-46	363.31						32				Disturbed clay
8-1, 106	409.06	1.67		1.78		1.76	29	2.58	52	3.04	Claystone
8-1, 146	409.46	1.76	1.67	1.77	1.81	1.79	29	2.61	51	2.76	Claystone
8, CC	409.55						28				Claystone
8, CC	409.60						6				Chert
8, CC	409.65	3.79		2.10						8.15	Chert
9-2, 100	458.00	1.77	1.71	1.83	1.87	1.81	26	2.55	48	3.20	Claystone
9-2, 133	458.33	3.77	3.13	2.11	2.09					6.67	Chert
9, CC	458.55	3.33		2.08						6.99	Chert
10-1, 142	504.42	1.88	1.76	1.98	2.00	1.98	24	2.86	47	3.50	Clayey siltstone
10-3, 0-12	506.00						22				Claystone
10-3, 62	506.62	2.51	2.12	2.03	1.99					4.24	Chert
10-3, 124	507.24		2.21		1.95					4.42	Chert
11-1, 0-10	550.50						22				Silty claystone
11-1, 67	551.17		1.71		1.86	1.89	26	2.72	48	3.27	Silty claystone
12-1, 101	599.01	1.88	1.76	2.07	1.98	1.94	23	2.69	44	3.56	Claystone
12-1, 135-150	599.35						20				Disturbed clay
12-2, 45	599.95	1.94	1.88	2.06	1.98	1.96	21	2.61	40	3.78	Claystone
13-5, 135-150	624.35						17				Silty claystone
13-5, 140	624.40	1.92	1.84	2.07	2.07	2.01	20	2.72	41	3.88	Claystone
13-5, 145	624.40	1.82	1.73		2.06	2.02	21	2.78	43	3.62	Clayey siltstone
13-6, 138	625.88	1.97	1.93	2.02	2.10	1.99	18	2.55	36	4.17	Claystone
14-1, 140-150	637.40						18				Claystone
14-2, 34	637.84	1.96	1.89	2.13	2.07	2.08	14	2.54	30	3.69	Claystone
14, CC	639.05	1.80	1.72	1.96	2.04	2.00	25	3.03(?)	51	3.50	Fe claystone
15-1, 79	656.04	1.82	1.75	1.99	1.99	1.84	27	2.67	50	3.60	Fe claystone
15-5, 48	661.73	1.80	1.70	1.95	2.02	1.86	28	2.79	52	3.54	Fe claystone
15-5, 140-150	662.65						22				Fe claystone
16-1, 31	664.81					2.10	19	2.86	41		Nanno claystone
16-1, 38	664.88	2.06	1.91	2.16	2.15					4.24	Nanno claystone
16-2, 63-65	668.13					2.02	20	2.73	41		Fe claystone
16-3, 135-150	668.85						24				Fe claystone
16-3, 135-150	668.85						22				Fe claystone
16-4, 148	670.48					1.92	24	2.70	46		Fe claystone
17-6, 143	682.93		1.84		1.95	1.90	25	2.67	46	3.72	Fe claystone
18-3, 19-21	696.19					1.99	23	2.86	47		Fe claystone
18-4, 22	697.72					1.91	24	2.66	45		Fe claystone
18-4, 76	698.26	1.90	1.82			1.87	26	2.67	48		Zeolitic claystone
18-4, 135-150	698.85						21				Zeolitic claystone
18-5, 125	700.25		1.80		2.36	1.97	24	2.84	47	4.34	Fe zeolitic claystone
18-6, 18	700.68	3.63	3.65		2.54					9.23	Basalt
19-1, 112	703.62	4.80	4.80	2.77						13.25	Basalt
19-2, 4	704.04	4.96	4.99		2.91					14.42	Basalt
19-3, 65	706.15	4.86	4.80	2.79	2.85					13.73	Basalt
19-4, 85	707.85	4.62		2.68						12.57	Basalt
19-4, 85	707.85	4.72		2.63						12.84	Basalt
20-1, 140	713.40	5.18		2.84						14.71	Basalt
20-1, 140	713.40	5.11		2.86						14.51	Basalt
20-2, 132	714.82	5.24		2.82						14.67	Across thin crack in basalt
20-2, 132	714.82	5.48		2.80						15.34	Basalt
20, CC	715.40	5.36		2.82						14.95	Basalt
20, CC	715.40	5.12		2.81						14.28	Basalt

[a] Syringe values.

[b] Calculated using bulk density from 2-1, 79-81 cm.

basal sediments there is evidence of a secondary mineral assemblage as is evident from a highly expandable illite/smectite (>80% smectite), clinoptilolite, and K-feldspar (?). Underlying basalts show alteration products: well-crystallized smectite, celadonite, and calcite. This is interpreted as evidence of influence from interactions with waters of hydrothermal origin. These waters may also have been responsible for the enrichment in barium, iron, and manganese in the overlying sediments. Depletions in δO^{18} of the interstitial waters suggest substantial ongoing alteration reactions in the basal sediments or underlying basalts.

The geochemistry of sediments and interstitial water is discussed and data are presented in greater detail in the Geochemistry section of this volume.

PHYSICAL PROPERTIES

Diatoms have a pronounced effect in increasing the porosity and water content in the upper 360 meters of sediments at Site 323 (Figure 7 and Table 3). Samples analyzed above 250 meters were all diatomaceous and several nondiatomaceous as well as diatomaceous samples cored between 250 and 360 meters were tested. At 250 meters the diatomaceous and nondiatomaceous samples differed by about 15% in both water content and porosity, but the difference decreased with depth so that porosities were essentially the same at 360 meters, and water contents varied by only about 5%. The decreasing void space with depth may be related to collapse of the diatom-clay lattice and crushing of the frustules. Consolidation tests on diatom oozes were made by Lee (1973); he suggested that at effective stresses exceeding 5-7 kg/cm^2, the crushing of diatom frustules may occur. Of course this stress value is highly variable and is sensitive to the sample's porosity, permeability, composition, grain size distribution, and cementation. In the sediments we studied, the diatoms are imbedded in a fine clay matrix comprising about 75% of the sediment.

In the nondiatomaceous clays, claystones, and siltstones, both porosity and water content show a progressive decrease down to 638 meters. The iron-rich claystones between this depth and basalt at 700 meters have slightly higher, uniform water contents of about 25% and porosities of 45% to 50%. A nannofossil claystone in the middle of this unit has values 3% to 5% lower for both parameters.

The downhole variation in saturated bulk density is grossly complementary to that of water content and porosity (Figure 7). Slight departures from this relationship are probably caused by downhole variations in grain density. The diatomaceous sediments have densities of less than 1.65 g/cm^3, and there is a steady density increase downhole to about 2.0 g/cm^3 at 638 meters. Slightly reduced densities (as low as 1.85 g/cm^3) occur in the iron-rich claystones in the lower 62 meters of the hole, but the nannofossil claystone in this unit has a high density (2.1 g/cm^3).

Measured sonic velocities show a remarkably steady increase with depth, from about 1.5 km/sec at 160 meters to 1.8-1.9 km/sec in the lowest 100 meters. The cherts (silicified claystones) which were encountered below 400 meters show the only marked deviation from this velocity trend. The highest measured velocity of 3.79 km/sec was in the shallowest chert cored, whereas the deeper cherts showed decreasing velocities, with 2.12 km/sec recorded for the silicified claystones at 507 meters. This velocity decrease appears to match a gradient of decreasing silicification downhole.

Velocities measured on basalt samples increased irregularly from 3.65 km/sec in the topmost basalt to a maximum of 5.48 km/sec 14 meters deeper. The lower velocities near the top of the unit may relate to progressive alteration of the basalt (see Vennum, this volume). Static GRAPE measurements indicate that the sample with velocity 3.65 km/sec has a bulk density of 2.54 g/cm^3, compared with densities greater than 2.63 g/cm^3 for deeper samples.

INTERPRETATION OF SEISMIC PROFILES IN VICINITY OF SITE 323

Basalt was encountered at 701 meters subbottom at Site 323. In the *Glomar Challenger* profiler record it correlates with a reflector of moderate amplitude at 0.72 sec beneath the sea floor (Figure 5), indicating an average sediment velocity of 1.95 km/sec. Two sonobuoy profiles recorded by *Eltanin*-42 on the Bellingshausen Abyssal Plain west of Site 323 suggest much lower velocities for the sediment column, but it is apparent from both the reflector correlation and the measured sample velocities (Figure 7) that higher velocities pertain at Site 323.

The major acoustic horizon within the sedimentary sequence lies at 0.42 sec subbottom, is sharp at its upper boundary, and is decreasingly reverberant over the next 0.15 sec (Figures 3 and 5). There is little doubt that this acoustic horizon corresponds to the chert encountered in the hole and first recovered at 409.1 meters. However, the interval velocities calculated using this depth (1.95 km/sec above the chert and 1.94 km/sec from chert to basement) are not consistent with the downhole velocity increase in directly measured samples (Figure 7). Thus it seems likely that the chert recovered at 409.1 meters actually came from a shallower depth in the hole between Cores 7 and 8 (370 to 408 m); this interval was drilled ("washed") with the core barrel in the drill string so it is entirely possible that the chert was encountered here. More reasonable interval velocities are obtained if the first occurrence of chert was at a true depth of, say, 390 meters (1.86 and 2.07 km/sec for the upper and lower intervals, respectively). Silicified claystones interlayered with claystones were recovered down to 507 meters, but the impedance contrast between these two sediment types decreases downhole (Figure 7). This may correlate with the downward-decreasing reverberation noted over these depths in the profiler record (Figure 5).

Except for the acoustic horizon just discussed, reflectors are weak or absent below about 0.3 sec subbottom, and the consolidated sediments below about 300 meters correspond closely to this acoustic interval. The strong basement reflection below the nonlaminated sediments suggests that signal attenuation does not fully account for the absence of reflectors in the overlying sediment.

Only three cores were obtained from the acoustically laminated sediments comprising the upper 300 meters of the sediment column. Impedance contrasts caused by rapid velocity/density changes in the unconsolidated sand, silt, and clay interbeds of this interval account for the reverberant character of sediment in the upper 0.3 sec of the profiler record. Our data are inadequate to identify any individual reflectors within this depth interval.

IGNEOUS ROCKS

Basalt (Lithologic Unit 6) was first recovered at a subbottom depth of 701.0 meters and was cored continuously for 30 meters. Recovery averaged 45% for Cores 19 and 20, but only a few fragments were recovered in the core catcher from Core 21. Approximately 150 cm was recovered from the base of Core 18.

Crustal Age

The oldest overlying sediments at Site 323 are zeolitic brown claystones of Maestrichtian age (70 m.y.). The basalt correlates with the deepest observed seismic reflector, but petrographic evidence suggests that a sill was penetrated and that still older sediments could be present below. The late Cretaceous age from nannoplankton in the overlying sediments (see Biostratigraphy section, this chapter) indicates that true basement lying below the deepest observed reflector is at least 70 m.y. old and is close to the 76 m.y. age suggested by the nearest magnetic anomaly (32?). Ap parent ages of 46-47 m.y.B.P. obtained from K-Ar ratios at this site are anomalously low (Seidemann, this volume).

Petrography

The basalt from Site 323 is dark gray (N3), aphanitic to extremely fine grained, and essentially aphyric although a very few scattered microphenocrysts of plagioclase and pseudomorphic olivine do occur. Most cores are moderately to extensively veined with calcite, and fracture surfaces are coated with smectite and reddish-brown iron oxides. Smectite-filled amygdules (0.5 mm), although nowhere numerous, occur scattered throughout most of the core. No glassy zones were found in the cores, nor was any brecciated basalt or hyaloclastite material recovered.

Microscopic examination of an essentially unbroken 7-meter section from the top of the drilled interval revealed a series of gradational textural changes which may be quite diagnostic of mode of occurrence. The uppermost basalt has an intergranular-intersertal texture. The intersertal matrix contains varioles of plagioclase and minute pyroxene quench crystals. This variolitic zone grades downward through intergranular and pilotaxitic basalt to subophitic and ophitic basalt which make up most of this 7-meter interval. Variolitic plagioclase and pyroxene quench crystals reappear in the basalt recovered from lower cores. This range of textures suggests that a sill was drilled. The virtual restriction of olivine to the lower variolitic zone can be attributed to gravitational settling also within a sill. Variolitic textures are usually found in pillow margins, but have been reported from sills (Wilson, 1960; Garrison, 1972). Pilotaxitic texture is a feature usually found in andesites and is uncommon in more mafic volcanics, although it has been reported from other DSDP basalts (Erlank and Reid, 1974; Thompson et al., 1974).

The origin of the basalt recovered in the core catcher from the lowermost core is problematic. This material has an intergranular to subophitic texture, contains scattered plagioclase phenocrysts up to 4 mm in length, and could have come from the interior of a flow, dike, or sill. The absence of glassy material in the lowermost two cores, and mineralogy and alteration identical to that in the overlying basalt suggest that a second sill was penetrated. Sediment was not recovered in either of the lower two cores, but increased drilling rates suggest that softer material was penetrated.

Subhedral to euhedral labradorite laths (An_{55}) range in length from 100 to 700 μm (average 400 μm), show very little zoning, and are essentially fresh. Plagioclase phenocrysts are blocky, fresh, and very slightly zoned (An_{55-50}). Most are twinned on the Carlsbad law. These grains average 1.5-2 mm in longest dimensions except in samples from Core 21 where they attain a size of 4 mm.

Clinopyroxene grains are anhedral, or in only a few cases subhedral, and mainly occur interstitial to the plagioclase. Phenocrysts (1.5 mm) are uncommon, and these generally occur in small rare glomeroporphyritic clots of 3-5 grains with or without plagioclase. Their average compositions range from calcic augite cores ($Ca_{38}Mg_{32}Fe_{30}$) to subcalcic ferroaugite rims ($Ca_{34}Mg_{26}Fe_{40}$). Groundmass grains are rather variable in composition, but most are subcalcic ferroaugites with a slightly higher Mg/Fe ratio than the phenocryst rims. Many of the plagioclase laths are strongly resorbed where in contact with the groundmass pyroxenes.

Euhedral microphenocrysts of olivine (1.5 mm) comprise 1% of the lower variolitic zone and also occur in the basalt recovered in Core 21. Those in Core 21 are moderately resorbed. Where present these grains have been completely replaced by calcite that is in some cases rimmed and/or veined by iddingsite and/or serpentine. Euhedral magnetite octahedrons and skeletal rods of ilmenite(?) are confined to the groundmass. Traces of apatite occur in about 30% of the thin sections.

Chemistry of Igneous Rocks

The pyroxene compositions, the rarity of olivine phenocrysts, the absence of groundmass olivine, and the resorption of the olivine from Core 21 suggests a tholeiitic composition. Except for a high K_2O content, this sample compares favorably with average mid-ocean ridge basalts (Engel et al., 1965). The anomalously low K-Ar date and high oxidation index suggest that the high potassium content is not a primary feature of the original magma. On a total silica-alkali diagram this sample plots near the boundary between alkalic basalt and tholeiite. Its alkaline tendencies are better displayed on a P_2O_5-TiO_2 diagram where it plots just inside the ocean island tholeiite field. Bass et al. (1973)

have described a possible sill from Site 170, DSDP Leg 17, in the central Pacific that has even stronger alkaline tendencies. The occurrence of possible sills with alkaline affinities in deep oceanic basins indicates that the oceanic crust may be far more "leaky" than was originally assumed.

The rather high total iron (12.07%) and titanium (2.89%), the low magnesium content (5.81%), and low solidification index (27.6) are indicative that considerable fractionation has taken place. Fractionation may have taken place either within the sill or in a shallow underlying reservoir. Normative computations based on the original analysis and those calculated on a volatile-free basis with excess Fe_2O_3 calculated as FeO both contain normative quartz and hypersthene and lie in the oversaturated tholeiite field in Yoder and Tilley's (1962) normative classification.

BIOSTRATIGRAPHY

Foraminifers

Cores 1 through 9 were barren of foraminifers although rare arenaceous specimens were observed in Sample 10, CC to Core 13. The fauna is similar to that observed at Site 322. It is characterized by *Cribrostomoides*, *Glomospira*, *Recurvoides*, *Reophax*, *Rhabdammina*, and *Rhizammina*. The stratigraphically important species *Haplophragmoides carinatus* and *Cyclammina* cf. *japonica* indicate an ? Oligocene to early Miocene age.

The composition of foraminiferal fauna shows a marked change within Core 14. The species *Bolivinopsis spectabilis* and *Rzehakina* spp. occurs in the interval from Core 14, Section 2 to Core 15, Section 4, indicating a relationship to the underlying Paleocene sediments. A sedimentary hiatus between the Paleocene and the ?Oligocene-early Miocene is therefore assumed.

Calcareous foraminifers are preserved in Core 15, Section 5 through Core 16, Section 2 and are accompanied by a higher diversity in arenaceous foraminifers. A large part of the fauna consists of planktonic forms. The species *Globigerina edita*, *G. fringa*, *G. triloculinoides*, *Globoconusa daubjergensis*, and *Chiloguembelina crinita* indicate a Danian age, assignable to the *Globigerina edita* Zone.

Below this unit and down to the basement (Core 18, Section 6) once again only arenaceous foraminifers are present. It is not possible to recognize the Cretaceous-Tertiary boundary based on the observed species. Characteristic species are: *Bolivinopsis spectabilis*, *Glomospira* spp., *Hormosina ovulum*, *Kalamopsis grzybowskii*, *Nodellum velascoense*, and *Rzehakina* spp.

Calcisphaerulidae

The occurrence of Calcisphaerulidae in Tertiary sediments is first noted in sediments of Site 323. They are abundant and occur with the Danian calcareous foraminifers from Core 15, Section 5 to Core 16, Section 2. Four new species are described: *Pithonella antarctica, P. bollii, P. fusiformis,* and *P. titanoplax* (see Rögl, this volume).

Nannoplankton

At Site 323 calcareous nannoplankton were first observed in Core 15, Section 6. All cores above this level are barren of nannoplankton. In the calcareous parts of Core 15, Section 6 to Core 16, Section 2, nannofossils are common, but are mostly fragmented. Only a few complete specimens which are poorly preserved are present.

From Core 15, Section 6 to the upper part of Core 16, Section 2, a flora typical of *Chiasmolithus danicus* Zone (upper Danian) was found including *C. danicus*, *Cruciplacolithus tenuis*, *Ericsonia subpertusa*, *Coccolithus cavus*, *Markalius astroporus*, and *Thoracosphaera* spp.

In the lower part of Core 16, Section 2, *Chiasmolithus danicus* is absent. At 50-51 cm of this section the flora is composed nearly entirely of a single dominant species: *Cruciplacolithus tenuis*. All of the lower part of Core 16, Section 2 is placed within the *C. tenuis* Zone (middle Danian). A few reworked Upper Cretaceous species were found throughout the calcareous sections.

Below Core 16, Section 2, all sections are essentially barren of calcareous nannoplankton except for Sample 17, CC, in which fragments of *Cribrosphaerella ehrenbergii* and *Watznauria barnesae* were found. (Similar fragments were also observed in Core 18, Section 4, but are most probably contaminants.) Sample 17, CC is thus most probably late Cretaceous in age. The Cretaceous-Tertiary boundary lies somewhere between Core 16, Section 2 and this level.

The parts of the Site 323 sequence placed here within the middle and upper Danian also contain the *G. eugubina* Zone (foraminiferal zone) of the lower Danian. Elsewhere the *G. eugubina* Zone has only been correlated with the *Markalius astroporus* nannoplankton Zone of the lower Danian. This discrepancy is difficult to explain since no evidence of extensive reworking or contamination was seen. It can only be assumed that *G. eugubina* has a longer range in these latitudes.

Radiolarians

At Site 323, 18 sediment cores were taken at periodic intervals with a total recovered length of 76.7 meters.

Sample 1-1, 129-131 cm through Sample 2, CC contains a poorly to moderately preserved Pliocene radiolarian assemblage. Although abundances of species fluctuate from common to rare, both the *Helotholus vema* Zone of Chen (1975) (Samples 323-1-2, 107-109 cm through 323-1, CC), and the Tau Zone of Hays and Opdyke (1967) (Samples 323-2-1, 65-67 cm through 323-2, CC) are recognized (Table 4).

Core 3, Section 1 and Core 3, Section 2 contain a few, moderately well preserved radiolarians which are long ranging and diagnostic of a Miocene age. Samples 323-3-2, 130-132 cm and 323-3, CC also contain numerous specimens of orosphaerid (spines only) and collosphaerid radiolarians.

A typical middle Miocene radiolarian assemblage which is well preserved occurs in Sample 3, CC. Common specimens representing the lower portion of the *Antarctissa conradae* Zone of Chen (1975) are present.

Distinctive species represented are (in order of decreasing abundance) *Cyrtocapsella tetrapera* (30%-40% of the entire fauna), *Lychnocanoma sphaerothorax*, *Antarctissa conradae*, *Prunopyle hayesi*, *Eucyrtidium cienkowskii* sp., *Actinomma tanyacantha*, *Dendrospyris megalocephalis*, *Cyrtocapsella* (?) *cornuta*, *C. isopera* (rare), *Amphistylus angelinus*, and *Sethoconus* sp. (Table 4).

Samples 4, CC through Core 6-1, 118-121 cm are essentially barren except for orosphaerids and a few of the more resistant high latitude Miocene radiolarians which include *C. tetrapera*, *P. hayesi*, *L. sphaerothorax*, and *A. angelinus*. None of the previously established radiolarian zones could be recognized within this interval.

The material recovered between Samples 323-6, CC and 323-8-1, 98-100 cm is middle Miocene in age. Preservation and abundance of specimens vary depending on the sediment lithologies. Based upon the co-occurrence and relatively high abundances of *Lophocyrtis golli*, *Lophocyrtis regipileus*, and *Eucyrtidium punctatum* group, the presence of *Cyrtocapsella isopera*, and the absence of *Actinomma tanyacantha*, this interval is assigned to the upper portion of the *Spongomelissa dilli* through the *Calocyclas disparidens* zones of Chen (1975) or early middle Miocene. Other species occurring within this interval include *Prunopyle hayesi*, collosphaerids, orosphaerids, *Eucyrtidium cienkowskii* group, *Amphistylus angelinus*, *Dendrospyris haysi*, *Sethoconus* sp., *Cyrtocapsella tetrapera*, and *Stylacontarium bispiculum*.

Middle Miocene index species, *Spongomelissa dilli*, *Calocyclas disparidens*, and *Thyrsocyrtis clausa*, were not recognized in any of the 11 samples analyzed from Cores 6 through 8, suggesting that the middle Miocene zonal scheme proposed by Chen (1975) may need some revision or redefinition in order for it to be applicable throughout the entire Southern Ocean.

Thirty-eight samples examined between Samples 323-8, CC and 323-18-2, 138-140 cm are entirely barren of radiolarians.

Common, but poorly preserved Cretaceous radiolarians were found in Samples 323-18-3, 63-65 cm through 323-18-6.

The siliceous tests are completely recrystallized, and only limited morphological characteristics are preserved (test outline, number of segments). A high percentage of the specimens examined belong to the genus *Dictyomitra* Zittel (1876), but species recognition is impossible due to the poor state of preservation.

Diatoms

Diatoms occurring in the interval from 323-1-1, 60-61 cm to 323-10-3, 47-48 cm are generally well to moderately well preserved and have moderate to high species diversity. The assemblage belongs to the Antarctic-Subantarctic assemblage of Jousé, Kozlova and Muhina (1971). Detailed climatical interpretations, however, are not possible because the section was not completely cored. Below 323-10-3, 47-48 cm diatoms are poorly preserved. Certain diatoms, including *Coscinodiscus* cf. *symbolophorus fossilis*, *Actinocyclus ehrenbergii*, and *Charcotia actinochilus* in cores containing Cretaceous foraminifers (323-16-4, 323-17-4, 323-17-1, 323-18-4) suggest downhole contamination inasmuch as a flora with almost identical species was encountered at 323-3-2, 32-33 cm. Moreover, diatoms have not previously been found in Cretaceous recrystallized radiolarian skeleton-bearing sediments.

The occurrence of a diatom assemblage below the chert-bearing sediment sequence at 323-8, CC (for example in Sample 323-10-3, 47-48 cm) is also interpreted as downhole contamination. Generally the diatom assemblage disappears gradually as opal is mobilized to form chert. All samples containing diatoms below the chert layers are mixed with younger downwashed material. The chert contained a few ghost shapes of radiolarian skeletons and is most probably of biogenic origin.

Displaced shallow-water benthonic and/or neritic species were found in almost all samples but with a considerable increase at 323-8, CC, 323-9, CC, 323-10-3, 47-48 cm, 323-11-2, 69-70 cm including mass occurrences of *Melosira sulcata*, *Stephanopyxis turris*, *Diploneis* sp., *Cocconeis*, and various other species.

Displaced fresh-water diatoms occur at 323-8, CC including *Pinnularia nobilis*, which inhabits fresh-water lakes in temperate climatic areas. This occurrence may serve as a link in the interpretation of Antarctic climatic during Miocene time.

The following biostratigraphic interpretation is tentative due to intermittent coring, poor recovery, and drilling displacement and disturbance; some important intervals were totally disturbed and sediment pieces were sorted on the basis of color.

Pliocene sediments were encountered from Samples 323-1-2, 55-56 cm to 323-2-1, 46-47 cm and are characterized by abundant *Nitzschia interfrigidaria*, *Nitzschia praeinterfrigidaria*, and *Cosmiodiscus insignis*. The occurrence of these species indicates that all samples above 323-1, 69-70 cm belong to the *Nitzschia interfrigidaria* Zone of McCollum (1975) which has been dated on the basis of correlation to the paleomagnetic stratigraphy and to the radiometric time scale as 2.8-3.65 m.y.B.P. Samples below 323-1-4, 109-110 cm to approximately 323-2-1, 46-47 cm are in the *Nitzschia praeinterfrigidaria* Zone of McCollum (1975) which has been dated by correlation to the paleomagnetic stratigraphy and the radiometric time scale as 3.65 — approximately 4.5 m.y.B.P. Thus, this boundary is very close to the Miocene-Pliocene boundary which is correlated to the boundary between magnetic epoch 5 and the reversed Gilbert epoch.

Samples from Core 3 are tentatively placed into the *Denticula hustedtii* Zone and *Denticula hustedtii-Denticula lauta* zones of McCollum (1975). These are correlative to the *Hemidiscus karstenii*, *Coscinodiscus yabei* zones (this paper) and are correlated to North Pacific Diatom Zones XVII/XVIII of Schrader (1973). These zones are of lower upper Miocene age and are approximately 10-12 m.y.B.P. on the radiometric time scale. Samples from Cores 4 through 7 are placed into the *Denticula antarctica-Coscinodiscus lewisianus* Zone of McCollum (1975) which is of lower middle Miocene age. This interpretation is sustained by the co-occurrence of *Raphidodiscus marylandicus* which is

TABLE 4
Occurrence of Radiolarians at Site 323

Species Sample (Interval in cm)	Abundance	Preservation	Age	Zone	*Antarctissa denticulata*	*A. strelkovi*	*A. conradae*	*A. antedenticulata*	*Stylatractus neptunus*	*Stylatractus universus*	*Stylodictya validispina*	*Lithelius nautiloides*	*Spongotrochus glacialis*	*Spongodiscus osculosus*	*Cornutella profunda*	*Saccospyris antarctica*	*S. conithorax*	*Theocalyptra bicornis*	*Prunopyle tetrapila*	*P. titan*	*P. hayesi*	*Peripyramis circumtexta*	*Collosphaeridae*	*Orosphaeridae*	*Eucyrtidium calvertense*	*E. cienkowskii* group	*E. punctatum* group	*Clathrocyclas bicornis*	*Desmospyris spongiosa*	*Helotholus vema*	*Siphocampe aquilonaris*	*Acanthodesmiidae*	*Triceraspyris coronatus*	*Lychnocanoma grande rugosum*	*Lychnocanoma sphaerothorax*	*Amphistylus angelinus*	*Dendrospyris haysi*	*D. megalocephalis*	*Lophocyrtis golli*	*Lophocyrtis regipileus*	*Druppatractus* sp.	*Saturnalis circularis*	*Sethoconus* sp.	*Cyrtocapsella tetrapera*	*C. cornuta* (?)	*C. japonica*	*C. isopera*	*Eucyrtidium* sp. aff. *E. inflatum*	*Actinomma tanyacantha*	*Stylacontrarium bispiculum*	*Lithomelissa* sp. C.
323-1-1, 74-76	–	–																							Barren																										
323-1-1, 129-131	R	M			R	–	–	–	F																																										
323-1-2, 29-31	R	P			–	–	–	–	–	–	–	–	–	–	–	–	–	–	–	–	–	–	–	–	R																										
323-1-2, 57-59	R	P			–	–	–	–	R	–	–	–	–	–	–	–	–	–	–	–	–	–	–	–	–	–	–	–	–	–	–	–	–	–																	
323-1-2, 107-109	C	M			C	C	–	+	R	–	R	R	C	F	R	R	–	–	–	+	–	–	–	–	F	–	–	R	C	R	–	–	–	R																	
323-1-2, 139-141	R	M			R	–	–	–	R	–	R	R	R	R	–	–	–	–	–	–	–	–	–	–	R	–	–	R	R	R	–	–	–	–																	
323-1-3, 14-16	F	M			F	R	–	–	–	–	–	R	F	R	R	R	–	R	–	+	–	–	–	–	R	–	–	–	R	R	–	–	–	–																	
323-1-3, 42-44	R	P			R	R	–	–	–	–	R	–	–	–	–	R	–	–	–	–	–	–	–	–	–	–	–	–	–	+	–	–	–	–																	
323-1-3, 67-69	R	P			–	–	–	–	R	–	–	–	–	–	–	–	–	–	–	–	–	–	–	–	–	–	–	–	–	–	–	–	–	–																	
323-1-3, 104-106	R	M			–	–	–	–	–	–	–	–	–	–	–	–	–	–	–	–	–	–	–	–	R	–	–	–	–	–	–	–	–	–																	
323-1-4, 16-18	–	–																							Barren																										
323-1-4, 71-73	R	M			–	–	–	–	R	–	–	–	R	–	–	–	–	–	R	–	–	–	–	–	R	–	–	–	R	–	–	–	–	–																	
323-1-4, 111-113	F	M			R	R	–	–	F	–	–	–	C	F	–	–	–	–	R	–	–	–	–	–	C	–	–	–	–	–	–	–	–	–																	
323-1-4, 142-144	C	M			R	R	–	–	F	R	–	R	F	F	–	–	–	–	R	+	–	–	–	–	C	–	–	R	F	–	–	–	–	–																	
323-1-5, 23-25	F	M			–	–	–	–	F	–	–	–	F	F	–	–	–	–	F	+	–	R	–	–	C	–	–	+	R	–	–	–	–	–																	
323-1-5, 65-67	R	M			–	–	–	–	–	–	–	–	F	F	–	–	–	–	–	–	–	–	–	–	C	–	–	–	R	–	–	–	–	–																	
323-1-5, 109-111	F	M			–	–	–	–	R	–	–	–	F	F	–	–	–	–	R	–	–	–	–	–	C	–	–	R	R	–	–	–	–	–																	
323-1-5, 125-127	F	M			–	R	–	–	F	–	–	–	F	F	–	–	–	–	–	–	–	R	–	–	C	–	–	–	R	–	–	–	–	–																	
323-1, CC	A	G			C	C	R	R	F	F	–	–	–	–	F	C	R	–	F	C	–	R	–	–	A	–	–	A	C	F	R	C	–	–																	
323-2-1, 65-67	F	P			–	–	–	–	–	–	–	–	F	–	–	–	–	–	–	R	–	–	–	–	F	–	–	–	–	–	–	–	R	F																	
323-2-1, 132-134	C	M			R	R	R	F	F	R	–	R	C	F	R	R	–	–	R	F	–	–	R	–	C	–	–	R	–	–	–	–	C	C	–	–	R	–	–	–	–	–	–	–	–	–	–	–	R	–	–
323-2, CC	C	G			R	F	F	F	–	R	–	R	F	–	R	R	–	R	R	–	R	R	R	–	R	–	–	–	–	–	–	–	R	C	–	–	–	–	–	–	F	R	–	–	–	–	–	R	–	–	–
323-3-1, 98-100	F	M			–	–	R	–	–	–	–	–	R	–	–	–	–	–	–	–	R	–	–	–	–	–	–	–	–	–	–	–	–	–	R	–	–	–	–	–	–	–	–	–	–	–	–	R	–	–	–
323-3-1, 135-137	–	–																							Barren																										
323-3-2, 33-35	F	M			–	–	–	–	–	–	–	–	–	–	–	–	–	–	–	–	F	–	R	–	–	–	–	–	–	–	–	–	–	–	R	–	–	–	–	–	–	–	–	–	–	–	–	–	–	–	–
323-3-2, 80-82	R	M			–		–	–	–	–	–	–	–	–	–	–	–	–	–	–	–	–	–	F	–	–	–	–	–	–	–	–	–	–	–	–	–	–	–	–	–	–	–	–	–	–	–	–	–	–	–
323-3-2, 130-132	F	M			–	–	–	–	–	–	–	–	–	–	–	–	–	–	–	–	C	–	–	C	–	–	–	–	–	–	–	–	–	–	–	–	–	–	–	–	–	–	–	–	–	–	–	–	–	–	–
323-3, CC	C	G			–	–	C	–	–	–	–	–	–	–	F	–	–	R	–	–	C	–	F	C	–	F	–	–	–	–	–	–	–	–	A	R	–	F	–	–		–	R	A	F	R	R	–	F	–	R
323-4, CC	–	–																							Barren																										
323-5-1, 134-137	F	M			–	–	–	–	–	–	–	–	–	–	–	–	–	–	–	–	–	–	–	C	–	–	–	–	–	–	–	–	–	–	–	–	–	–	–	–	–	–	–	–	–	–	–	–	–	–	–
323-5-1, 142-144	–	–																							Barren																										
323-5, CC	R	M			–	–	–	–	–	–	–	–	–	–	–	–	–	–	–	–	F	–	–	C	–	–	–	–	–	–	–	–	–	–	R	R	–	–	–	–	–	–	–	R	–	R	–	–	–	–	–
323-6-1, 100-102	F	M			–	–	–	–	–	–	–	–	–	–	–	–	–	–	–	–	R	–	R	F	–	R	–	–	–	–	–	–	–	–	–	–	–	–	–	–	–	–	–	R	–	–	–	–	–	R	–
323-6-1, 118-121	–	–																							Barren																										
323-6-1, 135-137	F	M			–	–	–	–	–	–	–	–	–	–	–	–	–	–	–	–	–	–	–	F	–	–	–	–	–	–	–	–	–	–	–	–	–	–	–	–	–	–	–	–	–	–	–	–	–	–	–
323-6, CC	C	G			–	–	–	–	–	–	–	–	–	–	–	–	–	–	–	–	C	–	C	C	–	C	F	–	–	–	–	–	–	–	–	R	R	+	F	C	–	–	R	R	–	–	F	–	–	R	–
323-7-1 (Gray)	R	P			–	–	–	–	–	–	–	–	–	–	–	–	–	–	–	–	R	–	–	–	–	–	–	–	–	–	–	–	–	–	–	–	–	–	R	–	–	–	–	–	–	–	–	–	–	–	–
323-7-1 (Brown	F	G			–	–	–	–	–	–	–	–	–	–	–	–	–	–	–	–	–	–	–	F	–	–	–	–	–	–	–	–	–	–	–	–	–	–	–	–	–	–	–	–	–	–	–	–	–	–	–
323-7-1 (Green)	R	G			–	–	–	–	–	–	–	–	–	–	–	–	–	–	–	–	–	–	–	R	–	–	–	–	–	–	–	–	–	–	–	–	–	–	–	–	–	–	–	–	–	–	–	–	–	–	–
323-7-1 (Dk. green)	R	M			–	–	–	–	–	–	–	–	–	–	–	–	–	–	–	–	–	–	–	R	–	–	–	–	–	–	–	–	–	–	–	–	–	–	–	–	–	–	–	–	–	–	–	–	–	–	–

<table>
<tr><td>323-7-3, 19-21</td><td>R</td><td>M</td><td></td><td></td><td>–</td><td>–</td><td>–</td><td>–</td><td>–</td><td>–</td><td>–</td><td>–</td><td>–</td><td>–</td><td>–</td><td>–</td><td>–</td><td>–</td><td>–</td><td>–</td><td>–</td><td>–</td><td>–</td><td>R</td><td>–</td><td>–</td><td>–</td><td>–</td><td>–</td><td>–</td><td>–</td><td>–</td><td>–</td><td>–</td><td>–</td><td>–</td><td>–</td><td>–</td><td>–</td><td>–</td><td>–</td><td>–</td><td>–</td><td>–</td><td>–</td><td>–</td><td>–</td><td>–</td><td>–</td><td>–</td><td>–</td></tr>
<tr><td>323-7, CC</td><td>F</td><td>M</td><td>-?-</td><td>-?-</td><td>–</td><td>–</td><td>–</td><td>–</td><td>–</td><td>–</td><td>–</td><td>–</td><td>–</td><td>–</td><td>–</td><td>–</td><td>–</td><td>–</td><td>–</td><td>–</td><td>F</td><td>–</td><td>–</td><td>–</td><td>–</td><td>F</td><td>R</td><td>–</td><td>–</td><td>–</td><td>–</td><td>–</td><td>–</td><td>–</td><td>–</td><td>–</td><td>R</td><td>–</td><td>–</td><td>C</td><td>–</td><td>–</td><td></td><td>R</td><td>–</td><td>–</td><td>–</td><td>–</td><td>–</td><td>–</td><td>–</td></tr>
<tr><td>323-8-1, 34-36</td><td>F</td><td>P</td><td></td><td></td><td>–</td><td>–</td><td>–</td><td>–</td><td>–</td><td>–</td><td>–</td><td>–</td><td>–</td><td>–</td><td>–</td><td>–</td><td>–</td><td>–</td><td>–</td><td>–</td><td>R</td><td>–</td><td>–</td><td>–</td><td>–</td><td>–</td><td>–</td><td>–</td><td>–</td><td>–</td><td>–</td><td>–</td><td>–</td><td>–</td><td>–</td><td>–</td><td>–</td><td>–</td><td>–</td><td>–</td><td>–</td><td>–</td><td>–</td><td>–</td><td>–</td><td>–</td><td>–</td><td>–</td><td>–</td><td>–</td><td>–</td></tr>
<tr><td>323-8-1, 40-42</td><td>R</td><td>M</td><td></td><td></td><td>–</td><td>–</td><td>–</td><td>–</td><td>–</td><td>–</td><td>–</td><td>–</td><td>–</td><td>–</td><td>–</td><td>–</td><td>–</td><td>–</td><td>–</td><td>–</td><td>–</td><td>–</td><td>–</td><td>–</td><td>–</td><td>–</td><td>–</td><td>–</td><td>–</td><td>–</td><td>–</td><td>–</td><td>–</td><td>–</td><td>–</td><td>–</td><td>–</td><td>–</td><td>–</td><td>–</td><td>–</td><td>–</td><td>–</td><td>R</td><td>–</td><td>–</td><td>–</td><td>–</td><td>–</td><td>–</td><td>–</td></tr>
<tr><td>323-8-1, 98-100</td><td>R</td><td>M</td><td></td><td></td><td>–</td><td>–</td><td>–</td><td>–</td><td>–</td><td>–</td><td>–</td><td>–</td><td>–</td><td>–</td><td>–</td><td>–</td><td>–</td><td>–</td><td>–</td><td>–</td><td>–</td><td>–</td><td>–</td><td>–</td><td>–</td><td>–</td><td>–</td><td>–</td><td>–</td><td>–</td><td>–</td><td>–</td><td>–</td><td>–</td><td>–</td><td>–</td><td>–</td><td>–</td><td>–</td><td>–</td><td>–</td><td>–</td><td>–</td><td>–</td><td>–</td><td>–</td><td>–</td><td>–</td><td>–</td><td>–</td><td>–</td></tr>
<tr><td>323-8, CC</td><td>–</td><td>–</td><td></td><td></td><td colspan="47">Barren</td></tr>
<tr><td>323-9, CC</td><td>–</td><td>–</td><td></td><td></td><td colspan="47">Barren</td></tr>
<tr><td>323-10-1, 96-98</td><td>–</td><td>–</td><td></td><td></td><td colspan="47">Barren</td></tr>
<tr><td>323-10-2, 103-104</td><td>–</td><td>–</td><td></td><td></td><td colspan="47">Barren</td></tr>
<tr><td>323-10-3, 67-68</td><td>–</td><td>–</td><td></td><td></td><td colspan="47">Barren</td></tr>
<tr><td>323-10, CC</td><td>–</td><td>–</td><td></td><td></td><td colspan="47">Barren</td></tr>
<tr><td>323-11-1, 36-38</td><td>–</td><td>–</td><td></td><td></td><td colspan="47">Barren</td></tr>
<tr><td>323-11-1, 130-132</td><td>–</td><td>–</td><td>?</td><td></td><td colspan="47">Barren</td></tr>
<tr><td>323-11-2, 66-68</td><td>–</td><td>–</td><td></td><td></td><td colspan="47">Barren</td></tr>
<tr><td>323-11, CC</td><td>–</td><td>–</td><td></td><td></td><td colspan="47">Barren</td></tr>
<tr><td>323-12-1, 129-131</td><td>–</td><td>–</td><td></td><td></td><td colspan="47">Barren</td></tr>
<tr><td>323-12-2, 14-16</td><td>–</td><td>–</td><td></td><td></td><td colspan="47">Barren</td></tr>
<tr><td>323-12-2, 74-76</td><td>–</td><td>–</td><td></td><td></td><td colspan="47">Barren</td></tr>
<tr><td>323-12, CC</td><td>–</td><td>–</td><td></td><td></td><td colspan="47">Barren</td></tr>
<tr><td>323-13-1, 104-106</td><td>–</td><td>–</td><td></td><td></td><td colspan="47">Barren</td></tr>
<tr><td>323-13-5, 83-84</td><td>–</td><td>–</td><td></td><td></td><td colspan="47">Barren</td></tr>
<tr><td>323-13-6, 31-32</td><td>–</td><td>–</td><td></td><td></td><td colspan="47">Barren</td></tr>
<tr><td>323-13-6, 108-110</td><td>–</td><td>–</td><td></td><td></td><td colspan="47">Barren</td></tr>
<tr><td>323-13, CC</td><td>–</td><td>–</td><td></td><td></td><td colspan="47">Barren</td></tr>
<tr><td>323-14-2, 69-71</td><td>–</td><td>–</td><td></td><td></td><td colspan="47">Barren</td></tr>
<tr><td>323-14-2, 122-124</td><td>–</td><td>–</td><td>?</td><td></td><td colspan="47">Barren</td></tr>
<tr><td>323-14, CC</td><td>–</td><td>–</td><td></td><td></td><td colspan="47">Barren</td></tr>
<tr><td>323-15-1, 110-112</td><td>–</td><td>–</td><td></td><td></td><td colspan="47">Barren</td></tr>
<tr><td>323-15-2, 105-107</td><td>–</td><td>–</td><td></td><td></td><td colspan="47">Barren</td></tr>
<tr><td>323-15-3, 116-118</td><td>–</td><td>–</td><td></td><td></td><td colspan="47">Barren</td></tr>
<tr><td>323-15-4, 24-26</td><td>–</td><td>–</td><td></td><td></td><td colspan="47">Barren</td></tr>
<tr><td>323-15-6, 18-20</td><td>–</td><td>–</td><td></td><td></td><td colspan="47">Barren</td></tr>
<tr><td>323-15, CC</td><td>–</td><td>–</td><td></td><td></td><td colspan="47">Barren</td></tr>
<tr><td>323-16-1, 37-39</td><td>–</td><td>–</td><td></td><td></td><td colspan="47">Barren</td></tr>
<tr><td>323-16-1, 94-96</td><td>–</td><td>–</td><td></td><td></td><td colspan="47">Barren</td></tr>
<tr><td>323-16-2, 40-42</td><td>–</td><td>–</td><td>?</td><td></td><td colspan="47">Barren</td></tr>
<tr><td>323-16-2, 90-92</td><td>–</td><td>–</td><td></td><td></td><td colspan="47">Barren</td></tr>
<tr><td>323-16-3, 90-92</td><td>–</td><td>–</td><td></td><td></td><td colspan="47">Barren</td></tr>
<tr><td>323-16-4, 57-59</td><td>–</td><td>–</td><td></td><td></td><td colspan="47">Barren</td></tr>
<tr><td>323-16, CC</td><td>–</td><td>–</td><td></td><td></td><td colspan="47">Barren</td></tr>
<tr><td>323-17-1, 81-83</td><td>–</td><td>–</td><td></td><td></td><td colspan="47">Barren</td></tr>
<tr><td>323-17, CC</td><td>–</td><td>–</td><td></td><td></td><td colspan="47">Barren</td></tr>
<tr><td>323-18-2, 138-140</td><td>–</td><td>–</td><td></td><td></td><td colspan="47">Barren</td></tr>
<tr><td>323-18-3, 63-65</td><td>C</td><td>P</td><td></td><td></td><td colspan="47">Silica Recrystallized</td></tr>
<tr><td>323-18-3, 127-129</td><td>A</td><td>P</td><td></td><td></td><td colspan="47">Silica Recrystallized</td></tr>
<tr><td>323-18-3, 143-145</td><td>C</td><td>P</td><td></td><td></td><td colspan="47">Silica Recrystallized</td></tr>
<tr><td>323-18-4, 58-60</td><td>C</td><td>P</td><td></td><td></td><td colspan="47">Silica Recrystallized</td></tr>
<tr><td>323-18-4, 85-87</td><td>C</td><td>P</td><td></td><td></td><td colspan="47">Silica Recrystallized</td></tr>
<tr><td>323-18-4, 105-107</td><td>–</td><td>–</td><td>Cretaceous</td><td></td><td colspan="47">Barren</td></tr>
<tr><td>323-18-5, 0-2</td><td>–</td><td>–</td><td></td><td></td><td colspan="47">Barren</td></tr>
<tr><td>323-18-5, 47-49</td><td>F</td><td>P</td><td></td><td></td><td colspan="47">Silica Recrystallized</td></tr>
<tr><td>323-18-5, 138-140</td><td>R</td><td>P</td><td></td><td></td><td colspan="47">Silica Recrystallized</td></tr>
<tr><td>323-18-6, (Basalt contact)</td><td>–</td><td>–</td><td></td><td></td><td colspan="47">Barren</td></tr>
</table>

short ranging and restricted to the NPD Zones XX-XXII which are correlative to N9-N10 standard foraminiferal zones. *R. marylandicus* is found at 323-6-1, 137-138 cm, 323-6, CC, and 323-7, CC. *Denticula nicobarica* becomes extinct in the North Pacific at the base of NPD Zone XIX (correlative to N10 foraminiferal standard zone, middle middle Miocene on the Berggren time scale). *D. nicobarica* was found at 7, CC placing Sample 323-7, CC in the middle middle Miocene or lower. Here it is tentatively placed near the middle/lower Miocene boundary, which is of approximately 15 m.y.B.P. on the Berggren (1969) time scale.

The co-occurrence of most North Pacific diatom biostratigraphic indicator species with indicator species endemic to the Antarctic could ultimately lead to the establishment of a high-resolution biostratigraphy in high latitude Cenozoic sediments.

RATES OF SEDIMENT ACCUMULATION

Accumulation rates for the sedimentary section at Site 323 are shown in Figure 8. The uppermost part down through Core 1 (85 m), from Holocene to early Pliocene (about 3.5 m.y.), has an accumulation rate of 2-3 cm/1000 yr. A strong increase in rate occurs in the early part of the early Pliocene between Cores 1 and 2; within this interval it reaches a maximum of 9-10 cm/1000 yr. From this level to Core 3, which lies within the middle Miocene at about 12 m.y., it decreases to 1.5 cm/1000 yr and then increases between 12 and 14 m.y. (Cores 3 to 5) to 3-4 cm/1000 yr. The rate calculated for the lower part of the middle Miocene (Cores 5-7) is 1.5 cm/1000 yr.

The biostratigraphic data below Core 7 (16 m.y.) are poor. Cores 10 to the upper part of 14 are tentatively dated as early Miocene to ? Oligocene. This age determination is reasonable since calculated accumulation rates are similar to those of the lower middle Miocene — about 1 to 2 cm/1000 yr.

Changes of accumulation rates may reflect climatic fluctuations in the area of Site 323; high rates occur in the early Miocene and Pliocene. The accumulation rate of the brown clay unit overlying the basalt is about 0.4-0.5 cm/1000 yr based on the assumption that the age of basal sediments is 70-72 m.y. The upper part of the unit would have a rate of 0.3 cm/1000 yr if all the Paleocene is included. In the case of an unchanged continuous sedimentation of the clay unit it is certain that not only the Eocene and most of the Oligocene, but also part of the Paleocene is missing.

SUMMARY AND CONCLUSIONS

Summary

Site 323 is located near the southern margin of the Bellingshausen Abyssal Plain in a water depth of 4993 meters. The single hole drilled at this site reached a total depth of 731 meters below the sea floor, penetrating 30 meters into basaltic rock at the bottom. The upper 701 meters consist of Upper Cretaceous and Cenozoic sedimentary deposits. A total of 199.5 meters was cored; 76.7 meters (38%) of core were recovered, including about 10 meters of basalt. Time on station was 113 hr. Coring results are summarized in Figures 9 and 10.

Six lithologic units are recognized, five sedimentary and one igneous; these units are numbered in descending order. Unit 1 is about 266 meters thick and consists of gray unconsolidated sandy silt, diatom clay, and diatom ooze (middle Miocene-Pliocene). The base of this semi-indurated clay unit apparently lies just below Core 3. Measured sonic velocities range from 1.54 to 1.73 km/sec.

Unit 2 is about 241 meters thick and consists of relatively indurated gray diatomitic claystone and cherts (Miocene). The cherts have formed by precipitation of cryptocrystalline silica within claystone. The basal contact occurs in Core 10. Measured sonic velocities range from 1.62 to 3.79 km/sec.

Unit 3 is about 130 meters thick and consists of gray claystone devoid of biogenic silica (? Oligocene to early Miocene). The lower contact occurs in Core 14 and is marked by a sharp color change. Measured sonic velocities range from 1.71 to 1.97 km/sec.

Unit 4 is 28 meters thick and is composed of yellow-brown iron-rich claystone and nanno-claystone overlying Unit 5, 35 meters thick, of brown zeolitic claystone (Late Cretaceous to Paleocene). The base of this unit rests upon basalt in Core 18, and there is no sign of contact metamorphism, although the exact contact is not preserved.

Unit 6 is at least 30 meters thick and consists of aphanitic aphyric basalt. Coring in this unit recovered 10 meters of solid, coherent core of rather fresh rock. A range of textures is present, but no evidence of glass, palagonite, or hyaloclastite was found. Many fractures and calcite veins occur throughout the core, along with a few very small amygdules. The rock consists mainly of augitic pyroxene and intermediate plagioclase, with minor olivine. Textures observed are intergranular-intersertal, variolitic, subophitic, and pilotaxitic. Measured sonic velocities range from 3.65 to 5.48 km/sec.

Seismic profiles near Site 323 reveal the following acoustical units in descending order: (I) flat-lying reverberant reflectors, (II) acoustically transparent layer, (III) reverberant, gently undulating reflector, (IV) acoustically transparent layer, (V) acoustically opaque, undulating reflector. Good correlations exist between these seismic units and the lithologic units encountered in the hole (see Figure 5).

Each of the first 18 cores taken yielded fossils of some kind. All of the five major microfossil groups are found in this sequence, diatoms being the most abundant fossil in Cores 1-9 and present in all 18 cores. Radiolarians are abundant only in Cores 1 and 3. They also occur near the base, but are absent in between. Foraminifers do not occur above 500 meters subbottom and are significant only in Core 15. Nannoplankton occur just above the basalt in Cores 15-17. Silicoflagellates were found in Cores 1-9.

The fossils recovered from the 18 cores yield ages ranging from Pliocene to late Cretaceous. Abundant

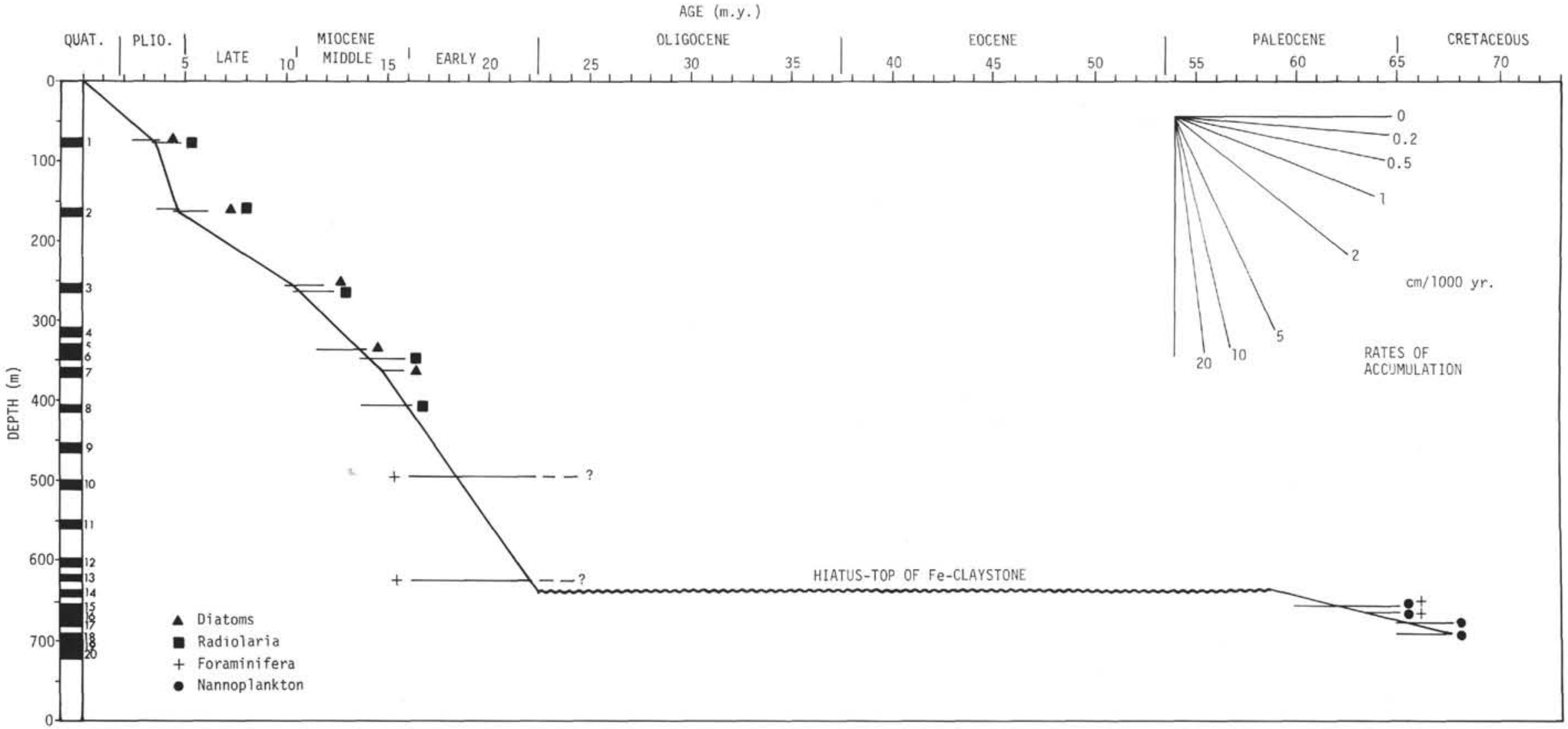

Figure 8. *Rate of sediment accumulation, Site 323.*

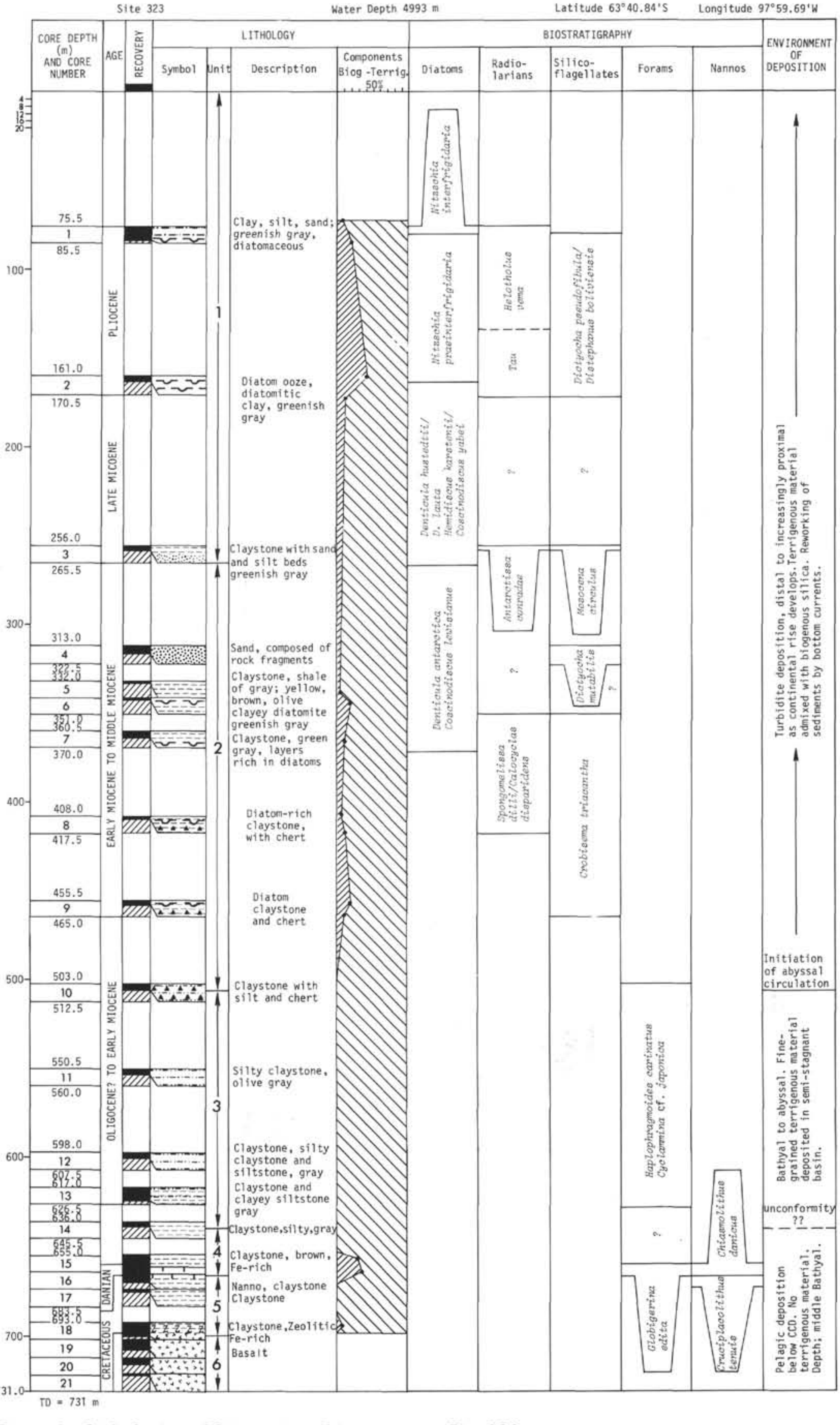

Figure 9. *Lithologic and biostratigraphic summary, Site 323.*

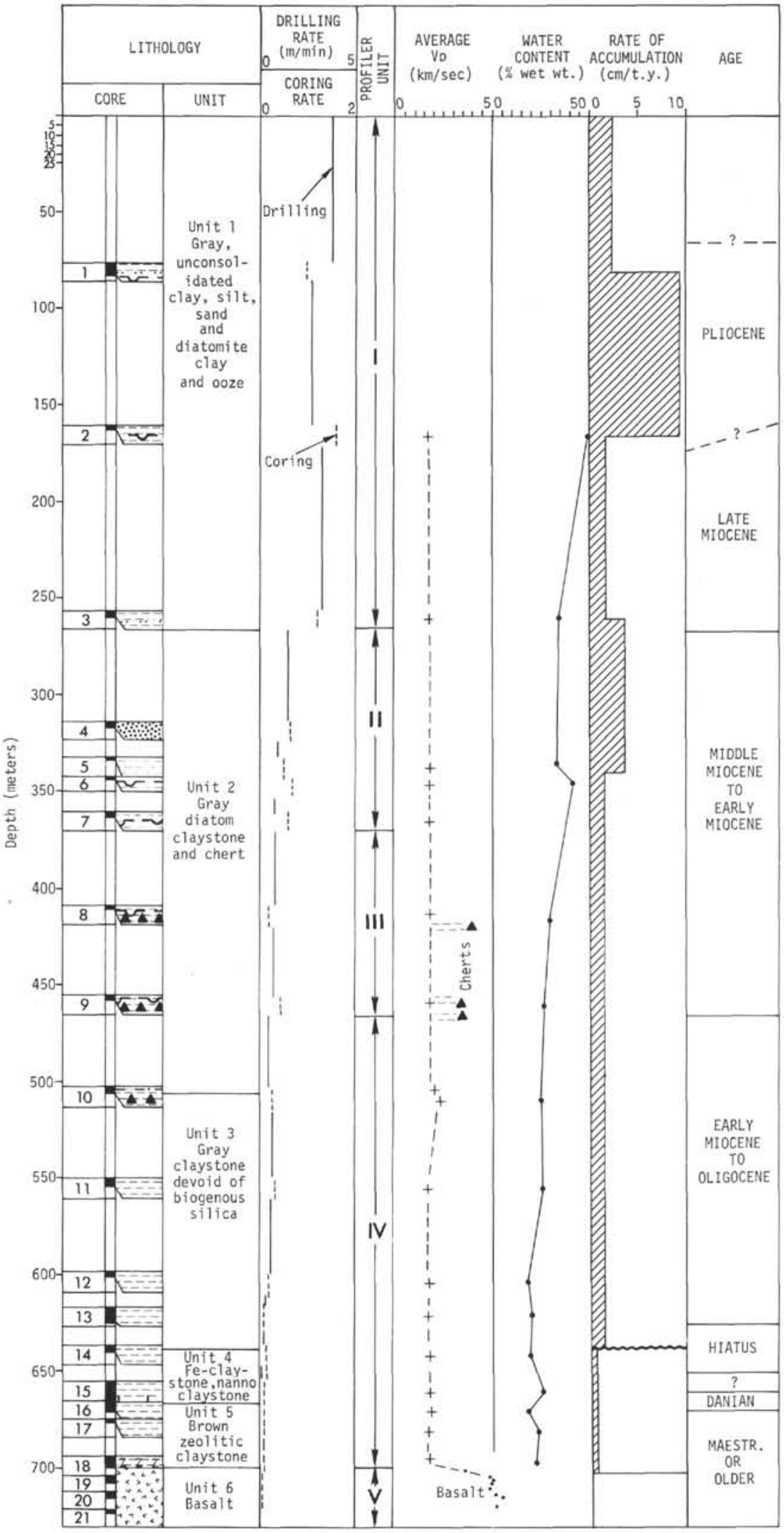

T.D.731 m

*Profile units are based on changes in drilling rates and acoustic reflectors.

Figure 10. *Correlation of lithology, physical properties, drilling rates and profiler units, Site 323.*

diatoms and radiolarians in Core 1 indicate a Pliocene age. A continuous stratigraphic sequence may exist downward through early Miocene or Oligocene into Core 14. Danian (early Paleocene) foraminifers and nannofossils occur in Cores 15 and 16. A probable unconformity is inferred in Core 14 representing part of Paleocene, all of Eocene, and at least some of Oligocene time. Below the Danian, and resting upon the basalt, the oldest beds in the sequence; nannoplankton and radiolarians indicate a late Cretaceous age.

Samples were taken from 16 cores in the sedimentary sequences for shipboard and shore-laboratory geochemical studies. Measurements of water content, porosity, formation factor, and certain chemical properties were made in the *Challenger* laboratories. Downhole increases in formation factor and dissolved calcium were observed, along with decreases in water content (%), porosity, and dissolved magnesium. Measured values of *p*H show no clear trend and cluster around a value of 8. Alkalinity and ammonia values increase to a maximum at about 300 meters and then decrease. Dissolved silica remains nearly the same to a depth of 300 meters, then decreases markedly down to 630 meters, and then increases steadily in the last three measurements.

Conclusions

The aphanitic holocrystalline basalt correlates with the deepest observed seismic reflector and probably represents one or more sills which have been intruded into sedimentary rocks. Petrographic evidence suggests that the volcanic rocks of true basement were not penetrated, and furthermore it is not possible to determine depth to that horizon from the geophysical record. The late Cretaceous age (Maestrichtian) obtained from nannoplankton in the sedimentary unit overlying the basalt indicates that the true basement (Layer 2) lying below the deepest observed reflector is at least 65 m.y. old and that it may be very close to the predicted age inferred from the closest magnetic anomaly (32), approximately 76 m.y.B.P.

The brown iron-rich pelagic clay just above the basalt was probably deposited in a tranquil, isolated environment mostly below the carbonate compensation depth. A diverse Danian benthonic foram assemblage and abundant well preserved nannoplankton occur 30 meters higher in the hole; these fossils suggest deposition of this unit above the carbonate compensation depth.

The upper part of this unit up to Core 14 again is lacking carbonate. It shows a fluctuation of the CCD throughout the late Cretaceous and early Paleocene.

An unconformity is indicated by the presence of ?Oligocene to early Miocene gray silty claystone 23 meters above the Danian nannofossil claystone. These 23 meters of carbonate-free claystones are considered also of Paleocene age according to the assemblage of arenaceous foraminifers and accumulation rates.

A subsequent abrupt increase in terrigenous detritus (between 500-640 m) with rare biogenic components suggests rapid deposition of continental rise hemipelagic silt and clays, probably originally transported downslope from Antarctica by turbidity currents, and penecontemporaneously entrained and redeposited by bottom currents flowing as part of the newly developed abyssal circulation. The gray and brown claystones (Cores 10-18) probably correspond to the acoustically transparent seismic unit lying above the deepest observed reflector.

During the later early Miocene siliceous biogenic contributions became more significant, and cherts formed by later silicification of claystones. This lithologic unit probably corresponds to the intermediate, reverberant acoustic reflector on the seismic profile.

Turbidity currents from Antarctica began reaching this site no later than the late Miocene. These first formed fine-grained distal deposits and, commensurate with the development of the continental rise, later formed proximal or base-of-rise sandy turbidites. These interbedded sands, silts, and clays are seen in seismic profiles as horizontal reverberant reflectors that typify profiles taken on modern abyssal plains.

Little definite evidence for ice rafting of detritus was observed, and this transportation mechanism appears to have been of minor importance at this site. One ice-rafted granite cobble was found in Core 7, Section 2, at 62 cm lying in sediment probably middle Miocene in age.

REFERENCES

Bass, M.A., Moberly, R., Rhodes, J.M., Shih, C., and Church, S.E., 1973. Volcanic rocks cored in the Central Pacific, Leg 17. *In* Winterer, E.L., Ewing, J.L., et al., Initial Reports of the Deep Sea Drilling Project, Volume 17: Washington (U.S. Government Printing Office), p. 429-504.

Berggren, W.A., 1969. Cenozoic chronostratigraphy, planktonic foraminiferal zonation and the radiometric time scale: Nature, v. 224, p. 1072-1075.

Böstrom, R. and Peterson, M.N.A., 1966. Precipitate from hydrothermal exhalations on the East Pacific Rise: Econ. Geol., v. 61, p. 1258.

Chen, P., 1975. Antarctic Radiolaria, Leg 28, Deep Sea Drilling Project. *In* Frakes, L.A., Hayes, D.E., et al., Initial Reports of the Deep Sea Drilling Project, Volume 28: Washington (U.S. Government Printing Office), p. 437-513.

Cook, H.E., 1972. Stratigraphy and sedimentation. *In* Hays, J.D., et al., Initial Reports of the Deep Sea Drilling Project, Volume 9: Washington (U.S. Government Printing Office), p. 933-943.

Craddock, C. (Ed.), 1970. Geologic Maps of Antarctica, Folio 12, Antarctic Map Folio Series: New York (Am. Geogr. Soc.).

———, 1972. Geologic Map of Antarctica, scale 1:5,000,000: New York (Am. Geogr. Soc.).

———, 1975. Tectonic evolution of the Pacific margin of Gondwanaland. *In* Campbell, K.S.W. (Ed.), Gondwana geology: Canberra (Australian National University Press), p. 609-618.

Craddock, C., Bastien, T.W., and Rutford, R.H., 1964. Geology of the Jones Mountains. *In* Adie, R.J. (Ed.), Antarctic Geology: Amsterdam (North Holland Publ. Co.), p. 171-187.

Engle, A.E.J., Engle, C.G., and Havens, R.G., 1965. Chemical characteristics of oceanic basalts and the upper mantle: Geol. Soc. Am. Bull., v. 76, p. 719-734.

Erlank, A.J. and Reid, D.L., 1974. Geochemistry, mineralogy, and petrology of basalts, Leg 25, Deep Sea Drilling Project. *In* Simpson, E.S.W., Schlich, R., et al., Initial Reports of the Deep Sea Drilling Project, Volume 25: Washington (U.S. Government Printing Office), p. 543-551.

Garrison, R.E., 1972. Inter and intrapillow limestone of the Olympic Peninsula, Washington: J. Geol., v. 80, p. 310.

Goodell, H.G., Houtz, R., Ewing, M., Hayes, D., Naini, B., Echols, R.J., Kennett, J.P., and Donahue, J.G., 1973. Marine sediments of the southern oceans, Folio 17, Antarctic Map Folio Series: New York (Am. Geogr. Soc.).

Gordon, A.L., 1967. Structure of Antarctic waters between 20°W and 170°W, Folio 6, Antarctic Map Folio Series: New York (Am. Geogr. Soc.).

———, 1972. On the interaction of the Antarctic circumpolar current and the Macquarie Ridge. *In* Antarctic Oceanology II, Antarctic Res. Series: Am. Geophys. Union, p. 71-78.

Hays, J.D. and Opdyke, P.D., 1967. Antarctic Radiolaria magnetic reversals, and climatic change: Science, no. 158, p. 1001.

Heezen, B.C. and Tharp, M., 1972. Morphology of the sea floor. *In* Folio 16, Antarctic Map Folio Series: New York (Am. Geogr. Soc.).

Houtz, R.E., Kennett, J.P., et al., 1975. Initial Reports of the Deep Sea Drilling Project, Volume 29: Washington (U.S. Government Printing Office).

Jousé, A.P., Kozlova, D.G., and Muhina, V.V., 1971. Distribution of diatoms in the surface layer of sediment from the Pacific Ocean. *In* Riedel, W.R. and Funnell, B.M. (Eds.), The micropaleontology of oceans: Cambridge (Cambridge University Press), p. 263-269.

Kennett, J.P., Burns, R.E., Andrews, J.E., Churkin, M., Jr., Davis, T.A., Dumitrica, P., Edwards, A.R., Galehouse, J.S., Packham, G.H., and van der Lingen, G.J., 1972. Australian-Antarctic continental drift, paleocirculation changes and Oligocene deep sea erosion: Nature, v. 239, p. 51-55.

Lancelot, Y., 1973. Chert and silica diagenesis in sediments from the Central Pacific. *In* Winterer, E.L., Ewing, J.I., et al., Initial Reports of the Deep Sea Drilling Project, Volume 17: Washington (U.S. Government Printing Office), p. 377-405.

Lee, H.J., 1973. Measurements and estimates of engineering and other physical properties, Leg 19. *In* Creager, J.S., Scholl, D.W., et al., Initial Reports of the Deep Sea Drilling Project, Volume 19: Washington (U.S. Government Printing Office), p. 701-719.

LeMasurier, W.E., 1972. Volcanic record of Cenozoic glacial history of Marie Byrd Land. *In* Adie, R.J. (Ed.), Antarctic geology and geophysics: Oslo (Universitetsforlaget), p. 251-259.

Margolis, S.V. and Kennett, J.P., 1970. Antarctic deep sea cores: Science, v. 170, p. 1085-1087.

McCollum, D.W., 1975. Leg 28 diatoms. *In* Hayes, D., Frakes, L.A., et al., Initial Reports of the Deep Sea Drilling Project, Volume 28: Washington (U.S. Government Printing Office), p. 515-571.

Pitman, W.C., Herron, E.M., and Heirtzler, J.R., 1968. Magnetic anomalies in the Pacific and sea floor spreading: J. Geophys. Res., v. 73, p. 2069-2085.

Reid, J.L. and Nowlin, W., 1971. Transport of water through the Drake Passage: Deep-Sea Res., v. 18, p. 51-64.

Rutford, R.H., Craddock, C., White, C.M., and Armstrong, R.L., 1972. Tertiary glaciation in the Jones Mountains. *In* Adie, R.J. (Ed.), Antarctic geology and geophysics: Oslo (Universitetsforlaget), p. 239-243.

Schrader, H.-J., 1973. Cenozoic diatoms from the Northeast Pacific, Leg 18. *In* Kulm, L.P., von Huene, R., et al., Initial Reports of the Deep Sea Drilling Project, Volume 18: Washington (U.S. Government Printing Office), p. 673-797.

Thompson, G., Bryan, W.B., Frey, F.A., and Sung, C.M., 1974. Petrology and geochemistry of basalts and related rocks from Sites 214, 215, and 217, Deep Sea Drilling Project Leg 22 Indian Ocean. *In* von der Borch, C.C., Sclater, J.G., et al., Initial Reports of the Deep Sea Drilling Project, Volume 22: Washington (U.S. Government Printing Office), p. 459-468.

Weissel, J.K. and Hayes, D.E., 1972. Magnetic anomalies in the southeast Indian Ocean. *In* Antarctic Oceanology II, Antarctic Res. Ser.: Am. Geophys. Union, p. 165-196.

Wilson, M.E., 1960. Origin of pillow structure in early Precambrian lavas of Western Quebec: J. Geol., v. 68, p. 97.

Yoder, H.S. and Tilley, C.E., 1962. Origin of basalt magmas: an experimental study of natural and synthetic rock systems: J. Petrol., v. 3, p. 342-352.

Zittel, K.A., 1876. Veber einige fossile Radiolarien aus der nord-deutschen kreidge: Deut. Geol. Ges., Z., v. 28, p. 75-86.

Hole 323, Core 1 Cored Interval: 75.5-85.0 m

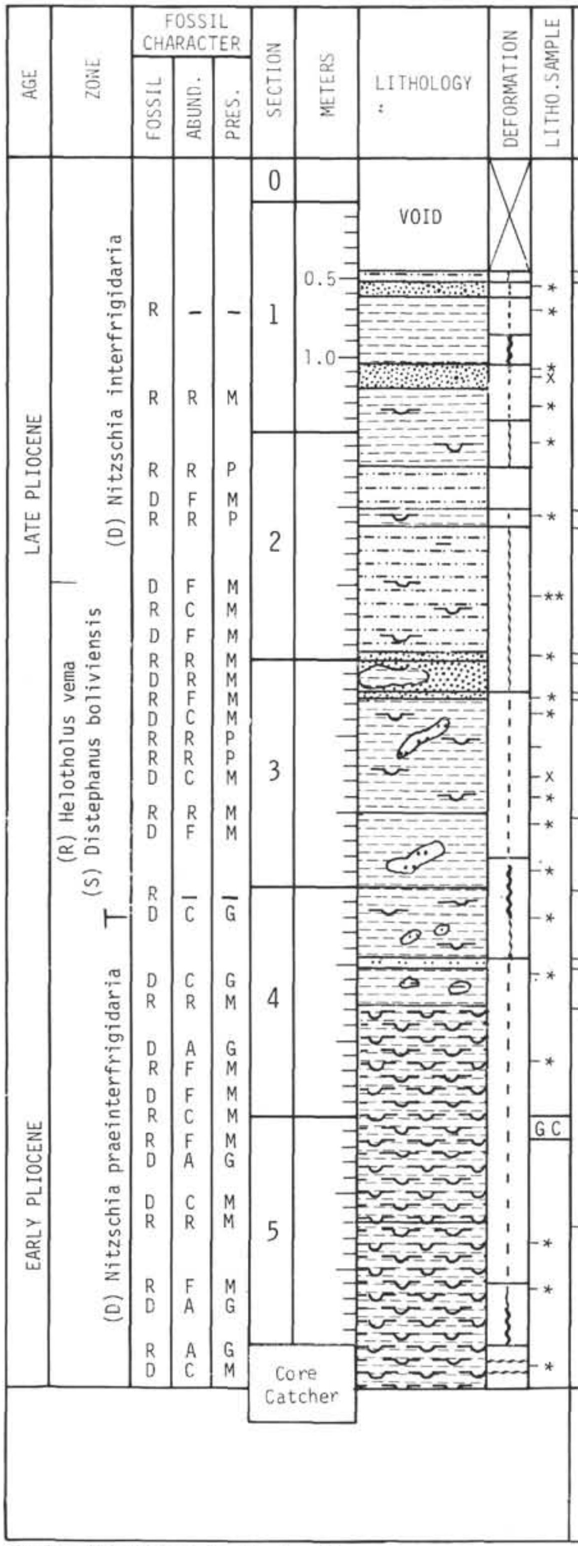

LITHOLOGIC DESCRIPTION

CLAY, DIATOM CLAY AND OOZE WITH SILT AND SAND INTERBEDS

SILTY CLAY: medium gray (N5).

CLAY AND INTERBEDDED QUARTZ SILTS AND SANDS: clay, greenish gray (5G 6/1, 5GY 6/1), firm, sticky, highly disturbed. Contains between 12-15% diatoms and sponge spicules, minor rads. Sands, medium gray (N5), no evidence of size grading, contacts sharp. Composition: 80% qtz., 5-10% fldspr., 5% rock frags., 2% heavy mins., 2% opaque mins.

DIATOM BEARING CLAY: greenish gray (5GY 6/1, 5GY 5/1), highly disturbed mixture of clay, sandy clay, and sand.

QUARTZ-CLAYEY SILT AND DIATOM BEARING CLAY: greenish gray (5G 6/1) and medium greenish gray (5GY 5/1), highly disturbed mixture.

QUARTZ-SANDY SILT: medium greenish gray (5GY 5/1). Sharp upper contact.

MIXED SAND AND CLAY: Sand, greenish gray (5G 5/1), and clay greenish gray (5GY 5/1).

QUARTZ SILTY SAND: medium gray (N5), unconsolidated, disturbed. Rich in heavy minerals.

DIATOM CLAY: greenish gray (5G 5/1), firm, some silt rich layers, 30-40% badly broken diatoms.

CLAY: greenish gray (5GY 5/1, 5G 5/1). Contains lumps of quartz silt, probably displaced.

DIATOM-RICH CLAY: greenish gray (5G 5/1) with streaks of 5GY 6/1 (disturbance) in lower part.

QUARTZ SILT: medium greenish gray (5GY 5/1), sharp contacts, no apparent grading. Contains 5% fldspr., 5% diats., rads., spicules.

CLAY: greenish gray (5G 5/1) with streaks of 5GY 6/1 (disturbance) and lumps of sand/clay mixtures (disturbance).

CLAYEY DIATOM OOZE: greenish gray (5GY 6/1), firm, but disturbed. Contains 50% well preserved diatoms, 20% rads.

CLAYEY DIATOM OOZE AND DIATOM CLAY: medium greenish gray (5GY 6/1) and greenish gray (5G 5/1).

BULK X-RAY

	1: 107-108	3: 75-76
Amorph.	33.8%	62.0%
Crystal.	66.2%	38.0%
Percent of Crystalline Component		
Quartz	45.3%	19.5%
K-Fldspr.	16.1%	3.7%
Plag.	28.8%	20.0%
Mica	5.6%	22.1%
Chlorite	1.7%	6.2%
Mont.	2.6%	26.7%
Clinop.	-	0.7%
Amphi.	-	1.1%

Explanatory notes in Chapter 2

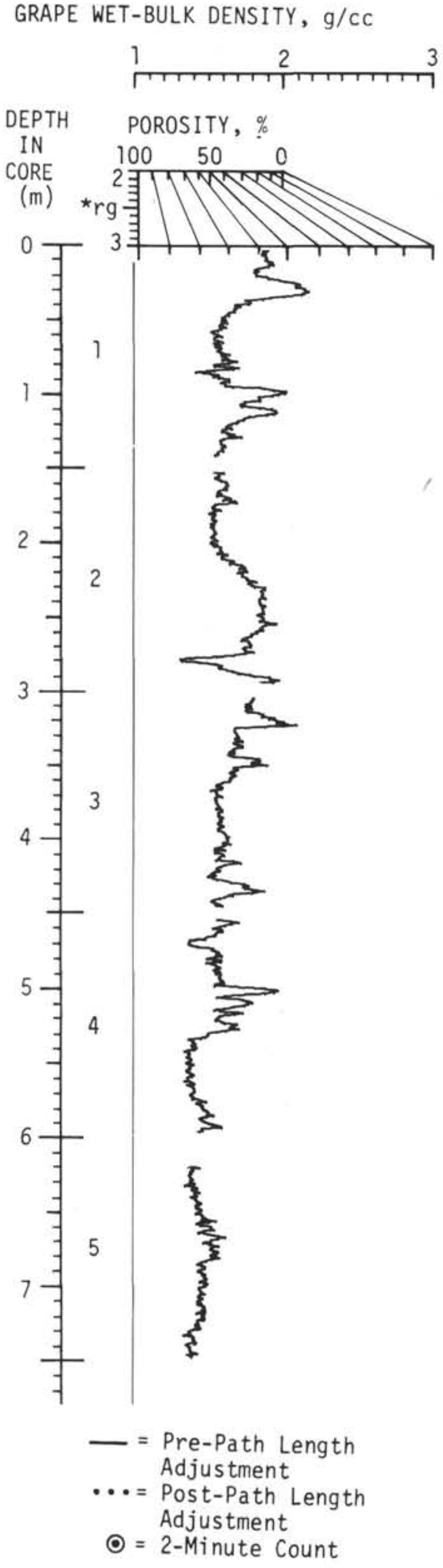
GRAPE WET-BULK DENSITY, g/cc
1
2
3
DEPTH IN CORE (m)
POROSITY, %
100
50
0
2
*rg
3
0
1
2
3
4
5
6
7
1
2
3
4
5
— = Pre-Path Length Adjustment
••• = Post-Path Length Adjustment
⊙ = 2-Minute Count
*rg = grain density, g/cc

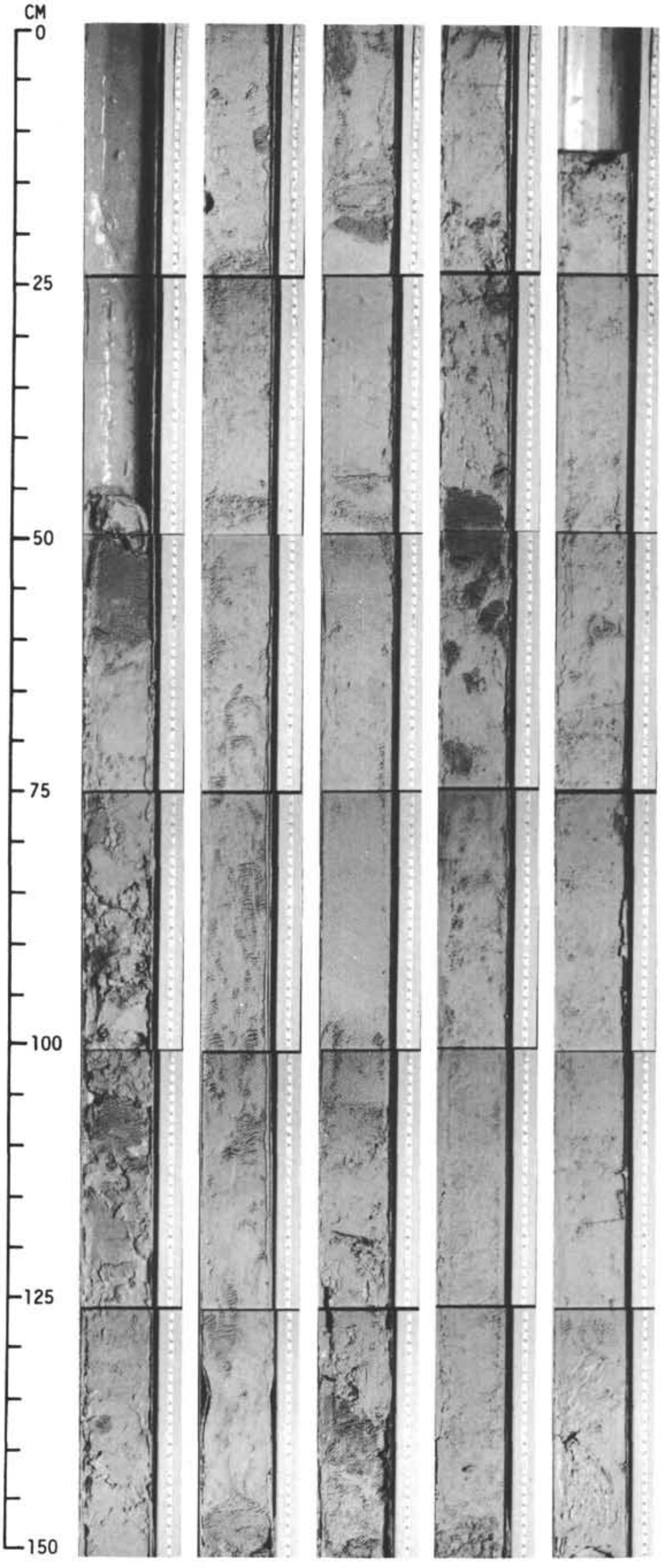
CM
0
25
50
75
100
125
150
1-1
1-2
1-3
1-4
1-5

Hole 323, Core 2   Cored Interval: 161.0-170.5 m

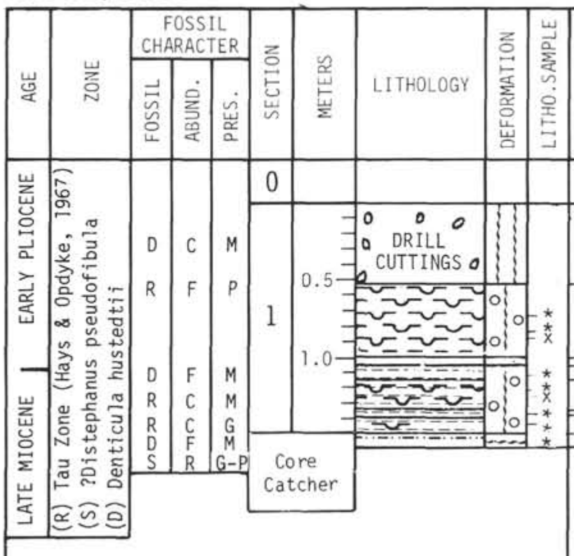

LITHOLOGIC DESCRIPTION

DIATOM OOZE, INTERBEDDED DIATOM CLAY AND CLAY

DRILL CUTTINGS:

DIATOM OOZE: medium greenish gray (5GY 5/1), diatoms moderately well preserved. Composition: 50-65% diatoms, 25-47% clay mins., 5% rads., Tr-5% qtz.

CLAY: medium greenish gray (5GY 5/1).

DIATOM RICH CLAY: medium greenish gray (5GY 5/1). Diatoms generally broken.

CLAY: dark greenish gray (5G 4/1). Composition: 93% clay mins., 5% diatoms, 2% opaque mins.

DIATOM BEARING CLAY: medium greenish gray (5G 5/1).

SILTY CLAY: quartzose. Composition: 53% clay mins., 40% qtz., 4% diatoms, 2% heavy mins.

BULK X-RAY

	1: 83-84	1: 119-120
Amorph.	66.0%	54.2%
Crystal.	34.0%	45.8%
Percent of Crystalline Component		
Quartz	16.0%	16.9%
K-Fldspr.	9.7%	5.7%
Plag.	14.3%	15.9%
Kaol.	0.8%	0.9%
Mica	24.9%	15.9%
Chlorite	1.3%	0.6%
Mont.	31.7%	42.5%
Clinop.	0.3%	0.6%
Amphi.	0.9%	0.9%

Explanatory notes in Chapter 2

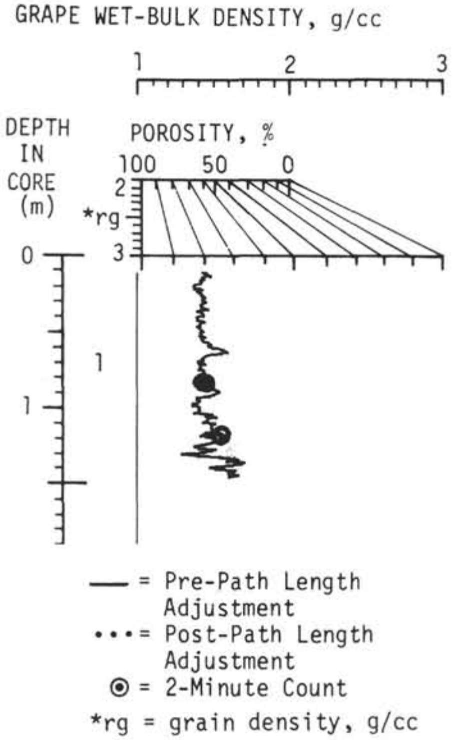
GRAPE WET-BULK DENSITY, g/cc
1
2
3
DEPTH IN CORE (m)
POROSITY, %
100
50
0
2
*rg
3
0
1
1
— = Pre-Path Length Adjustment
••• = Post-Path Length Adjustment
⊙ = 2-Minute Count
*rg = grain density, g/cc

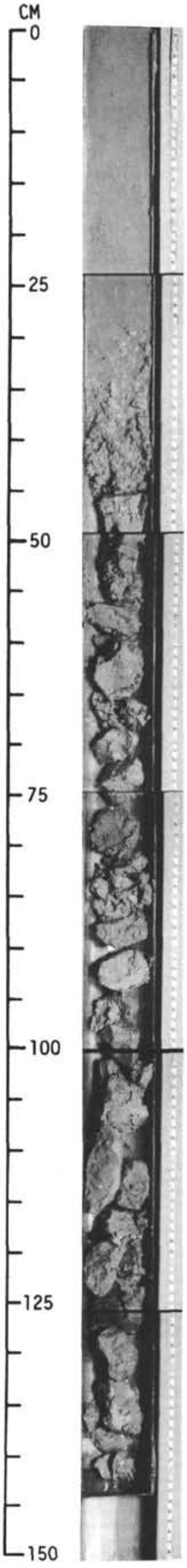
CM
0
25
50
75
100
125
150

2-1

Hole 323, Core 3 Cored Interval: 256.0-265.5 m

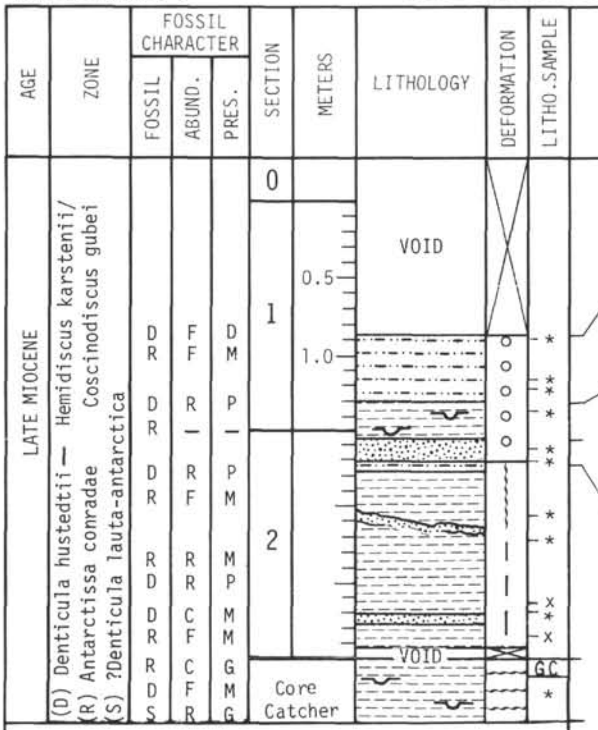

LITHOLOGIC DESCRIPTION

DIATOM BEARING AND SILTY CLAY AND CLAYSTONE

QUARTZ-SILT-RICH CLAYSTONE: olive gray (5Y 4/1), firm to consolidated. Olive gray (5Y 3/1) band at 120 cm. No contacts preserved. Composition: 92% clay mins., 5% diatoms (broken), 3% opaque mins.

QUARTZ-SILTY CLAYSTONE: olive gray (5Y 4/1), firm No contacts preserved. Composition: 90% clay mins., 10% diatoms (broken).

QUARTZ-SANDY SILT: moderate greenish black (5GY 3/1), contacts obscured, no structures or apparent size grading. Composition: 57% qtz., 25% rock frags., 5% heavy mins., 5% opaque mins., 5% sponge spicules, 3% fldspr.

CLAY: medium greenish gray (5G 5/1), no primary structures. Contains: a) quartz silt-rich pocket (20 cm), moderate greenish black (5GY 3/1, b) quartz silty sand layer (57 cm), olive gray (5Y 4/1), c) quartz silty sand layer (121 cm), dark olive gray (5Y 3/1).

DIATOM-RICH CLAY: Composition: 70% clay mins., 20% diatoms, 5% radiolarians, 5% qtz.

BULK X-RAY

	2: 119-120	2: 136-137
Amorph.	32.2%	46.9%
Crystal.	67.8%	53.1%
Percent of Crystalline Component		
Quartz	42.7%	13.2%
K-Fldspr.	13.2%	7.7%
Plag.	35.7%	15.1%
Mica	2.6%	11.7%
Chlorite	1.5%	-
Mont.	2.5%	51.1%
Clinop.	0.7%	0.5%
Amphi	1.1%	0.7%

Explanatory notes in Chapter 2

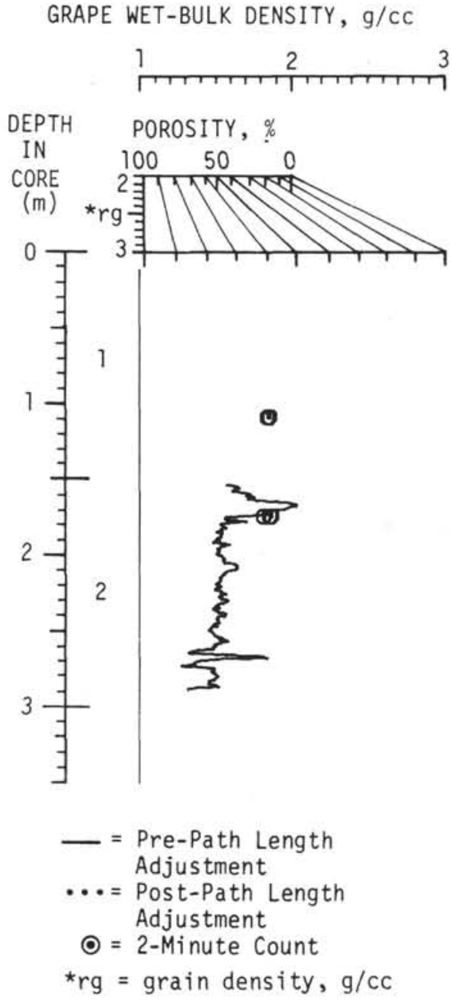
GRAPE WET-BULK DENSITY, g/cc
1
2
3
DEPTH IN CORE (m)
POROSITY, %
100
50
0
2
*rg
3
0
1
2
3
1
2
— = Pre-Path Length Adjustment
••• = Post-Path Length Adjustment
⊙ = 2-Minute Count
*rg = grain density, g/cc

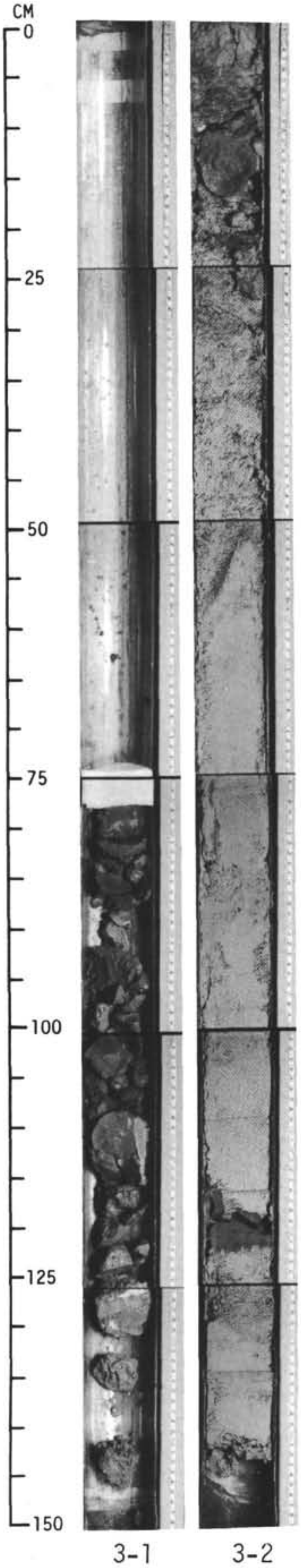
CM
0
25
50
75
100
125
150
3-1
3-2

Hole 323, Core 4 Cored Interval: 313.0-322.5 m

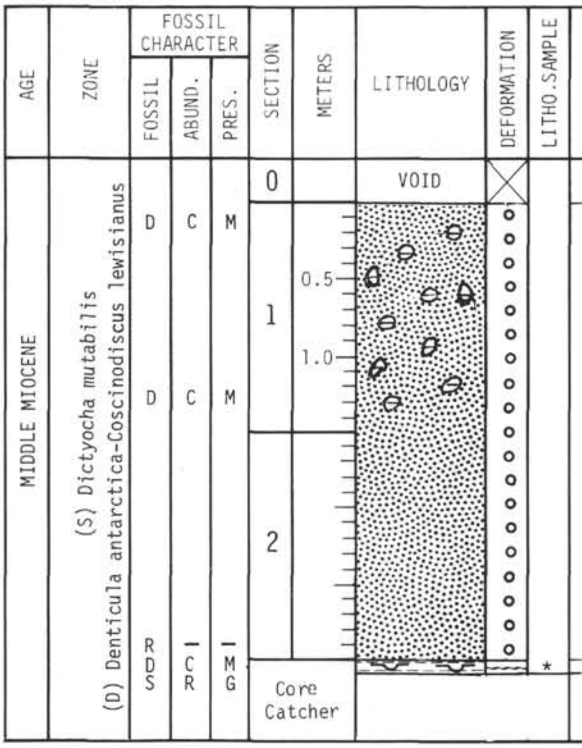

LITHOLOGIC DESCRIPTION

SAND

SAND: totally disturbed and unconsolidated. Very coarse, but well sorted to size. Composed predominantly of rock fragments of great variety. Some clay fragments in Section 1. Although disturbed, size sorting suggests material is from sand bed rather than drill cuttings.

DIATOM BEARING CLAY: Composition: 83% clay mins., 7% qtz., 7% diatoms., 3% opaque mins.

Hole 323, Core 5 Cored Interval:332.0-341.5 m

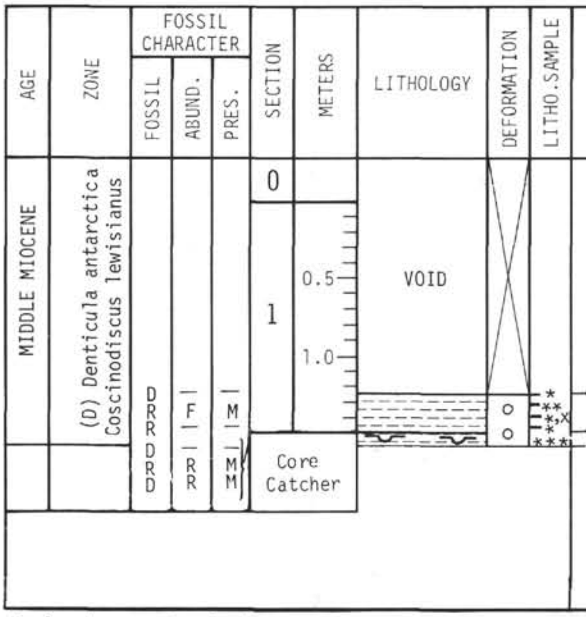

LITHOLOGIC DESCRIPTION

CLAYSTONE

CLAYSTONE: pieces of yellowish gray (5Y 6/2), greenish gray (5GY 5/1), light olive gray (5Y 5/2), medium dark gray (N4), and moderate yellowish brown (10YR 5/4). Vein of 100% authigenic carbonate at 135 cm. Trace-5% micronodules.

CLAYSTONE: olive gray (5Y 5/2), black specks, hard. Composition: 90-98% clay mins., 5-8% diatoms, traces rads., sponge spicules, calc. nannos.

BULK X-RAY (1: 140-141)

Amorph. 57.8% Crystal. 42.2%

Percent of Crystalline Component

Quartz	15.6%	Chlorite	0.6%
K-Fldspr.	2.3%	Mont.	40.0%
Plag.	19.0%	Clinop.	0.8%
Kaol.	0.4%	Amphi.	0.9%
Mica	20.4%		

Explanatory notes in Chapter 2

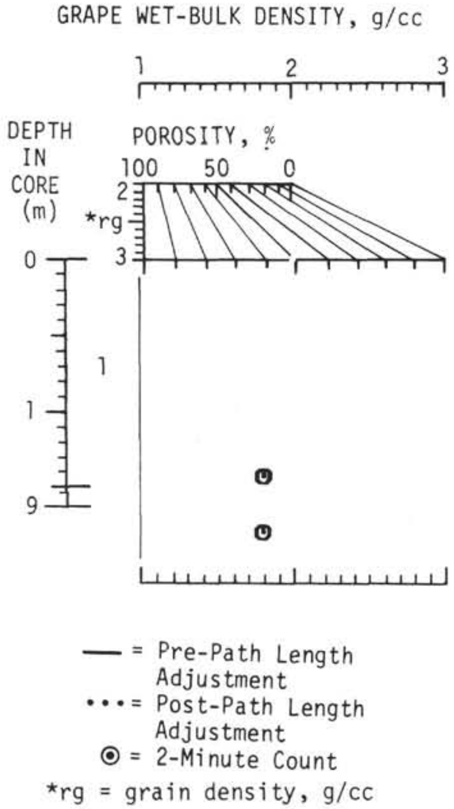
GRAPE WET-BULK DENSITY, g/cc
1
2
3
DEPTH IN CORE (m)
POROSITY, %
100
50
0
2
*rg
3
0
1
1
9
— = Pre-Path Length Adjustment
• • • = Post-Path Length Adjustment
⊙ = 2-Minute Count
*rg = grain density, g/cc

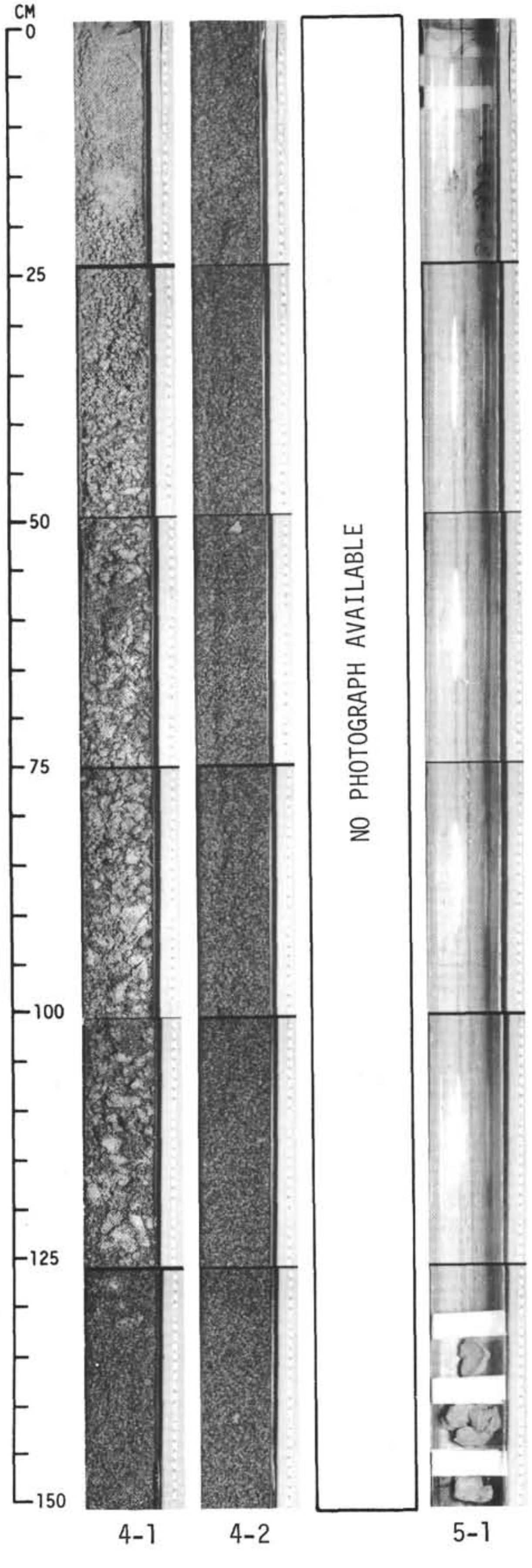
CM
0
25
50
75
100
125
150
NO PHOTOGRAPH AVAILABLE
4-1
4-2
5-1

Hole 323, Core 6 Cored Interval:341.5-351.0 m

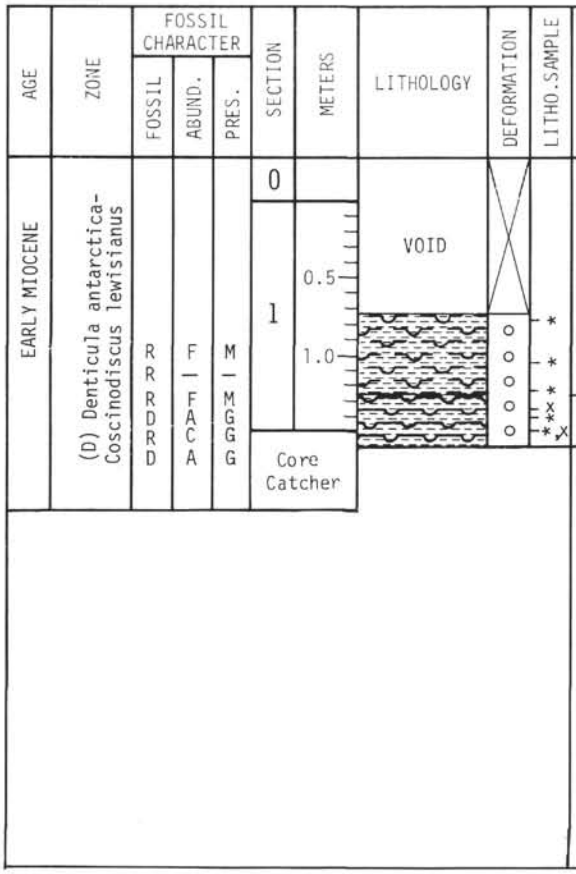

LITHOLOGIC DESCRIPTION

DIATOM CLAYSTONE AND CLAYEY DIATOMITE

DIATOM CLAYSTONE: fragments washed from drill cuttings. Fresh broken surfaces indicate that fragments are from cored interval, but are not in stratigraphic order. Primary lithologies are: a) diatom-bearing claystone, moderate and dark yellowish brown (10YR 5/4, 10YR 4/2) and greenish gray (5G 5/1), b) diatom-rich claystone, yellowish brown (10YR 5/2), and c) clayey diatomite, moderate greenish gray (5GY 5/1).

CLAYEY DIATOMITE: greenish gray (5GY 6/1), structureless. Composition: 50-55% diatoms (20% of which are well preserved), 45-50% clay mins.

BULK X-RAY

	1: 135-147	1: 47-48
Amorph.	60.5%	62.6%
Crystal.	39.5%	37.4%
Percent of Crystalline Component		
Quartz	13.0%	14.6%
K-Fldspr.	8.1%	4.5%
Plag.	13.6%	15.1%
Kaol.	0.7%	0.8%
Mica	19.7%	19.9%
Chlorite	0.2%	-
Mont.	43.8%	43.9%
Clinop.	0.2%	0.3%
Gibb.	-	-
Amphi.	0.8%	0.9%

Explanatory notes in Chapter 2

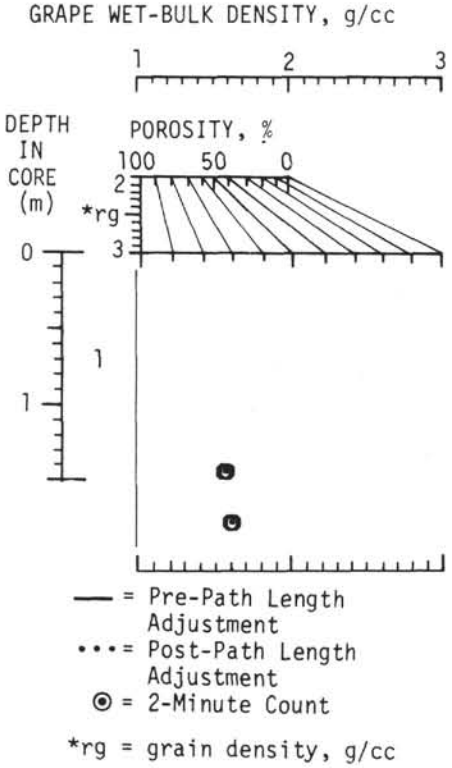
GRAPE WET-BULK DENSITY, g/cc
1
2
3
DEPTH IN CORE (m)
POROSITY, %
100
50
0
2
*rg
3
0
1
1
— = Pre-Path Length Adjustment
• • • = Post-Path Length Adjustment
⦿ = 2-Minute Count
*rg = grain density, g/cc

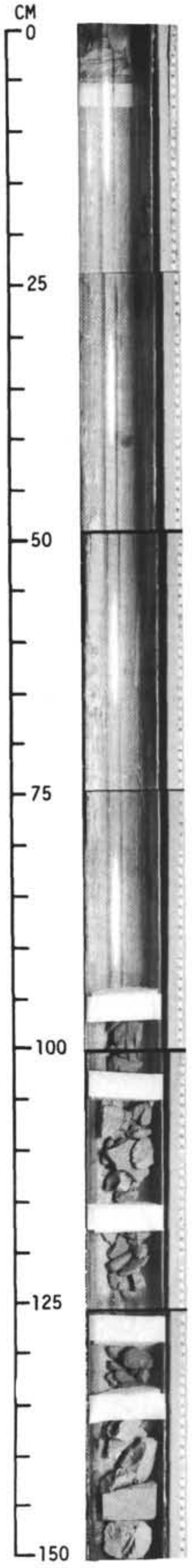
CM
0
25
50
75
100
125
150

6-1

Hole 323, Core 7 Cored Interval: 360.5-370.0 m

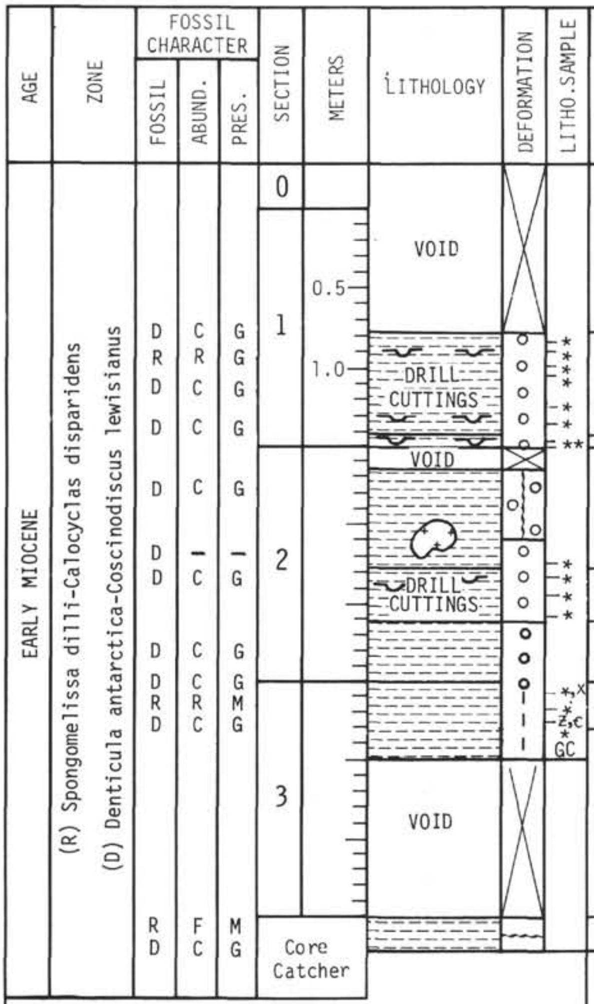

LITHOLOGIC DESCRIPTION

CLAY AND DIATOM-RICH CLAYSTONE

DIATOM-RICH CLAYSTONE AND CLAYSTONE: fragments washed from drill cuttings. Fresh broken surfaces indicate that fragments are from cored inerval, but they have been artifically grouped by color and are not in stratigraphic order. Lithologies include: claystone, dusky yellow brown (10YR 2/2), and greenish gray (5G 5/1) and dark greenish gray (5GY 4/1), diatom claystone, yellow brown (10YR 5/4, 10YR 4/2), quartz sand with auth. carb., medium olive gray (5Y 5/1), diatom rich claystone, medium olive gray (5Y 5/1).

DIATOM-RICH CLAYSTONE: dark greenish gray (5GY 4/1) and moderate and dark yellowish brown (10YR 5/4, 10YR 4/2), structureless. Composition: 75-88% clay mins., 7-20% diatoms, 0-5% qtz., traces fldspr., heavy mins., rads., sponge spicules.

CLAY: Totally disturbed drilling hash. Contains varying colored clays and diatom clay. Granite cobble, Sect. 2, 60 cm.

DIATOM-RICH CLAY AND CLAYSTONE: fragments washed from drill cuttings as in Sect. 1. Lithologies include: diatom claystone, moderate and dark yellowish brown (10YR 5/4, 10YR 4/2) and dark greenish gray (5GY 4/1), diatom clay, greenish gray (5GY 5/1) and clay, greenish gray (5G 5/1).

CLAY: totally disturbed drilling hash. Contains varying colored clays and diatom clays.

CLAY: dark greenish gray (5GY 4/1). Featureless except for two sand pods containing up to 30% rock fragments, 15% heavy mins., 5% fldspr. Grain size: 3-25: (0-25-75). C/CO_3: 3-23 (0.1-0.1-0.0).

CLAY: dark greenish gray (5GY 4/1), faintly mottled, minor small sand pods and ice-rafted gravel.

BULK X-RAY (3: 5-6)

Amorph. 48.6% Crystal. 51.4%

Percent of Crystalline Component

Quartz	16.2%	Chlorite	2.2%
K-Fldspr.	8.5%	Mont.	38.2%
Plag.	17.1%	Clinop.	0.3%
Kaol.	0.4%	Amphi.	0.9%
Mica	16.2%		

Explanatory notes in Chapter 2

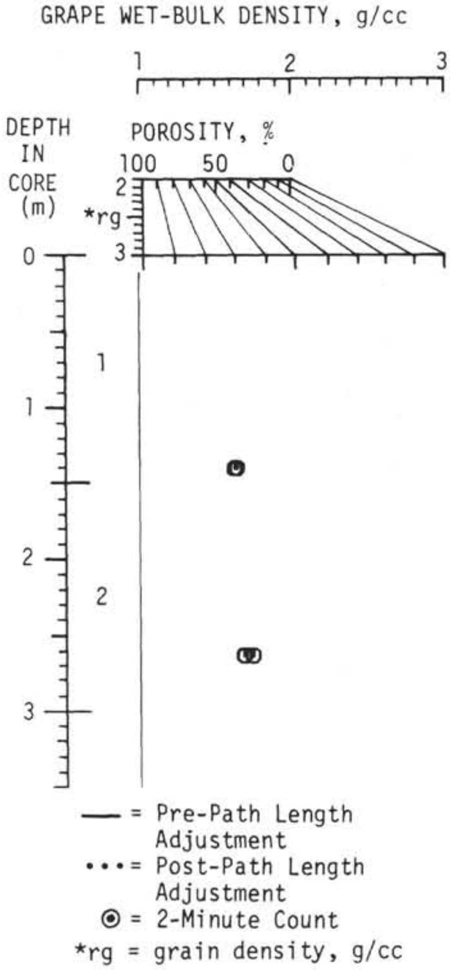
GRAPE WET-BULK DENSITY, g/cc
1
2
3
DEPTH IN CORE (m)
POROSITY, %
100
50
0
2
*rg
3
0
1
1
2
2
3
— = Pre-Path Length Adjustment
•••= Post-Path Length Adjustment
⊙ = 2-Minute Count
*rg = grain density, g/cc

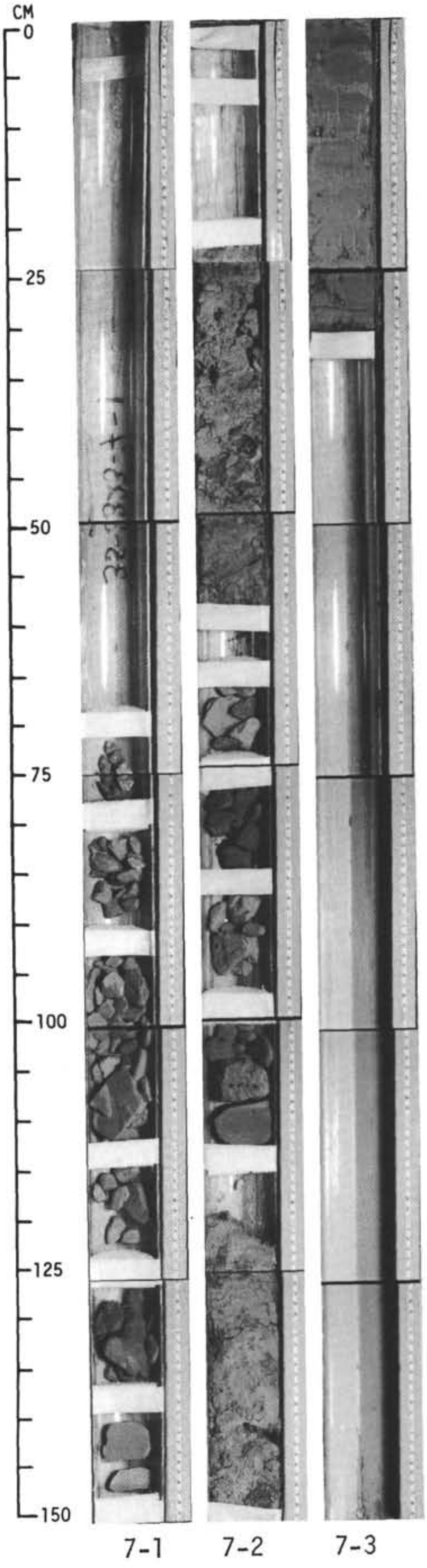
CM
0
25
50
75
100
125
150
7-1
7-2
7-3

Hole 323, Core 8 Cored Interval: 408.0-417.5 m

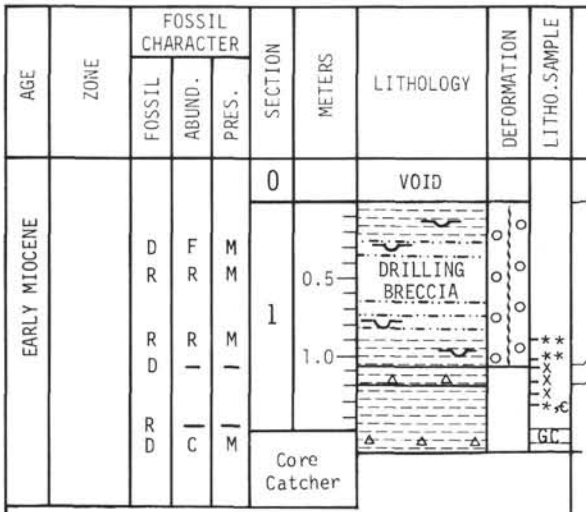

LITHOLOGIC DESCRIPTION

DIATOM-RICH CLAY, CLAYEY SILT, AND CLAYSTONE

DIATOM-RICH CLAY AND QUARTZ CLAYEY SILT: drilling breccia, intensely mixed. Clay is light bluish gray (5B 7/1), silt is dark gray (N4).

SILICIFIED CLAYSTONE: dark gray (N3). Can be scratched with knife. Contact between claystone and silicified claystone intact and sharp.

CLAYSTONE: dark greenish gray (5GY 3/1), slight silicified, massive, uniform texture, very faint bedding. Composition: 83% clay mins., 10% qtz., 7% diatoms. Core catcher contains some dark gray (N3) silicified claystone. Carbon/carbonate: 1-130 (0.6-0.6-0.0).

BULK X-RAY

	1: 106-107	1: 117-118	1: 143-148
Amorph.	38.0%	67.8%	70.2%
Crystal.	62.0%	32.2%	28.8%
	Percent of Crystalline Component		
Quartz	12.9%	8.5%	22.1%
Crist.	-	57.5%	15.8%
K-Fldspr.	5.6%	2.6%	6.3%
Plag.	15.8%	6.2%	17.0%
Kaol.	0.3%	0.2%	-
Mica	20.8%	7.8%	21.9%
Chlorite	1.5%	1.4%	6.6%
Mont.	42.1%	2.3%	8.2%
Trid.	-	13.4%	1.7%
Clinop.	0.2%	-	0.4%
Amphi.	0.7%	-	

Explanatory notes in Chapter 2

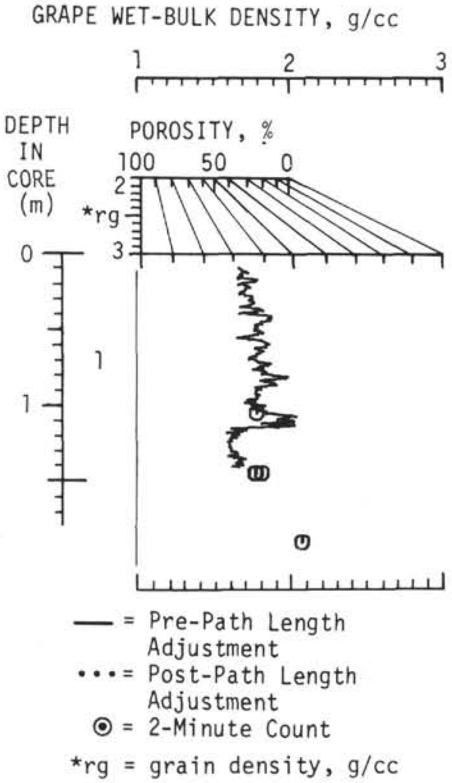
GRAPE WET-BULK DENSITY, g/cc
1
2
3
DEPTH IN CORE (m)
POROSITY, %
100
50
0
2
*rg
3
0
1
1
— = Pre-Path Length Adjustment
• • • = Post-Path Length Adjustment
⊙ = 2-Minute Count
*rg = grain density, g/cc

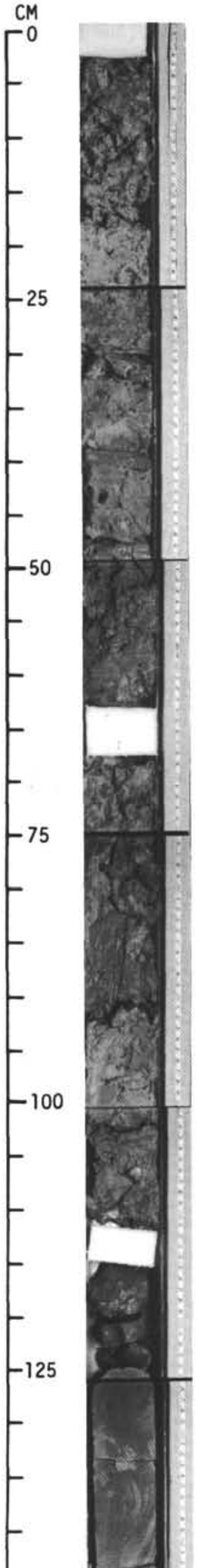
CM
0
25
50
75
100
125
150

8-1

Hole 323, Core 9 Cored Interval: 455.5-465.0 m

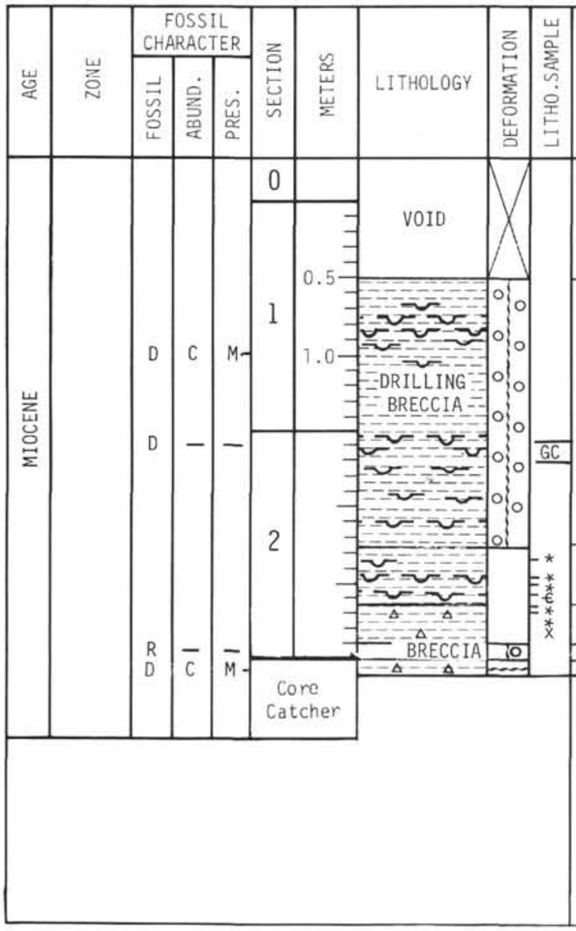

LITHOLOGIC DESCRIPTION

DIATOM CLAYSTONE AND SILICIFIED CLAYSTONE

DRILLING BRECCIA: pebbles of mixed lithology including claystone and diatom claystone. Totally disturbed. Includes many small fragments of silicified claystone.

DIATOM CLAYSTONE-CLAYSTONE: dark greenish gray (5GY 4/1), massive, featureless. Diatoms decrease down section. Contact with underlying silicified claystone intact and sharp. Composition: 53-80% clay mins., 7-30% diatoms, 10% detritals, 3-7% sponge spicules. C/CO_3: 2-107 (0.1-0.1-0.0).

SILICIFIED CLAYSTONE: dark greenish gray (5GY 4/1) and greenish black (5GY 2/1, 5G 2/1). Can be scratched with knife. Composition: 90% clay mins., 10% detritals, traces diatoms, rads., sponge spicules.

DRILLING BRECCIA: as above in Sect. 1.

CLAYSTONE AND SILICIFIED CLAYSTONE: dark greenish gray (5GY 4/1).

BULK X-RAY

	2: 99-100	2: 131-132
Amorph.	60.5%	49.6%
Crystal.	39.5%	50.4%
Percent of Crystalline Component		
Quartz	24.1%	6.2%
Crist.	-	70.9%
K-Fldspr.	17.4%	2.8%
Plag.	21.3%	4.7%
Mica	15.9%	4.7%
Chlorite	2.4%	0.7%
Mont.	17.4%	-
Trid.	-	10.0%
Amphi.	1.6%	-

Explanatory notes in Chapter 2

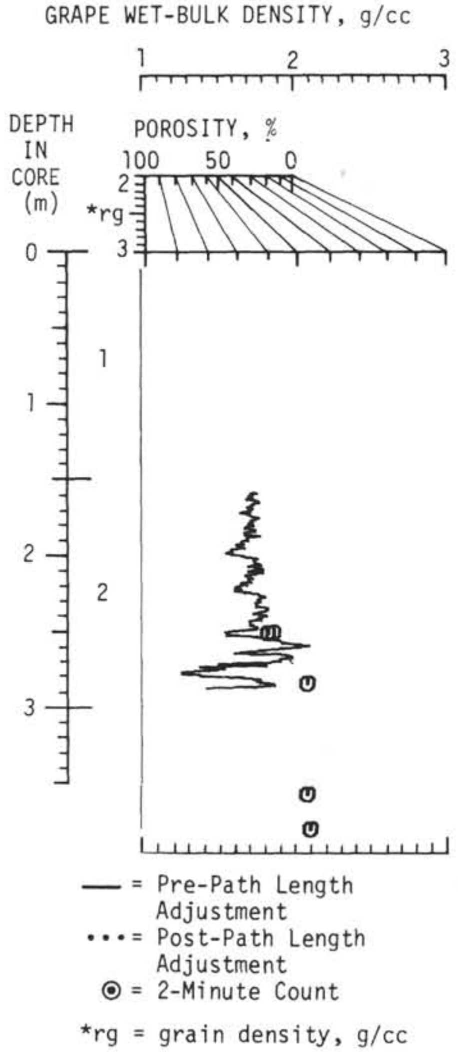
GRAPE WET-BULK DENSITY, g/cc
1
2
3
DEPTH IN CORE (m)
POROSITY, %
100
50
0
*rg
2
3
0
1
2
3
1
2
— = Pre-Path Length Adjustment
••• = Post-Path Length Adjustment
⊙ = 2-Minute Count
*rg = grain density, g/cc

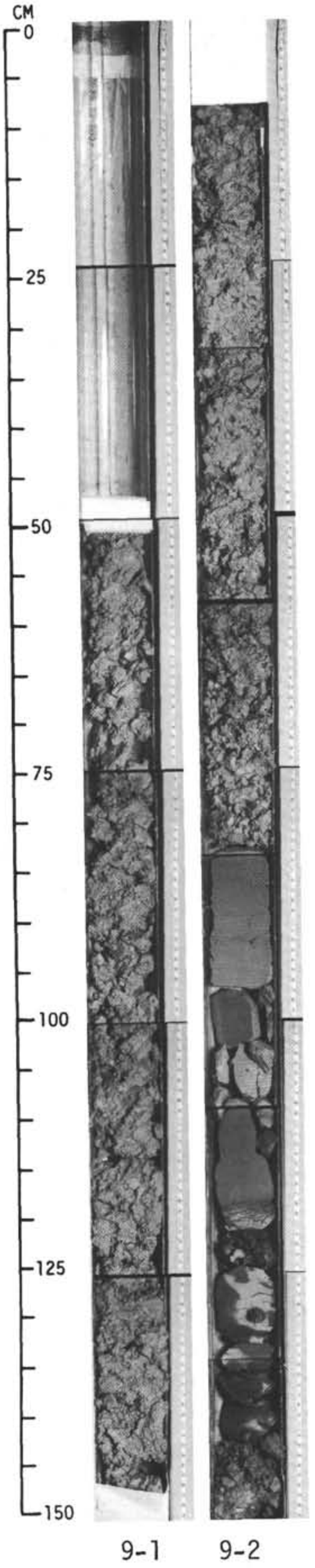
CM
0
25
50
75
100
125
150
9-1
9-2

Hole 323, Core 10

Cored Interval: 503.0-512.5

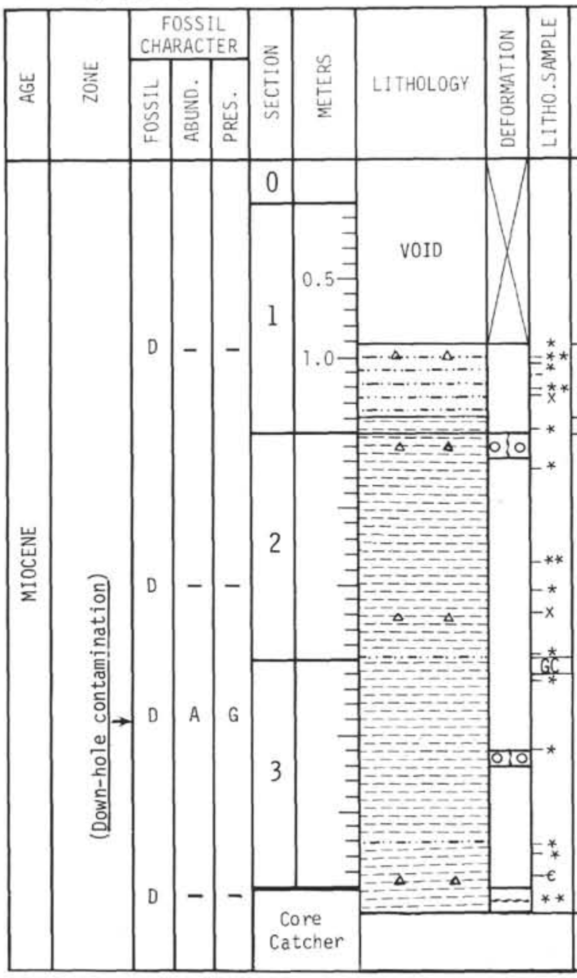

LITHOLOGIC DESCRIPTION

CLAYEY SILT, CLAYSTONE, AND SILTY CLAYSTONE

CLAYEY QUARTZ-SILT: dark greenish gray (5GY 4/1). Fragment of dark gray (N3) silicified claystone at 92 cm. Well developed parting along bedding planes at 100-102 cm. Faint wavey bedding throughout which may be bioturbated bedding planes. Some burrowing evidence. White specks (zeolite concentrations) throughout.

CLAYSTONE: dark greenish gray (5G 4/1), minor trace fossils in lower part, otherwise featureless. Composition: ≈100% clay mins. with traces of qtz. and opaque mins.

CLAYSTONE AND SILTY CLAYSTONE: dark greenish gray (5G 4/1) with some dark gray (N3) chert or siliceous claystone. Wavey (bioturbated?) bedding and white specks as in Sect. 1. Distinctive vertical burrow at 84 cm. Carbon/carbonate: 3-142 (0.1-0.1-0.0).

BULK X-RAY

	1: 122-126	2: 117-120	3: 125-127
Amorph.	46.2%	51.6%	52.3%
Crystal.	53.8%	48.4%	47.7%
	Percent of Crystalline Component		
Quartz	22.3%	21.8%	20.1%
K-Fldspr.	9.4%	7.2%	11.4%
Plag.	22.4%	20.8%	18.6%
Kaol.	-	0.5%	0.5%
Mica	11.6%	18.7%	19.9%
Chlorite	3.4%	2.1%	3.5%
Mont.	29.9%	26.9%	24.8%
Clinop.	0.4%	0.7%	0.7%
Amphi.	0.6%	1.2%	0.6%

Hole 323, Core 11

Cored Interval: 550.5-560.0 m

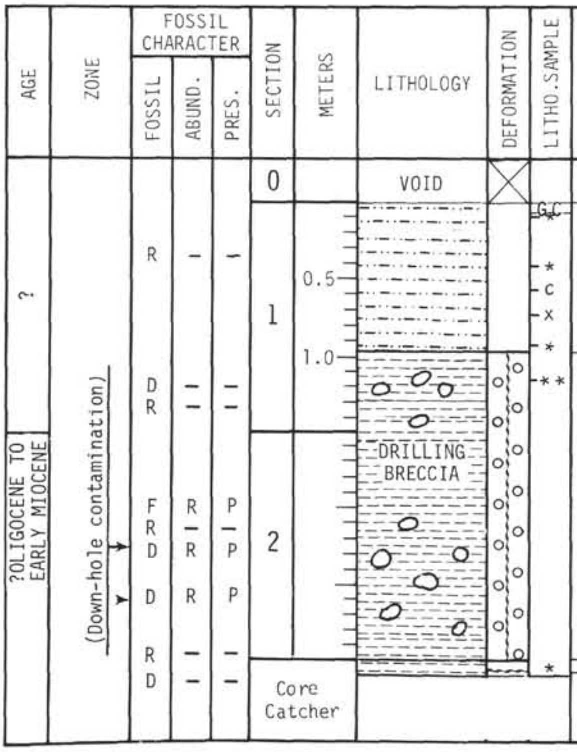

LITHOLOGIC DESCRIPTION

QUARTZ-SILTY CLAYSTONE, AND CLAYSTONE

QUARTZ-SILTY CLAYSTONE: olive gray (5Y 5/1), 10-30% silt. Minor bedding structures and laminations. White specks are foraminifera. Pyritized diatoms in small silt layer at 43 cm. Carbon/carbonate: 1-58 (0.5-0.5-1.0).

DRILLING BRECCIA: Mixed clay and pebbles. Basic lithology is clay. Totally disturbed.

BULK X-RAY (1: 70-72)

Amorph. 57.2% Crystal. 42.8%

Percent of Crystalline Component

Quartz	24.9%	Mica	27.0%
K-Fldspr.	11.4%	Chlorite	7.6%
Plag.	16.3%	Mont.	11.9%
Kaol.	0.6%	Clinop.	0.4%

CLAYSTONE: Composition: 92% clay mins., 6% qtz., 2% opaque mins.

Explanatory notes in Chapter 2

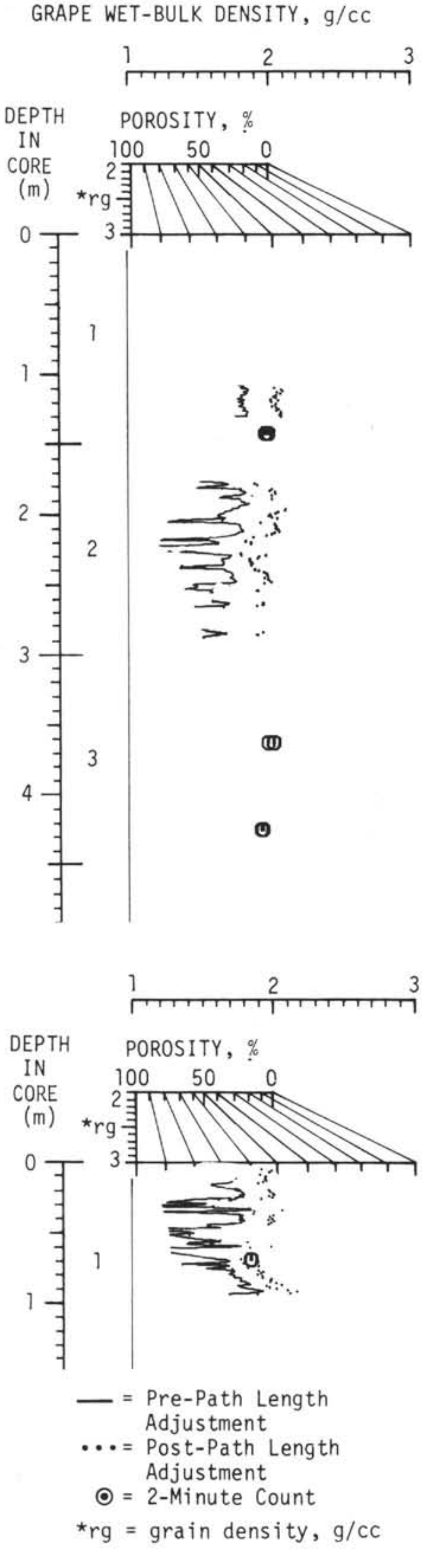
GRAPE WET-BULK DENSITY, g/cc
1
2
3
DEPTH IN CORE (m)
POROSITY, %
100
50
0
2
*rg
3
0
1
2
3
4
1
2
3
1
2
3
DEPTH IN CORE (m)
POROSITY, %
100
50
0
2
*rg
3
0
1
1
— = Pre-Path Length Adjustment
•••= Post-Path Length Adjustment
⊙ = 2-Minute Count
*rg = grain density, g/cc

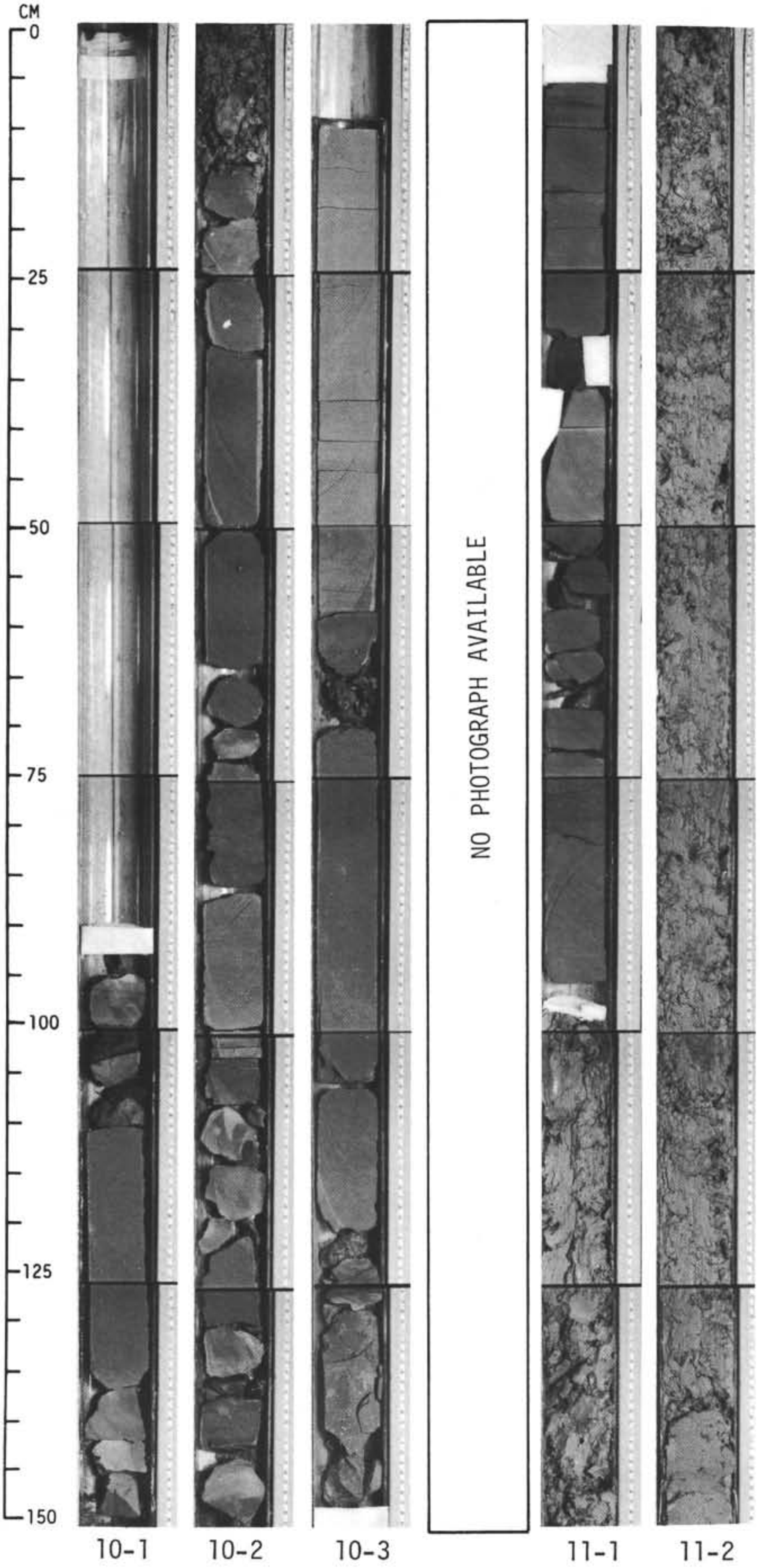
CM
0
25
50
75
100
125
150
NO PHOTOGRAPH AVAILABLE
10-1
10-2
10-3
11-1
11-2

Hole 323, Core 12 Cored Interval: 598.0-607.5 m

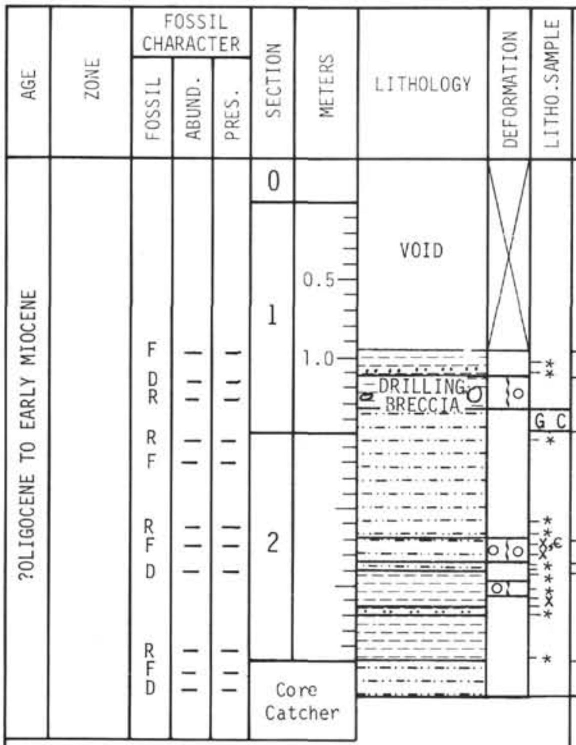

LITHOLOGIC DESCRIPTION

CLAYSTONE, SILTY CLAYSTONE, AND SILTSTONE

CLAYSTONE: dark greenish gray (5GY 5/1), small lenses of quartz silt. Composition: 95% clay mins., 5% qtz., traces of opaque and heavy mins.

DRILLING BRECCIA: mixture of clay and pebbles. Totally disturbed.

QUARTZ-SILTY CLAYSTONE: color grades downward from medium dark gray (N4) to dark greenish gray (5GY 4/1). Faint bioturbation especially between 20-30 cm. Few forams.

QUARTZ-SILT BEARING CLAY: olive gray (5Y 4/1), friable. Forms distinct "brown" layer in greenish gray sequence. C/CO_3: 2-71 (0.1-0.1-0.0).

QUARTZ-SILTY CLAY: medium dark gray (N4), soft, friable.

CLAYSTONE: olive gray (5Y 4/1) and dark greenish gray (5GY 5/1), faint wavy banding. Silt layer at 115 cm contains 70% qtz., 20% clay mins., 3% heavy mins., 5-7% pyrite.

CLAYSTONE, SILTSTONE AND CLAYEY SILTSTONE: dark gray claystone overlies 1.2 cm of light yellowish green, soft siltstone containing fine laminations of silty clay. This overlies 1.5 cm of dark red, soft, clayey siltstone which is moderately laminated and dissected by thin mottles of yellowish green and dark greenish gray.

BULK X-RAY

	2: 71-72	2: 78-80	2: 106-108
Amorph.	39.6%	39.8%	41.8%
Crystal.	60.4%	60.2%	58.2%
	Percent of Crystalline Component		
Quartz	32.1%	28.4%	19.2%
K-Fldspr.	10.0%	9.1%	8.7%
Plag.	18.5%	17.8%	9.6%
Kaol.	-	-	1.2%
Mica	9.9%	19.9%	29.1%
Chlorite	1.2%	1.1%	7.3%
Mont.	27.8%	23.7%	24.9%
Clinop.	0.5%	-	-

Explanatory notes in Chapter 2

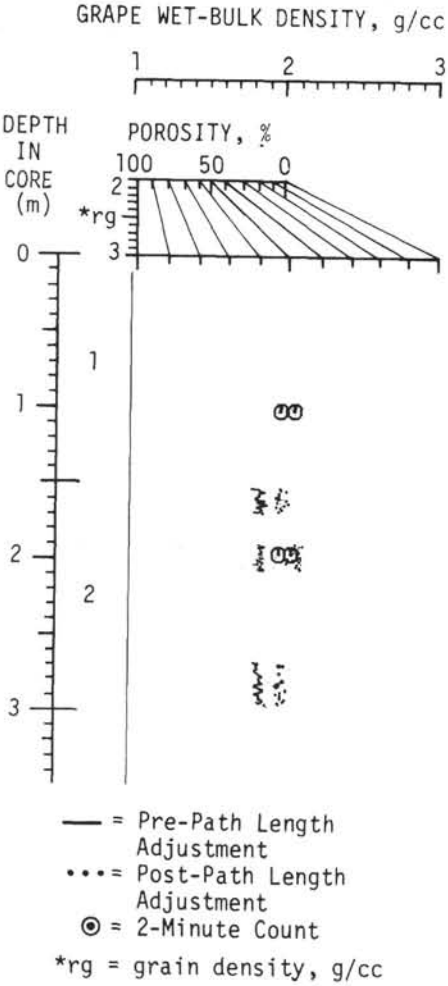
GRAPE WET-BULK DENSITY, g/cc
1
2
3
DEPTH IN CORE (m)
POROSITY, %
100
50
0
2
*rg
3
0
1
2
3
1
2
—— = Pre-Path Length Adjustment
• • • = Post-Path Length Adjustment
⊙ = 2-Minute Count
*rg = grain density, g/cc

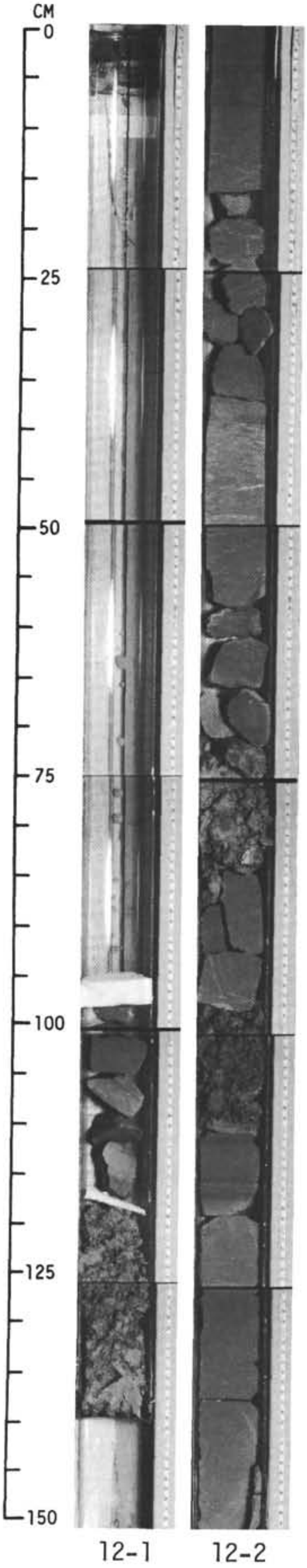
CM
0
25
50
75
100
125
150
12-1
12-2

Hole 323, Core 13 Cored Interval: 617.0-626.5 m

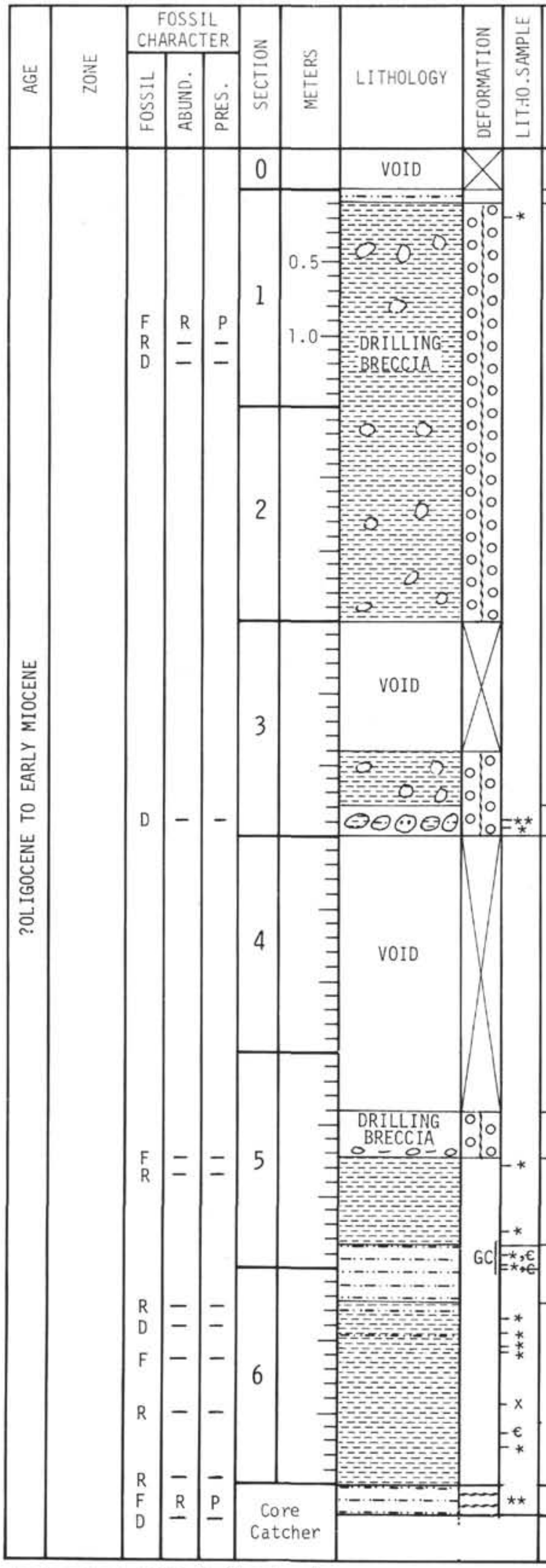

LITHOLOGIC DESCRIPTION

CLAYSTONE, SILTY CLAYSTONE, AND CLAYEY SILTSTONE

SILTY CLAYSTONE: olive gray (5Y 4/1), quartz rich. Composition: 85% clay mins., 15% qtz., traces mica, heavy and opaque mins.

DRILLING BRECCIA: contains mud and pebbles. Totally mixed.

BULK X-RAY

	5: 123-125	6: 92-94
Amorph.	56.0%	46.3%
Crystal.	44.0%	53.7%
Percent of Crystalline Component		
Quartz	28.1%	26.4%
K-Fldspr.	11.5%	12.0%
Plag.	16.6%	11.7%
Kaol.	1.3%	1.3%
Mica	17.8%	15.0%
Chlorite	4.8%	4.0%
Mont.	19.9%	29.6%

PEBBLES: washed from drilling breccia immediately above. Lithologies include clay, silty clay, silt. Quartz silt pebbles contain up to 30% authigenic $CaCO_3$.

DRILLING BRECCIA: contains mud and pebbles. Totally mixed.

CLAYSTONE: olive gray (5Y 4/1) and brownish gray (5YR 5/2) with light bluish gray (5B 7/1) mottles and white specks which are arenaceous benthic forams.

CLAYEY SILTSTONE AND SILTY CLAY: greenish gray (5GY 6/1), bioturbated. Contains 10% recrystallized silica. C/CO_3: 5-139 (0.1-0.1-0.0), 5-145 (0.4-0.2-2.0).

CLAYSTONE AND SILTY CLAY: pronounced color changes and bioturbations. 25-36 cm - light olive gray (5Y 5/2) to light gray (N7), thin quartz silt lense at base. 36-53 cm, similar to above sequence with greenish gray (5GY 5/1) to "rusty" bands (5YR 4/4) to light gray (N7) bands. 53-150 cm, greenish gray (5GY 5/1) to olive gray (5Y 4/1) clay with laminations of brown (5YR 5/4) clay. C/CO_3: 6-115 (0.1-0.1-0.0).

CLAYEY SILTSTONE: quartz rich (60%) interbedded with silty claystone.

Explanatory notes in Chapter 2

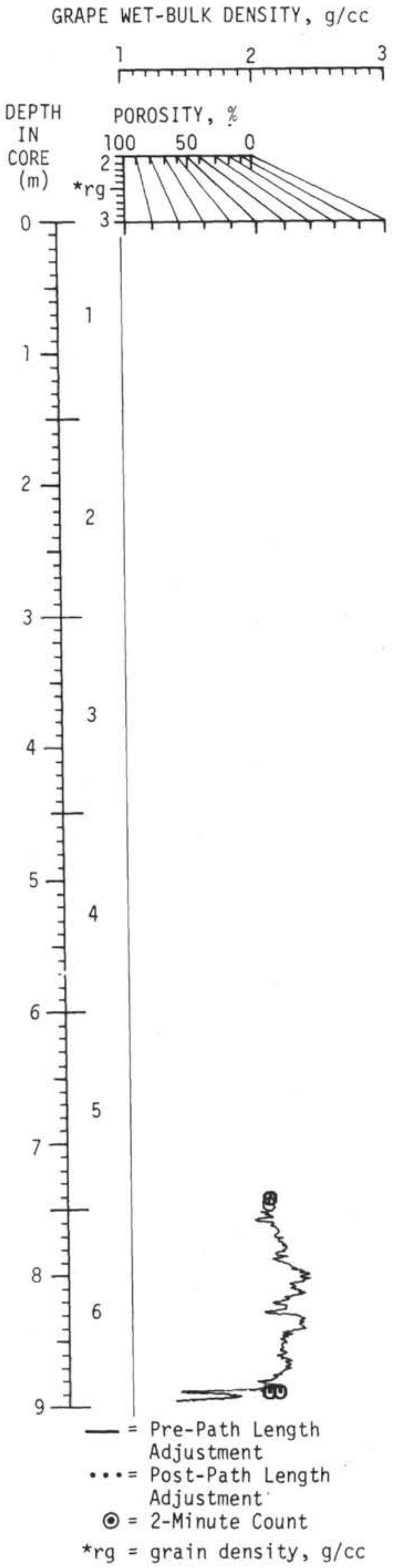
GRAPE WET-BULK DENSITY, g/cc
1
2
3
DEPTH IN CORE (m)
POROSITY, %
100
50
0
2
*rg
3
0
1
2
3
4
5
6
7
8
9
1
2
3
4
5
6
— = Pre-Path Length Adjustment
••• = Post-Path Length Adjustment
⊙ = 2-Minute Count
*rg = grain density, g/cc

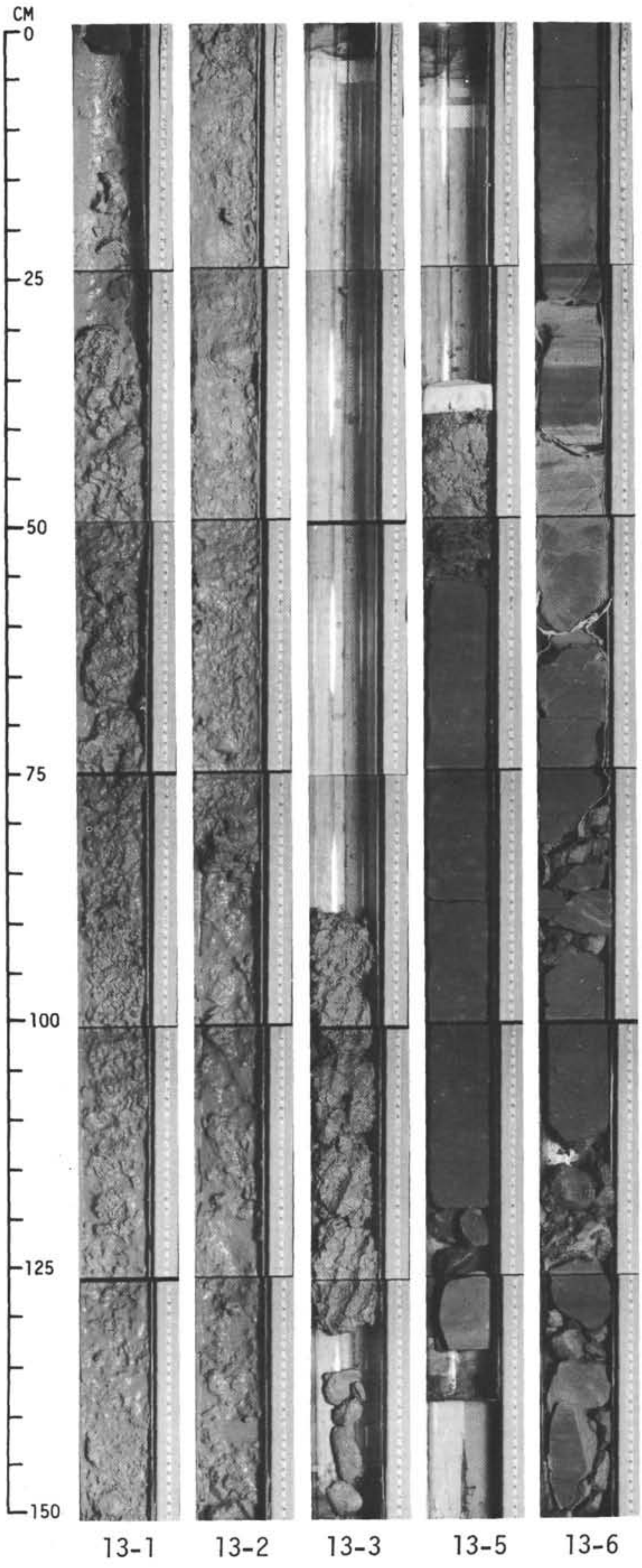
CM
0
25
50
75
100
125
150
13-1
13-2
13-3
13-5
13-6

Hole 323, Core 14 Cored Interval: 636.0-645.5 m

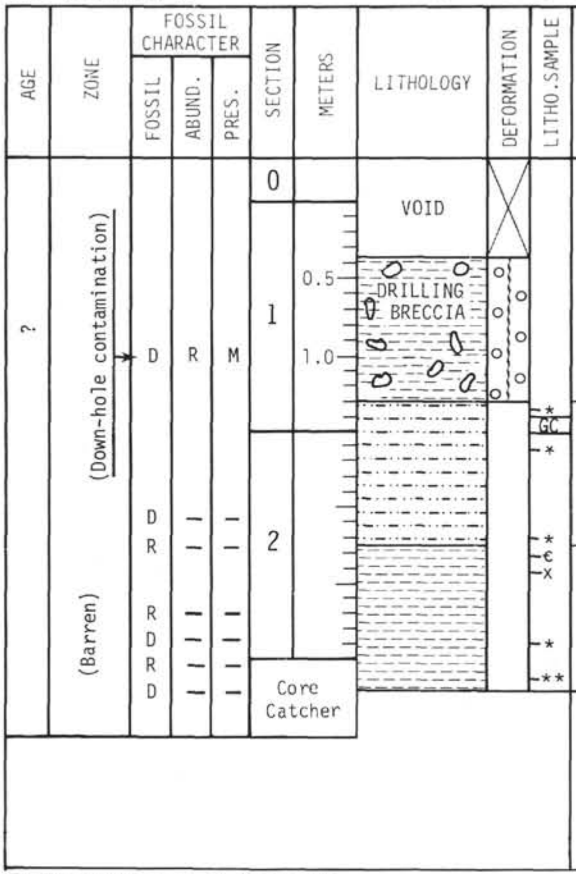

LITHOLOGIC DESCRIPTION

QUARTZ-SILT BEARING CLAYSTONE, FE-CLAYSTONE

DRILLING BRECCIA.

QUARTZ-SILT BEARING CLAYSTONE: brown (5YR 5/1) at top with bioturbations with greensih gray (5G 6/1) mottles surrounding pyrite. Color becomes increasingly greenish gray (5G 6/1) downward to 70 cm. Sharp color change at 70 cm to light bluish gray (5B 7/1).

Composition: 85-90% clay mins., 10% qtz., traces fldspr. glauc., pyrite(?), heavy and opaque mins., volc. glass, auth. carb.

FE-CLAYSTONE: dusky yellowish brown (10YR 2/2) with moderate yellowish brown (10YR 5/2) mottles (probably trace fossils. Carbon/carbonate: 2-85 (0.1-0.0-0.0).

BULK X-RAY (2: 93-97)

Amorph. 47.1% Crystal. 52.9%

Percent of Crystalline Component

Quartz	11.3%	Chlorite	2.5%
K-Fldspr.	7.7%	Goethite	5.8%
Plag.	7.3%	Mont.	54.6%
Kaol.	0.9%	Gibbsite	0.1%
Mica	9.9%		

Explanatory notes in Chapter 2

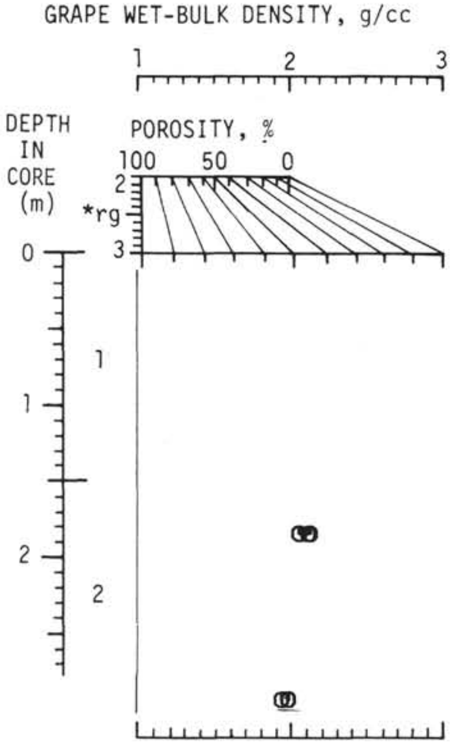

—— = Pre-Path Length Adjustment
•••= Post-Path Length Adjustment
⊙ = 2-Minute Count
*rg = grain density, g/cc

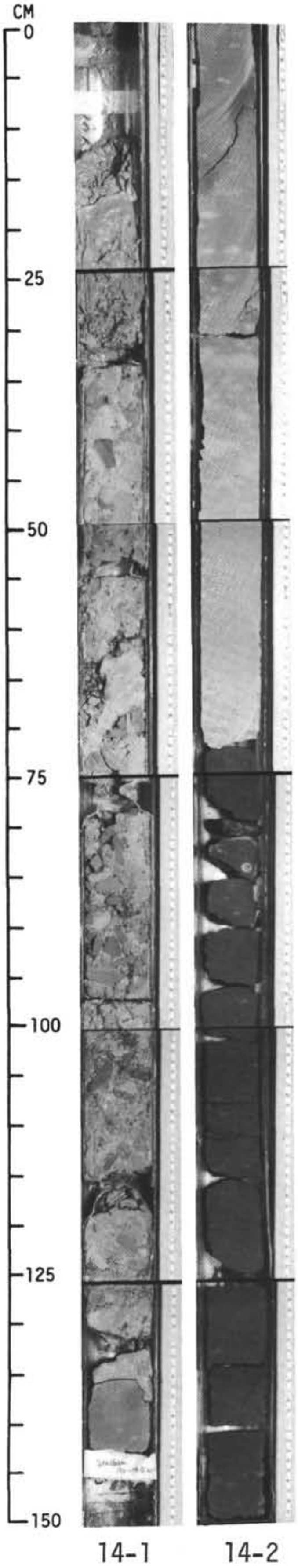

Hole 323, Core 15 Cored Interval: 655.0-664.5 m

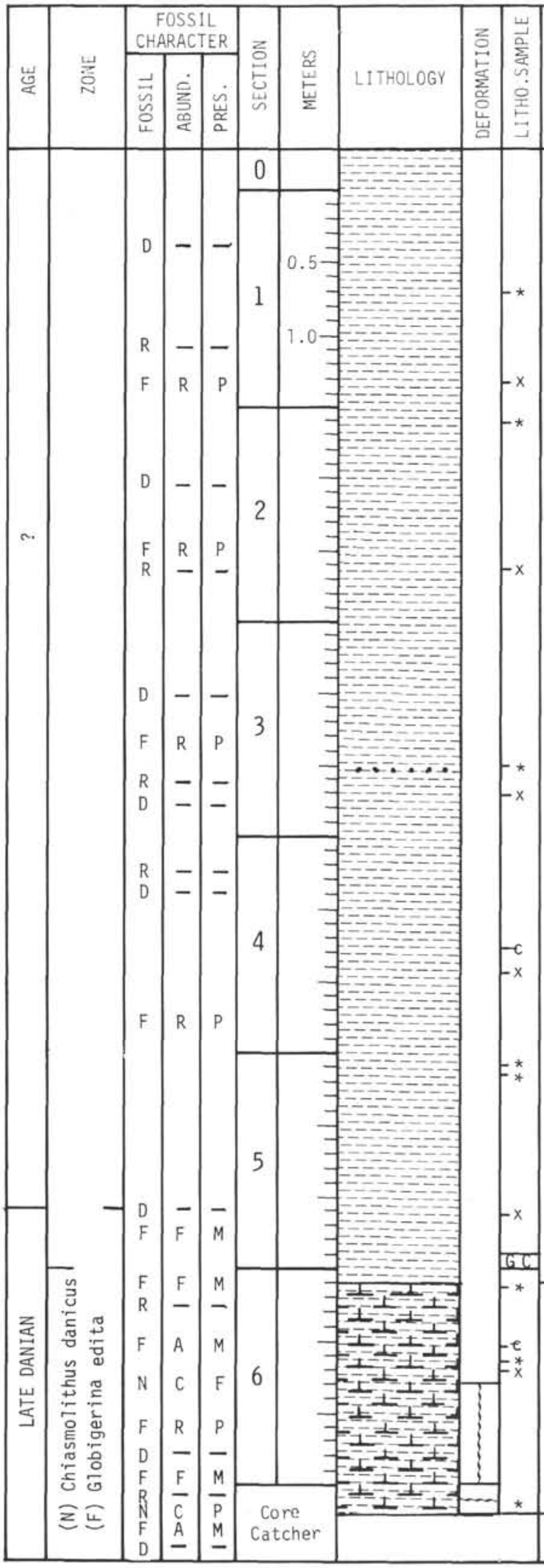

LITHOLOGIC DESCRIPTION

FE-CLAYSTONE AND NANNOFOSSIL CLAYSTONE

FE-CLAYSTONE: dusky yellowish brown (10YR 2/2) and brownish black (5YR 2/1) with moderate yellowish brown (10YR 5/4) and brownish black (5YR 2/1) trace fossils. Well developed burrows, Sect. 1, 50-150 cm. 2% $CaCO_3$ Sect. 1 at 79 cm.

Clay between pieces of claystone is probably drilling slurry.

Carbon/carbonate: 4-77 (0.0-0.0-0.0).

Few Fe-Mn micronodules, Sect. 3, 101 cm, 2 mm maximum diameter.

BULK X-RAY

	1: 132-134	2: 114-117	3: 121-124
Amorph.	41.7%	53.3%	43.1%
Crystal.	58.3%	46.7%	56.9%
	Percent of Crystalline Component		
Calc.	-	-	-
Quartz	11.3%	12.6%	11.9%
K-Fldspr.	13.7%	14.5%	13.5%
Plag.	8.9%	8.6%	6.9%
Kaol.	1.2%	2.0%	1.8%
Mica	8.0%	7.9%	7.4%
Chlorite	1.9%	1.6%	2.0%
Goet.	6.5%	8.2%	6.7%
Mont.	48.4%	44.4%	49.7%
Gibb.	-	-	0.3%

	4: 95-98	5: 111-115	6: 69-72
Amorph.	45.3%	59.8%	64.8%
Crystal.	54.7%	40.2%	35.2%
	Percent of Crystalline Component		
Calc.	-	-	73.1%
Quartz	10.2%	12.3%	3.2%
K-Fldspr.	12.6%	18.3%	3.9%
Plag.	3.7%	3.7%	1.3%
Kaol.	2.3%	2.3%	-
Mica	5.3%	7.9%	2.7%
Chlorite	1.6%	2.6%	-
Goet.	7.2%	10.3%	3.3%
Mont.	57.2%	42.6%	12.7%
Gibb.	-	-	-

(2% $CaCO_3$, Sect. 5, 48 cm - shipboard determination)

NANNOFOSSIL CLAYSTONE: dusky brown (5YR 2/2) 0-18 cm, dusky yellowish brown (10YR 2/2) 18-88 cm, brownish black (5Y 2/1) 88-150 cm. Mottling (trace fossils), 0-88 cm. Contains 30-50% nannoplankton. Carbon/carbonate: 6-55 (5.4-0.0-45.0).

Explanatory notes in Chapter 2

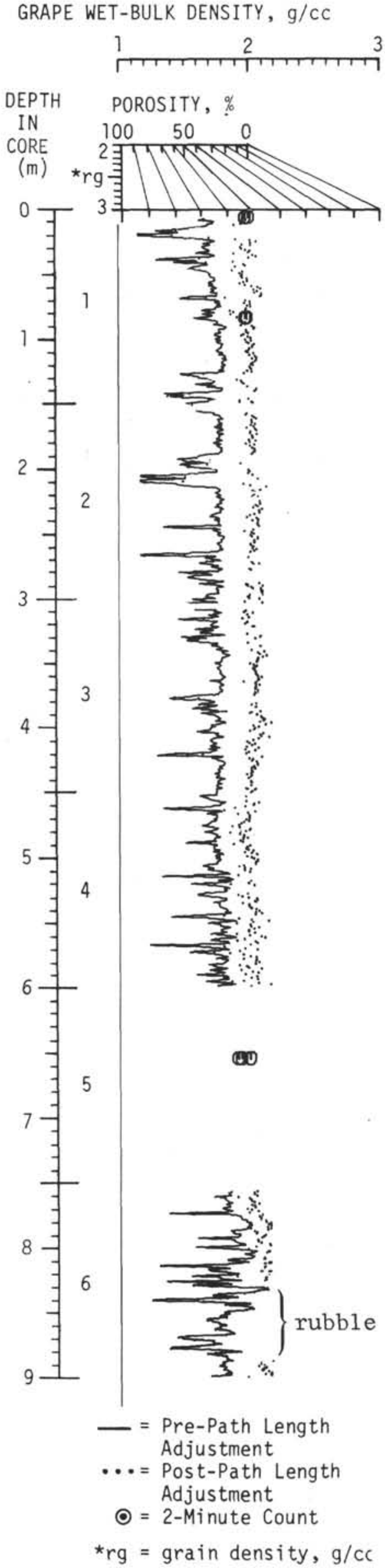
GRAPE WET-BULK DENSITY, g/cc
1
2
3
DEPTH IN CORE (m)
POROSITY, %
100
50
0
2
*rg
3
0
1
2
3
4
5
6
7
8
9
1
2
3
4
5
6
rubble
— = Pre-Path Length Adjustment
•••= Post-Path Length Adjustment
⊙ = 2-Minute Count
*rg = grain density, g/cc

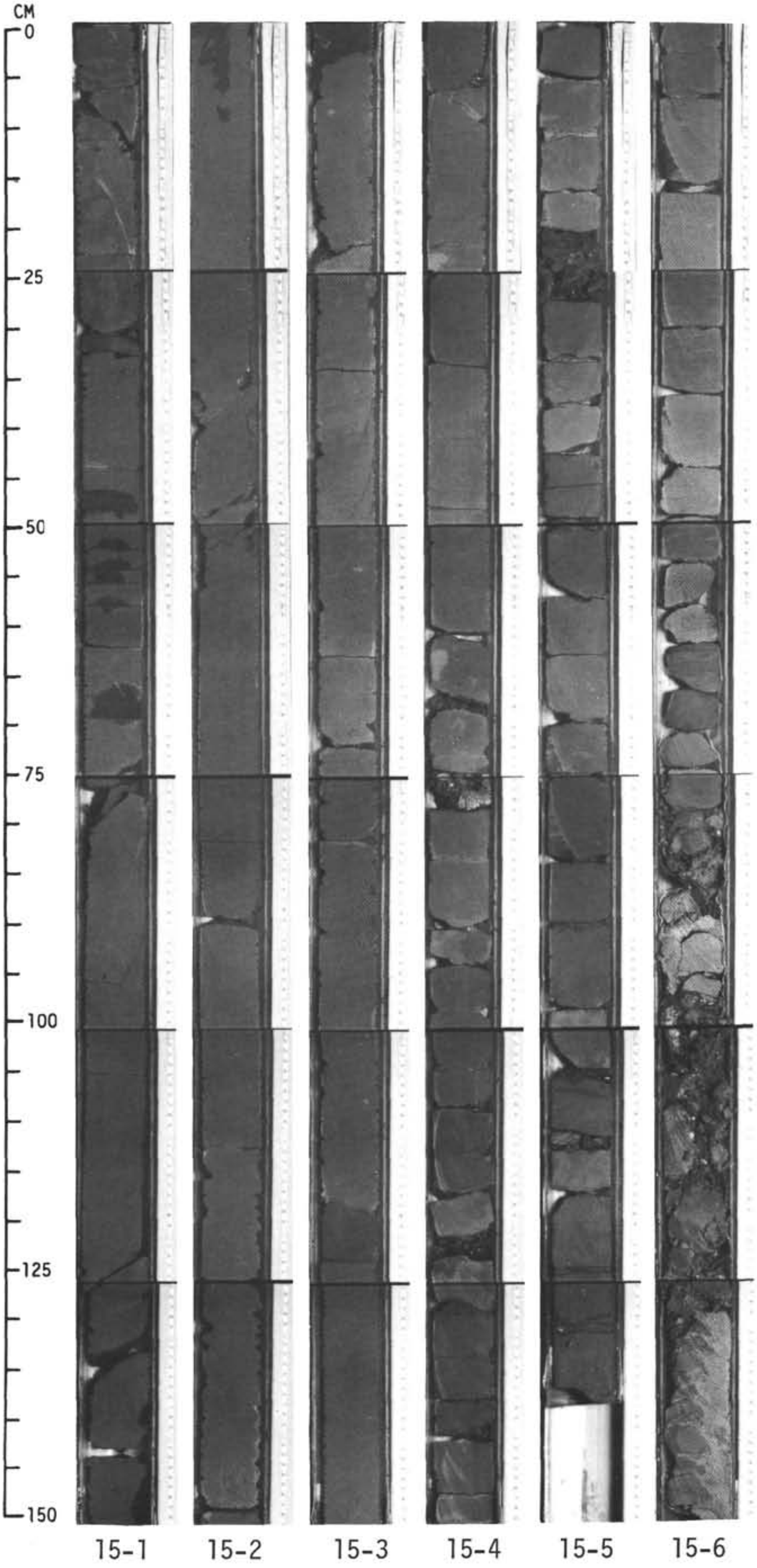
CM
0
25
50
75
100
125
150
15-1
15-2
15-3
15-4
15-5
15-6

Hole 323, Core 16

Cored Interval: 664.5-674.0 m

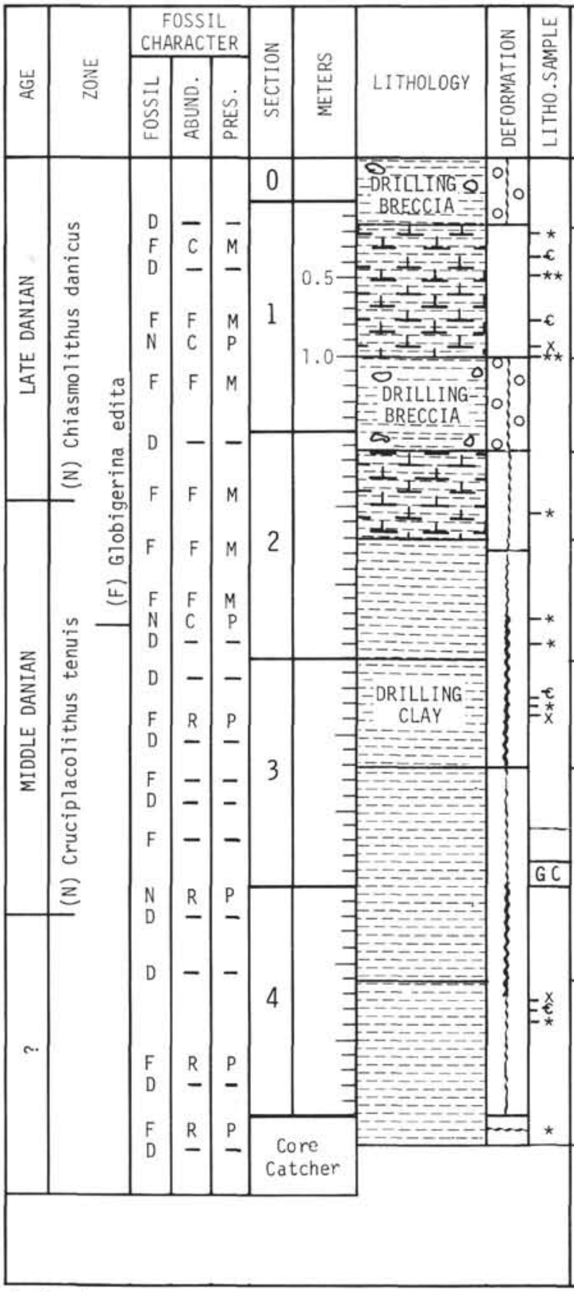

LITHOLOGIC DESCRIPTION

NANNOFOSSIL CLAYSTONE AND CLAYSTONE

DRILLING BRECCIA:

NANNOFOSSIL CLAYSTONE: dark yellowish brown (10YR 4/2) and olive black (5Y 2/1), numerous trace fossils. Brown zones contain 10-20% Fe aggregates; black areas, 50% Fe aggregates or amorphous iron. (34% $CaCO_3$ at 31 cm.) Carbon/carbonate: 1-36 (5.4-0.0-45.0), 1-78 (6.8-0.1-57.0).

DRILLING BRECCIA:

NANNOFOSSIL CLAYSTONE: dark yellowish brown (10YR 4/2). Contains up to 50% clay. (35% $CaCO_3$ at 65 cm - shipboard determination).

CLAYSTONE: varying colors of brown (10YR 4/2, 5YR 6/4, 5YR 5/6, 5YR 2/1), layered and mottled. Mixed from drilling disturbance.

DRILLING CLAY: compacted, but contains reddish yellow fragments from underlying(?) claystone. Carbon/carbonate: 3-29 (0.0-0.1-0.0).

CLAYSTONE: reddish brown (5YR 4/4) and dusky yellow brown (10YR 2/2). Drilling disturbance resulted in formation of wafer-like fragments separated by hard, compacted drilling slurry. (Section 4, 0-62 cm is mostly drilling slurry.)

CLAYSTONE: medium brown (7.5YR 4/4) with brownish black (5YR 2/1) streaks. Drilling disturbance increases down hole. Carbon/carbonate; 4-80 (0.0-0.1-0.1) 0% $CaCO_3$ at 148 cm, Sect. 4 - shipboard determination).

BULK X-RAY

	1: 90-94	3: 31-33	4: 73-74
Amorph.	35.5%	42.9%	16.3%
Crystal.	64.5%	58.1%	83.7%
	Percent of Crystalline Component		
Calc.	55.3%	-	-
Dolo.	0.2%	-	-
Quartz	3.8%	8.1%	5.8%
K-Fldspr.	4.5%	11.8%	18.4%
Plag.	1.0%	3.8%	2.1%
Kaol.	-	0.8%	-
Mica	-	4.1%	6.7%
Chlorite	-	0.3%	-
Mont.	35.2%	71.1%	63.6%
Clinop.	-	-	3.5%

Explanatory notes in Chapter 2

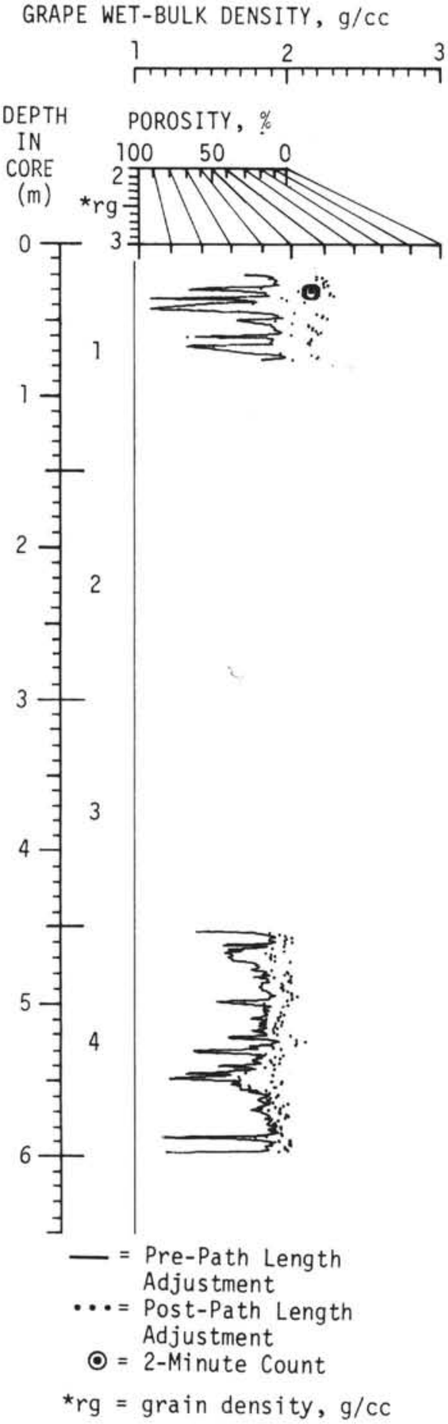
GRAPE WET-BULK DENSITY, g/cc
1
2
3
DEPTH IN CORE (m)
POROSITY, %
100
50
0
2
*rg
3
0
1
2
3
4
5
6
1
2
3
4
— = Pre-Path Length Adjustment
• • • = Post-Path Length Adjustment
⊙ = 2-Minute Count
*rg = grain density, g/cc

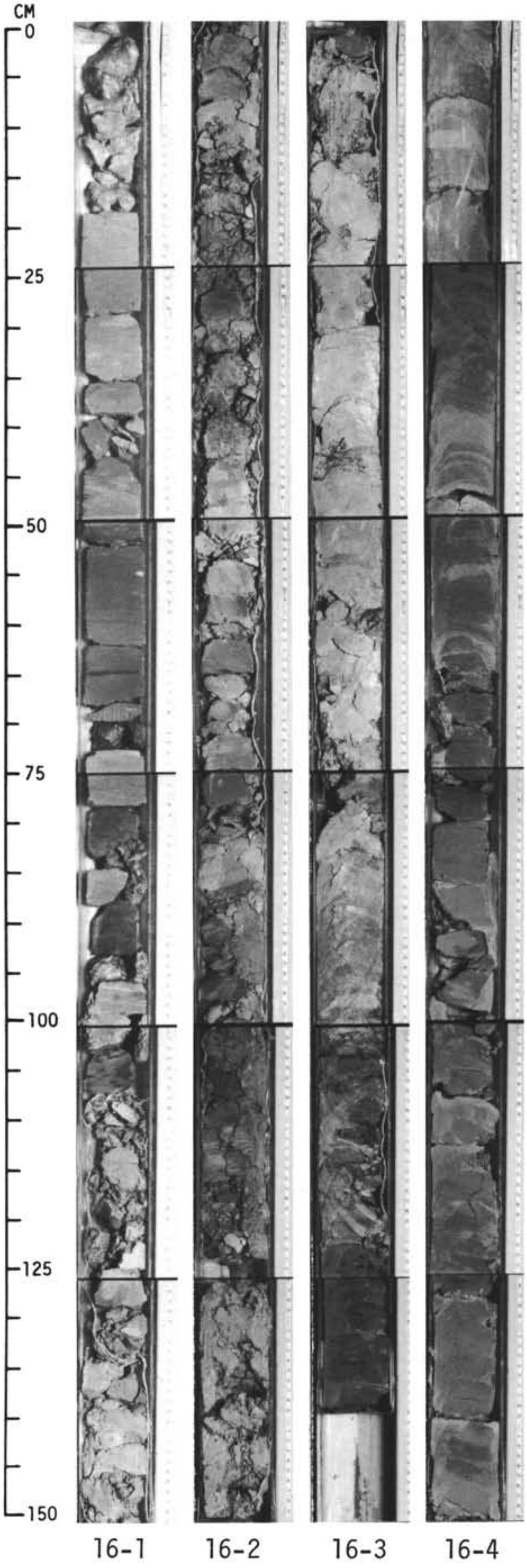
CM
0
25
50
75
100
125
150
16-1
16-2
16-3
16-4

Hole 323, Core 17 Cored Interval: 674.0-683.5 m

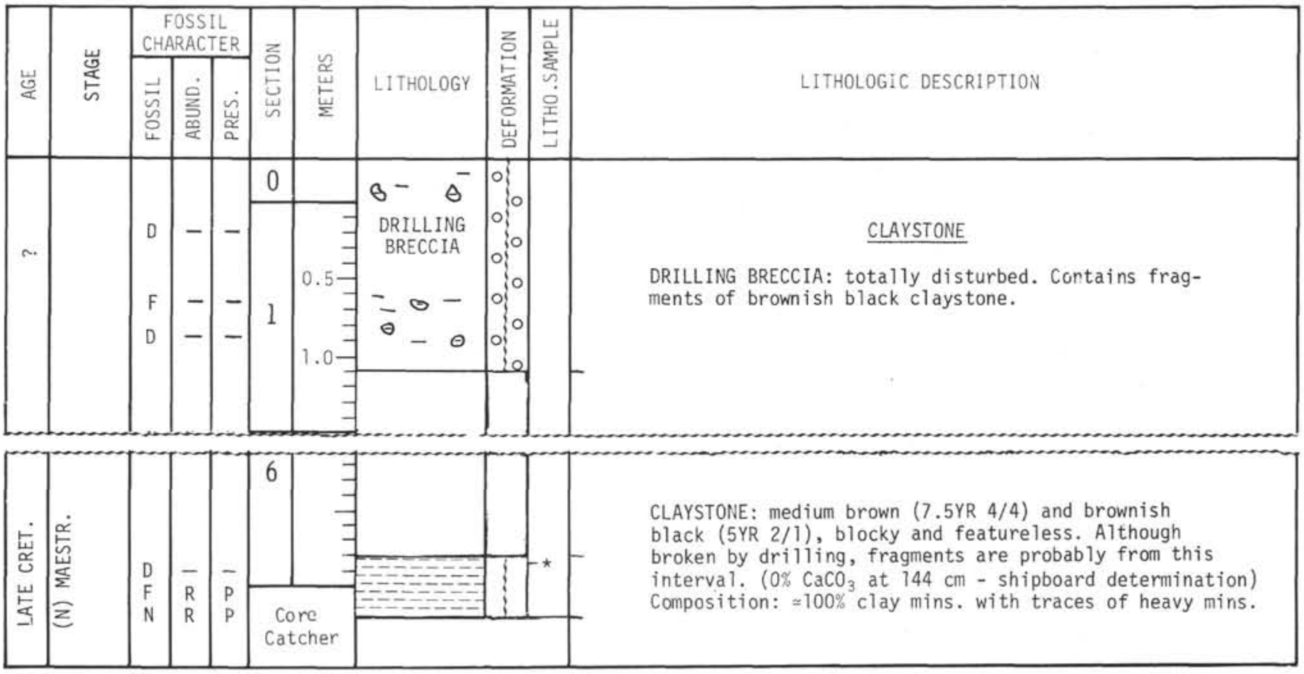

CLAYSTONE

DRILLING BRECCIA: totally disturbed. Contains fragments of brownish black claystone.

CLAYSTONE: medium brown (7.5YR 4/4) and brownish black (5YR 2/1), blocky and featureless. Although broken by drilling, fragments are probably from this interval. (0% $CaCO_3$ at 144 cm - shipboard determination) Composition: ≈100% clay mins. with traces of heavy mins.

Explanatory notes in Chapter 2

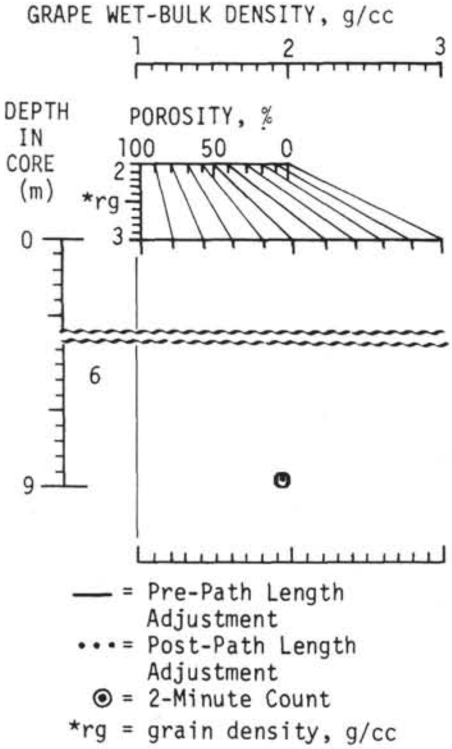
GRAPE WET-BULK DENSITY, g/cc
1
2
3
DEPTH IN CORE (m)
POROSITY, %
100
50
0
2
*rg
3
0
6
9
— = Pre-Path Length Adjustment
••• = Post-Path Length Adjustment
⊙ = 2-Minute Count
*rg = grain density, g/cc

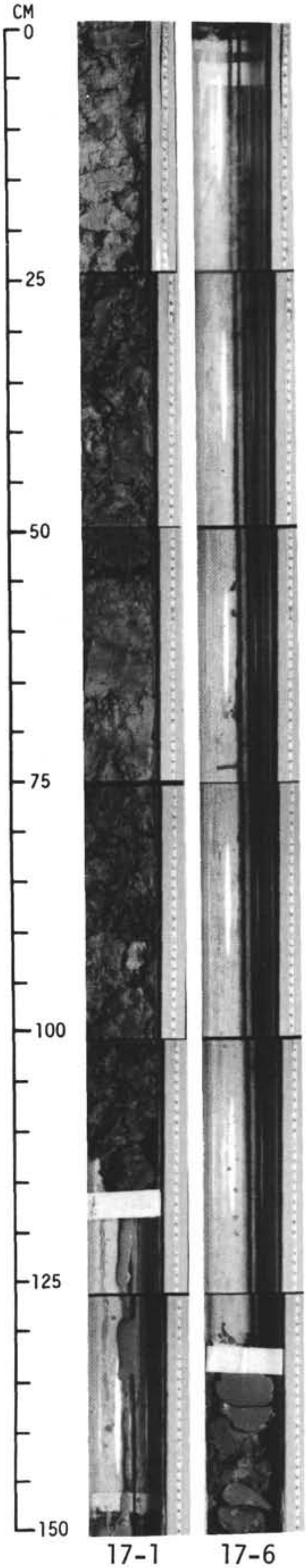
CM
0
25
50
75
100
125
150
17-1
17-6

Hole 323, Core 18

Cored Interval:693.0-702.5 m

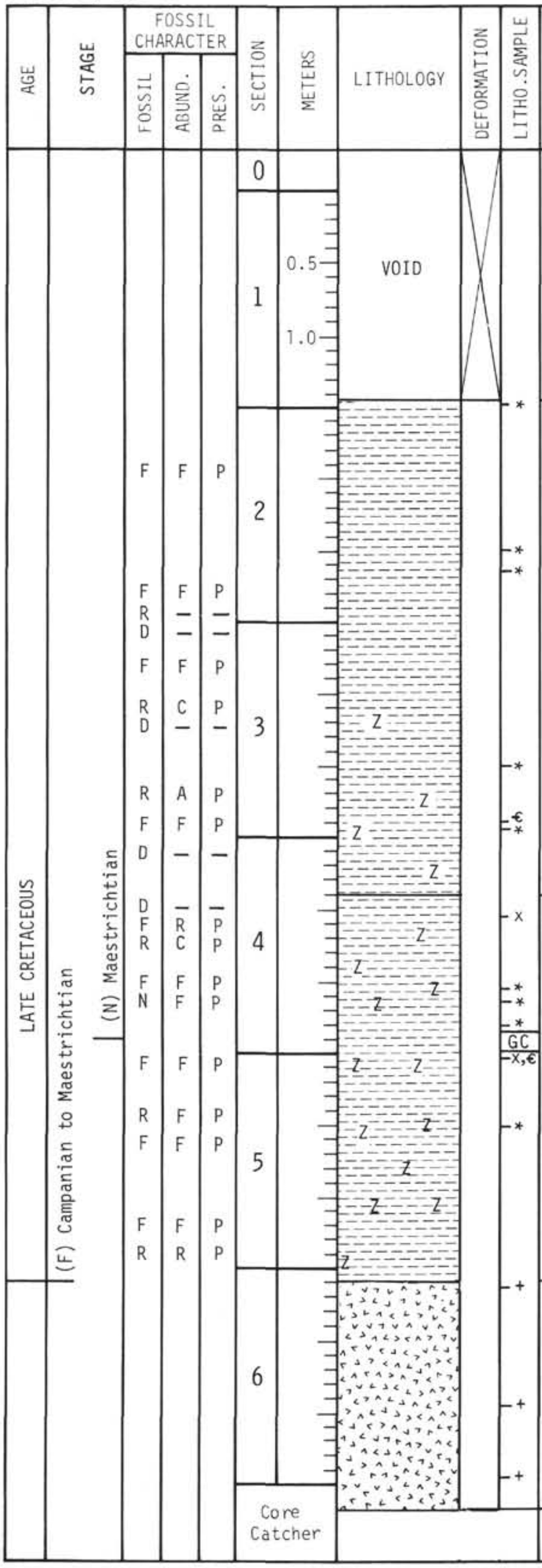

LITHOLOGIC DESCRIPTION

CLAYSTONE, ZEOLITIC CLAYSTONE, AND BASALT

CLAYSTONE: brown (10YR 4/3, 10YR 5/3) with white specks, uniform, structureless. Arenaceous forams present. Carbon/carbonate: 3-140 (0.0-0.1-0.0).

BULK X-RAY

	2: 116-118	3: 99-101	4: 52-54	5: 0-2
Amorph.	28.6%	54.7%	30.1%	36.1%
Crystal.	71.4%	45.2%	69.9%	63.9%
	Percent of Crystalline Component			
Quartz	10.7%	12.8%	13.7%	14.7%
K-Fldspr.	15.8%	14.5%	5.7%	9.3%
Plag.	3.1%	6.4%	9.2%	9.6%
Mica	8.6%	11.0%	5.9%	7.6%
Chlorite	0.3%	0.3%	-	-
Mont.	58.0%	44.5%	46.2%	45.6%
Clinop.	3.5%	10.5%	18.8%	12.7%
Amphi.	-	-	0.4%	0.5%

ZEOLITIC CLAYSTONE: varicolored dark yellowish brown (10YR 4/4), very dark grayish brown (10YR 3/2), dusky yellowish brown (10YR 2/2), brown (7.5YR 4/4) and minor brownish black (5YR 2/1). Contains arenaceous forams, trace fossils (Zoophycos, Sect. 4, 110 cm), 10-50% zeolites, 5-20% Fe aggregates. Carbon/carbonate 5-0 (0.0-0.0-0.0).

BASALT: dark gray (N3), extremely fine-grained aphyric and diabasic. No glass. Trace of amygdules filled with greenish clay. Fractures coated with green clay mins., calcite, Fe oxides. Contact not preserved; no evidence of baking. Horizontal calcite vein at 76-80 cm. Basalt is completely aphanitic below 142 cm.

Explanatory notes in Chapter 2

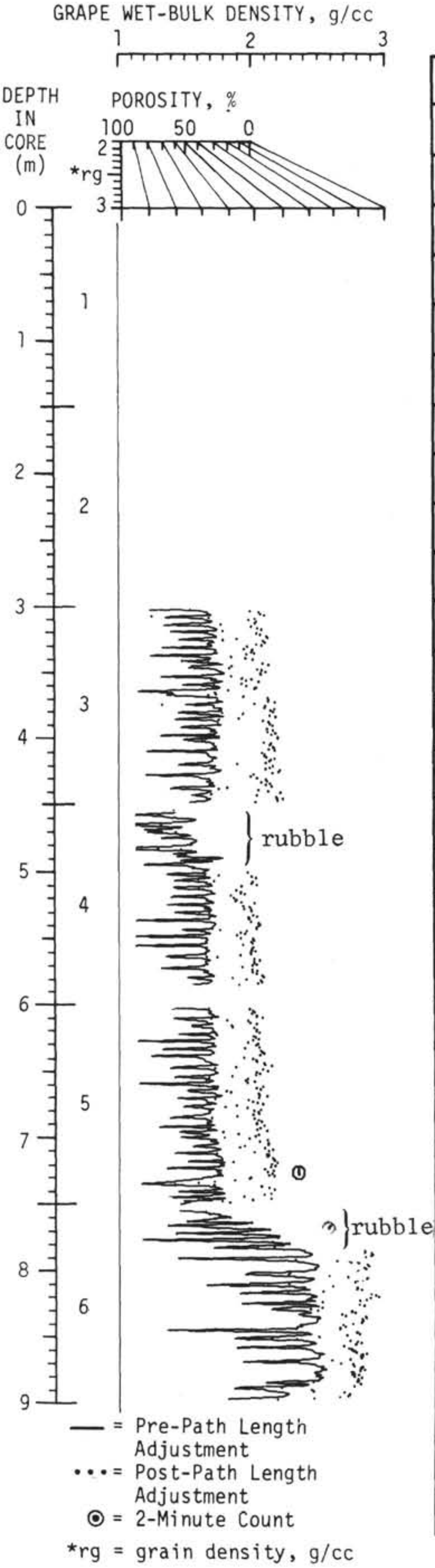
GRAPE WET-BULK DENSITY, g/cc
1
2
3
DEPTH IN CORE (m)
POROSITY, %
100
50
0
2
*rg
3
0
1
2
3
4
5
6
7
8
9
1
2
3
4
5
6
rubble
rubble
— = Pre-Path Length Adjustment
•••• = Post-Path Length Adjustment
⊙ = 2-Minute Count
*rg = grain density, g/cc

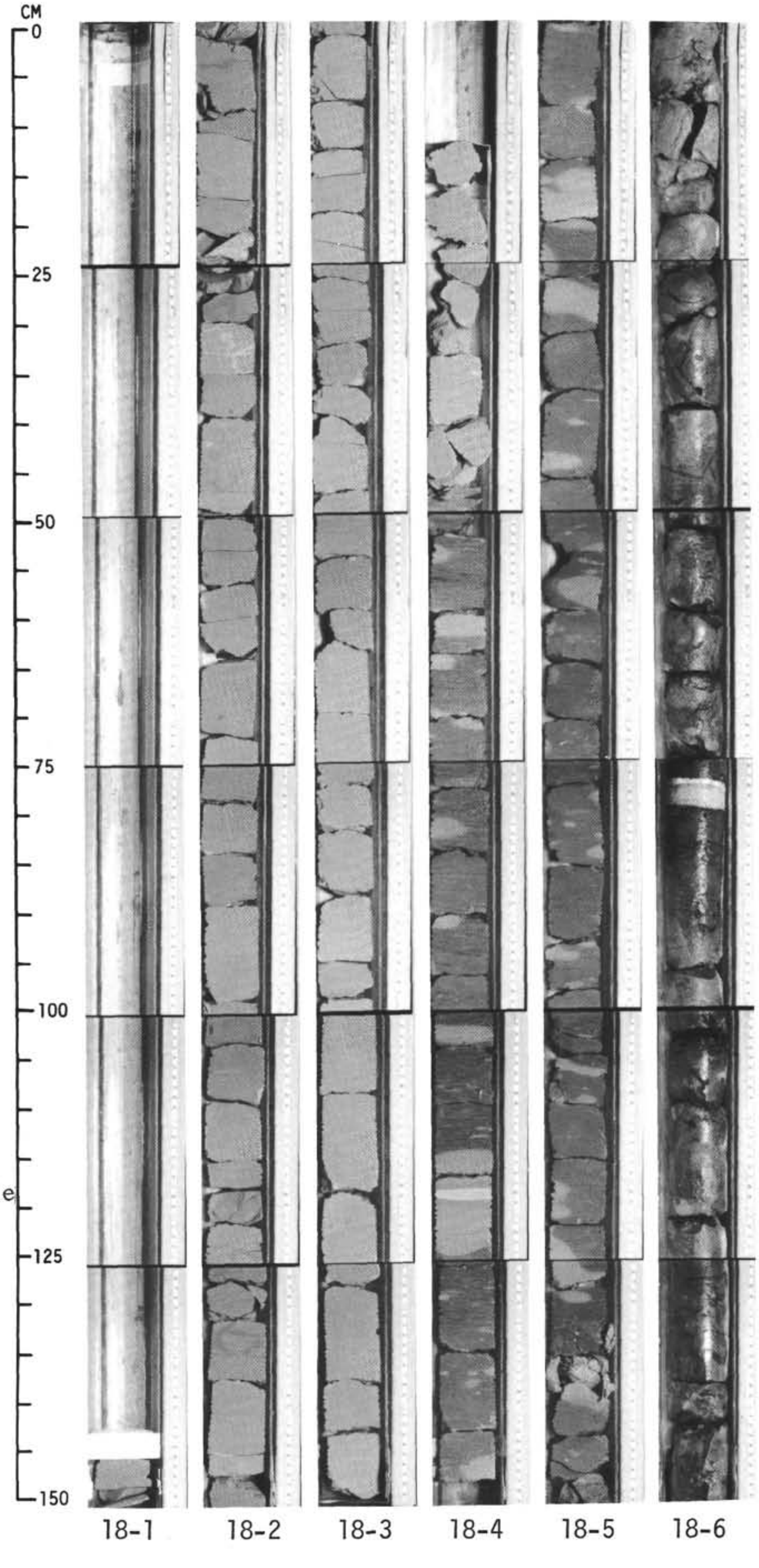
CM
0
25
50
75
100
125
150
18-1
18-2
18-3
18-4
18-5
18-6

Hole 323, Core 19

Cored Interval: 702.5-712.0 m

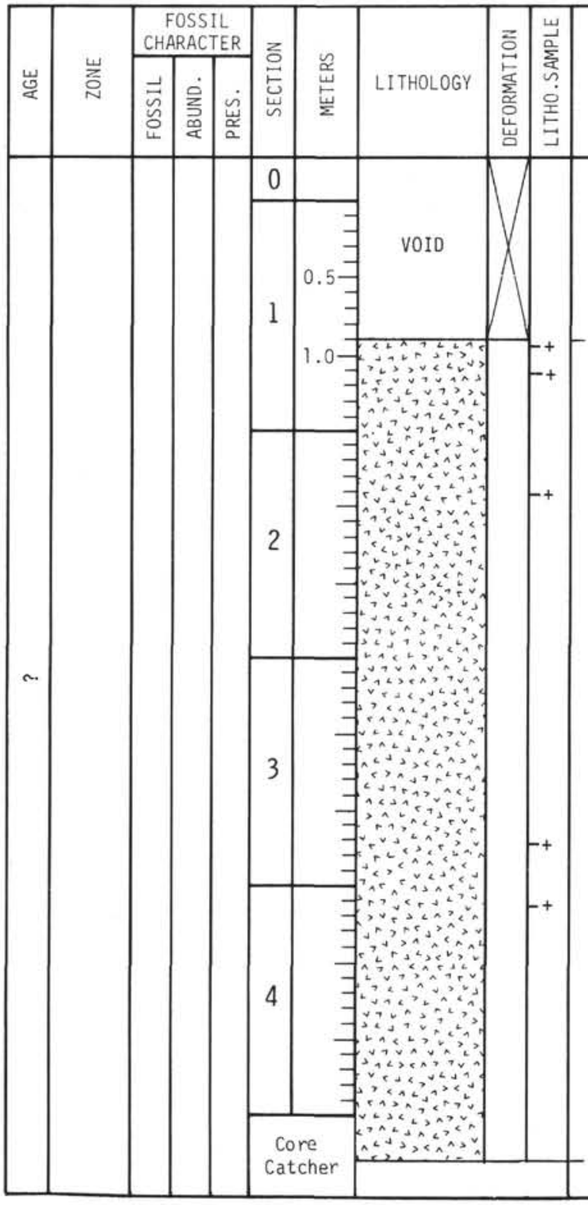

LITHOLOGIC DESCRIPTION

BASALT

BASALT: dark gray (N3), extremely fine-grained aphyric and diabasic. No glass. Trace of amygdules filled with greenish clay. Fractures coated with green clay, calcite, Fe-oxides.
Sect. 1, 90-100 cm - completely aphanitic, pilotaxitic texture.

Sect. 2, 20-55 cm - amygdule-rich zone.

Sect. 2, 65 cm - Sect. 3, 50 cm - very extensive veining with extensive staining adjacent to veins.

Sect. 3, 70 cm - large calcite vein.
Sect. 3, 90-93 cm - large clay filled vein.
Sect. 3, 100-150 cm - scattered plagioclase microphenocrysts.

(Amygdules very scarce and small in Sections 3 and 4.)

Sect. 4, 120-135 cm - scattered plagioclase microphenocrysts.

Explanatory notes in Chapter 2

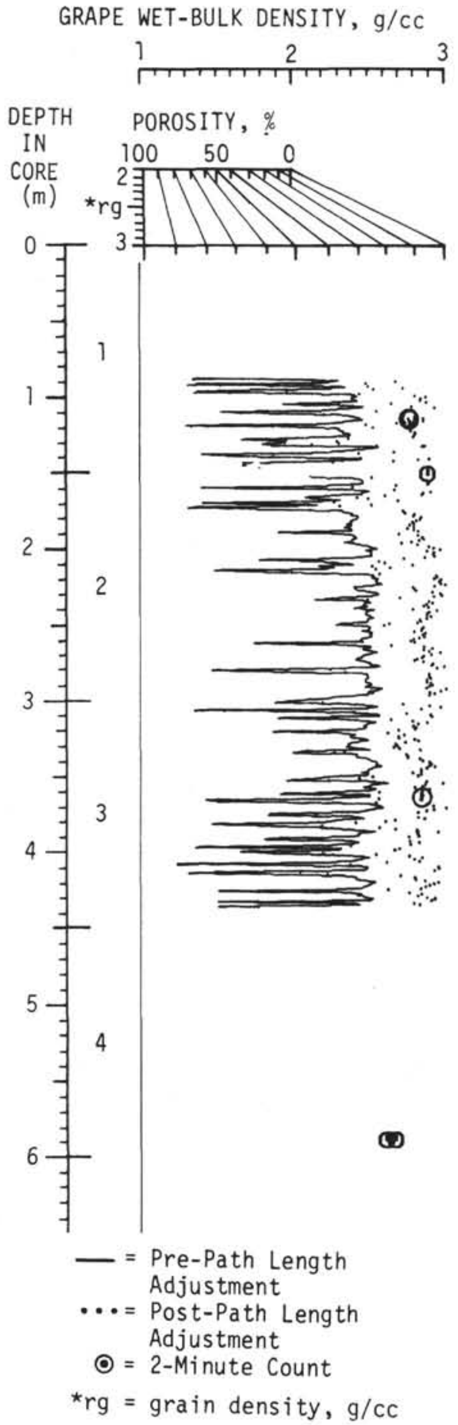
GRAPE WET-BULK DENSITY, g/cc
1
2
3
DEPTH IN CORE (m)
POROSITY, %
100
50
0
2
*rg
3
0
1
2
3
4
5
6
1
2
3
4
— = Pre-Path Length Adjustment
• • • = Post-Path Length Adjustment
⊙ = 2-Minute Count
*rg = grain density, g/cc

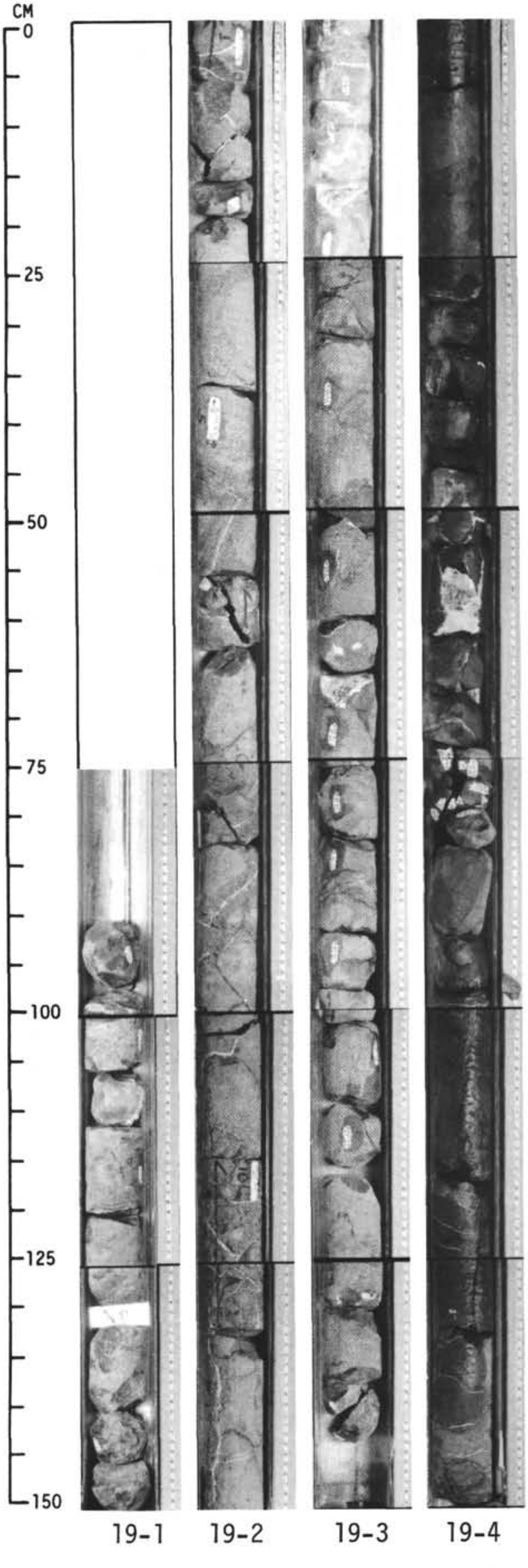
CM
0
25
50
75
100
125
150
19-1
19-2
19-3
19-4

Hole 323, Core 20 Cored Interval: 712.0-721.5 m

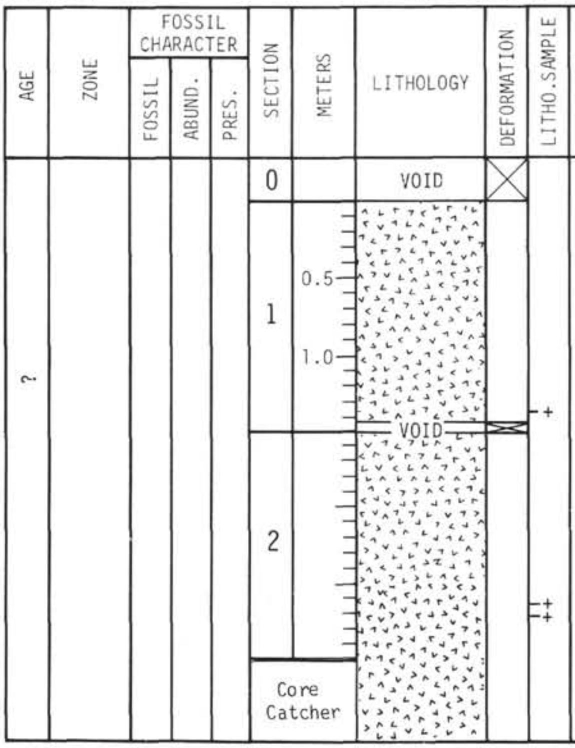

LITHOLOGIC DESCRIPTION

BASALT

BASALT: dark gray (N3), aphanitic to very fine-grained aphyric diabasic. No glass. Very small (<<0.5 mm) amygdules filled with greenish clay are scattered throughout Sect. 1, and between 65-70 cm and 112-116 cm in Sect. 2. Moderate amount of veining with calcite, green clay and Fe-oxides. No noticeable staining adjacent to veins.
Sect. 1, 72-78 cm - scattered plagioclase microphenocrysts.
Sect. 1, 98-120 cm - iddingsite pseudomorphs after olivine.

Sect. 2, 50-60 cm - thick calcite vein, subvertical.
Sect. 2, 72-80 cm and 120-150 cm - scattered plagioclase microphenocrysts.

Core catcher - scattered plagioclase microphenocrysts, iddingsite pseudomorphs after olivine, greenish amygdules and minor veining.

Hole 323, Core 21 Cored Interval: 721.5-731.0 m

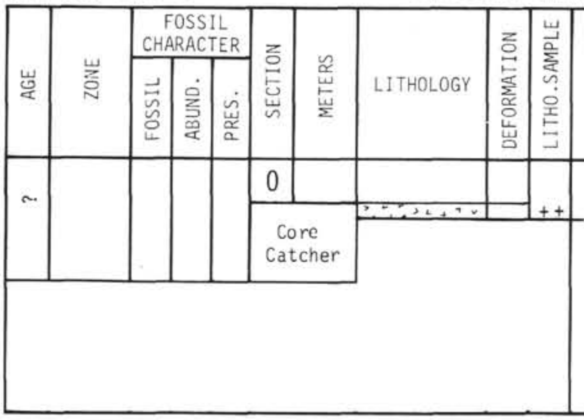

LITHOLOGIC DESCRIPTION

BASALT

BASALT: dark gray (N3), very fine-grained diabasic. Contains: 2% fresh plagioclase microphenocrysts, 0.5% greenish amygdules (<0.5 mm), no glass. Calcite veins are 0.5-1.0 mm thick, randomly oriented with 2-4 mm stains along sides. Tiny fractures contain small amount of green clay.

(Total recovery for Core 21 was a single 8 cm long segment in the core catcher.)

Explanatory notes in Chapter 2

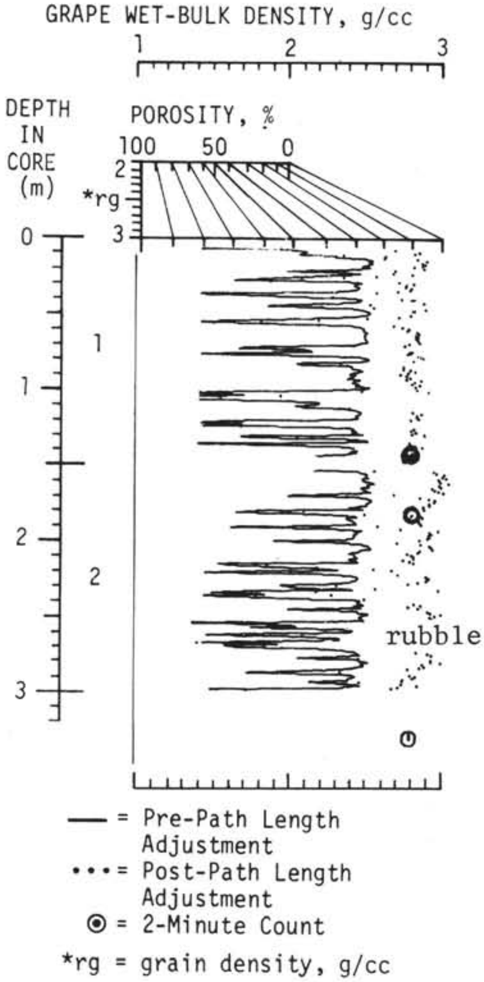
GRAPE WET-BULK DENSITY, g/cc
1
2
3
DEPTH IN CORE (m)
POROSITY, %
100
50
0
2
*rg
3
0
1
2
3
1
2
rubble
— = Pre-Path Length Adjustment
••• = Post-Path Length Adjustment
⊙ = 2-Minute Count
*rg = grain density, g/cc

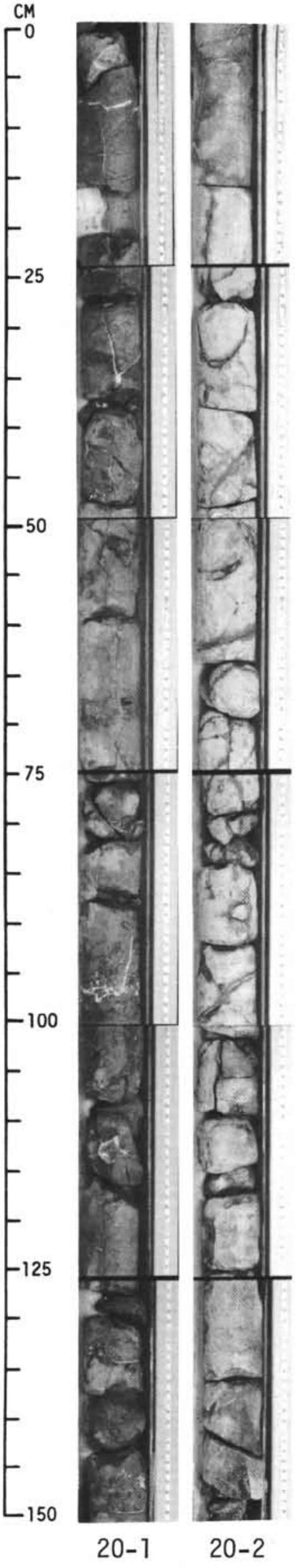
CM
0
25
50
75
100
125
150
20-1
20-2

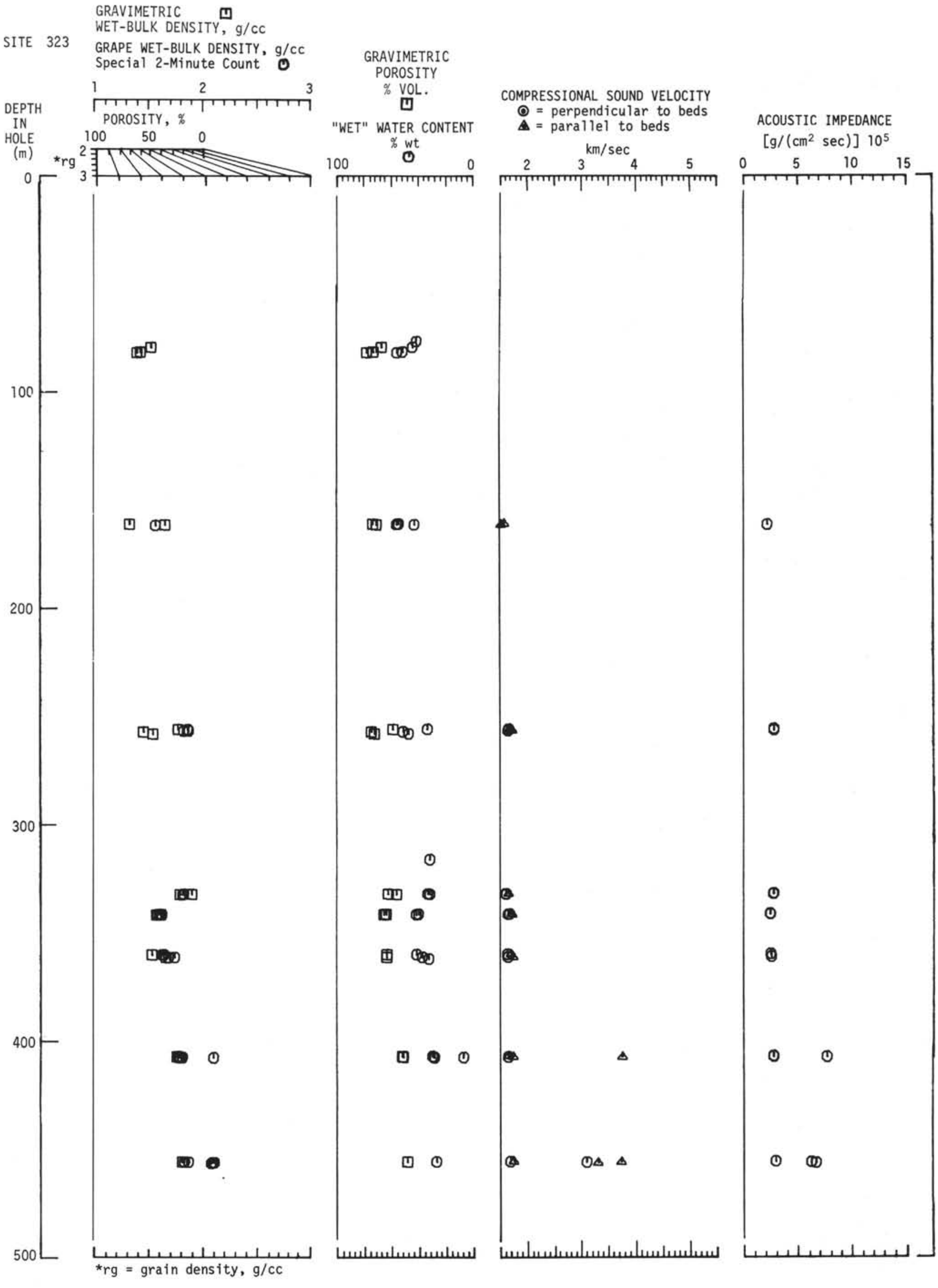
SITE 323
GRAVIMETRIC WET-BULK DENSITY, g/cc
GRAPE WET-BULK DENSITY, g/cc
Special 2-Minute Count
1
2
3
POROSITY, %
100
50
0
*rg
2
3
DEPTH IN HOLE (m)
0
100
200
300
400
500
GRAVIMETRIC POROSITY % VOL.
"WET" WATER CONTENT % wt
100
0
COMPRESSIONAL SOUND VELOCITY
= perpendicular to beds
= parallel to beds
km/sec
2
3
4
5
ACOUSTIC IMPEDANCE
[g/(cm^2 sec)] 10^5
0
5
10
15
*rg = grain density, g/cc

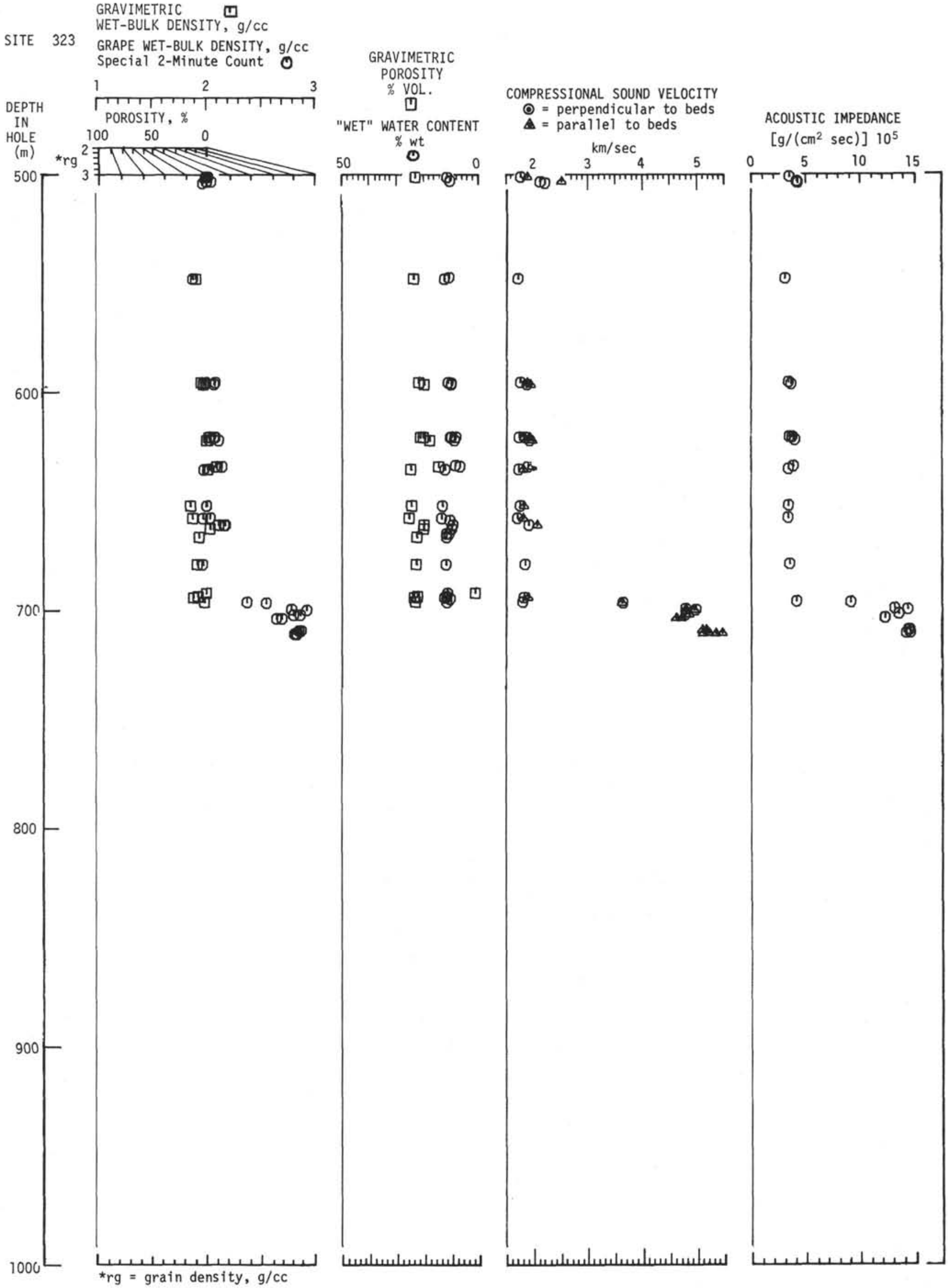

SITE 323
GRAVIMETRIC WET-BULK DENSITY, g/cc
GRAPE WET-BULK DENSITY, g/cc
Special 2-Minute Count
1
2
3
DEPTH IN HOLE (m)
POROSITY, %
100
50
0
*rg
2
3
500
600
700
800
900
1000
*rg = grain density, g/cc
GRAVIMETRIC POROSITY % VOL.
"WET" WATER CONTENT % wt
50
0
COMPRESSIONAL SOUND VELOCITY
◉ = perpendicular to beds
▲ = parallel to beds
km/sec
2
3
4
5
ACOUSTIC IMPEDANCE
[g/(cm² sec)] 10⁵
0
5
10
15